Latest ATLAS studies on Higgs to diboson states

Fabrice Hubaut (hubaut@in2p3.fr)

CPPM/IN2P3 – Aix-Marseille Université (Marseille, FRANCE)

On Behalf of the ATLAS Collaboration

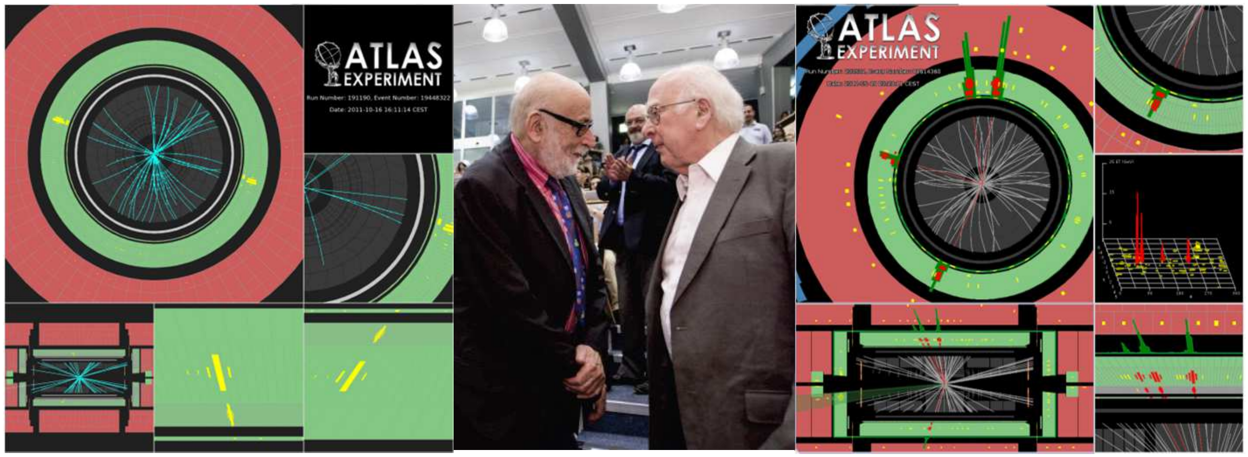

Rencontres de Moriond 2013, EW session, March 2-9

Introduction and outline

ATLAS new boson discovery paper based on diboson channels $\gamma\gamma$, $ZZ^{(*)}$, $WW^{(*)}$

[6 months ago]

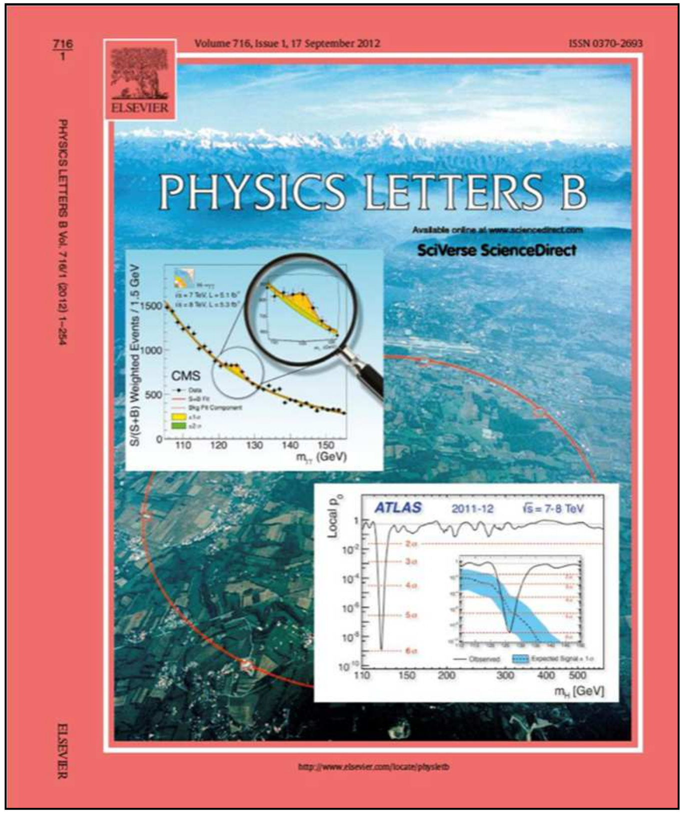

PLB 716 (2012) 1-29

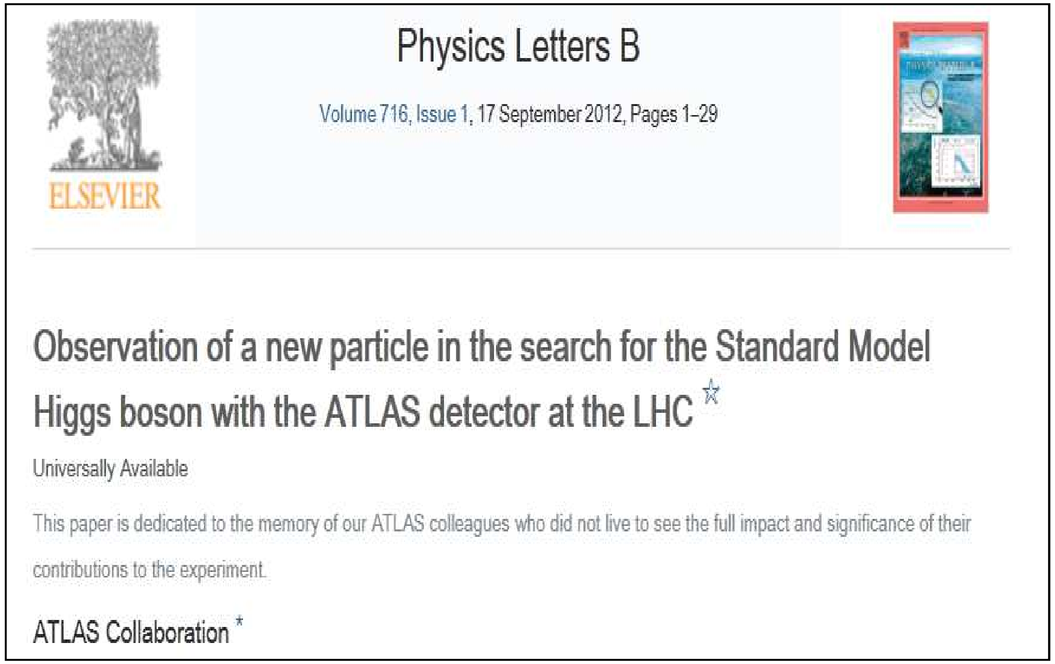

Introduction and outline

Since then, Higgs to diboson states analyses mostly focused on:

- Refining property measurements (mass, spin/parity, couplings), driven by these channels

  ➔ Today: $H \to \gamma\gamma$ and $H \to ZZ^{(*)} \to 4l$ analyses updates with full LHC dataset [~25 fb^{-1}]

- Keeping looking for other possible signals of (beyond SM) Higgs(es)

  ➔ Today: updated high-mass search in $H \to ZZ \to 4l$ channel

Outline

1. **Updated results in $H \to \gamma\gamma$ channel and property measurements** — New
2. **Updated results in $H \to ZZ^{(*)} \to 4l$ channel and property measurements** — New
3. **Analysis in $H \to WW^{(*)} \to l\nu l\nu$ channel with 13 fb^{-1} of 8 TeV data**
4. **First results on $H \to Z\gamma$ channel** — New
5. **High-mass BSM Higgs searches in diboson states** — New

Remark: overview of latest SM dibosons cross-section measurements @LHC → S. Hassani's talk

SM-Higgs production @ LHC and decay

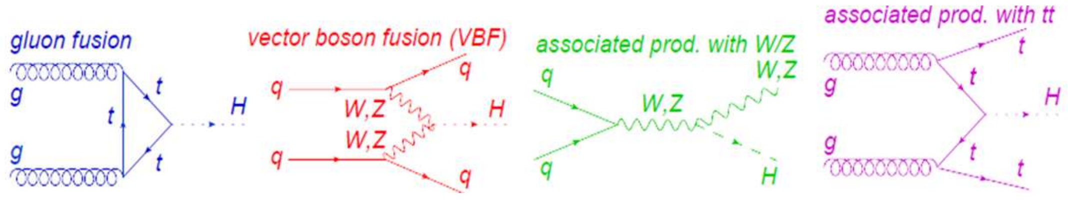

19.5 pb (87%)	1.6 pb (7%)	1.1 pb (5%)	0.1 pb (1%)

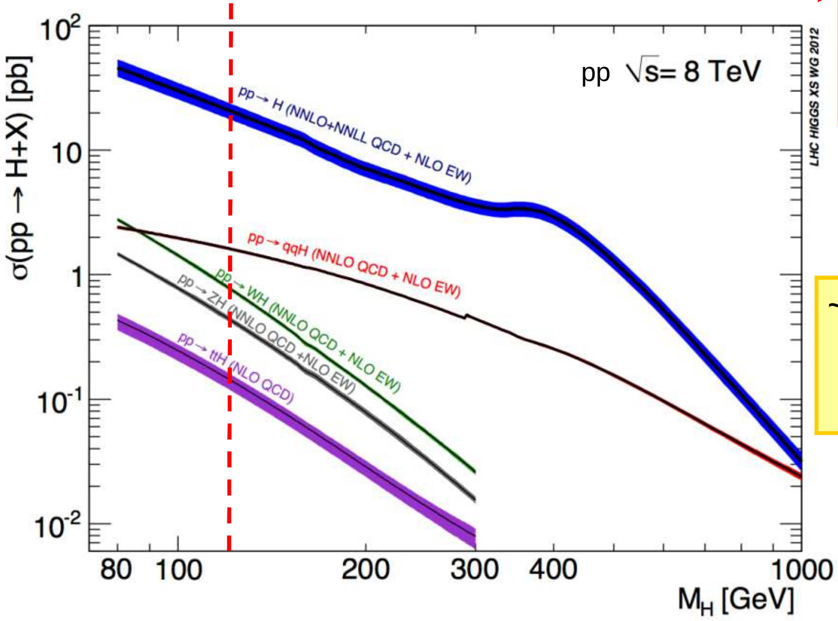

σ(pb) @125 GeV for pp √s=8TeV

Total 22.3 pb

~2 Higgs bosons @ 125GeV produced at LHC out of 10^{10} pp collisions

Branching ratios at 125 GeV:

bb:	57.7%	ZZ:	2.6%
WW:	21.5%	γγ:	0.23%
ττ:	6.3%		

σ*BR for « useable » final states

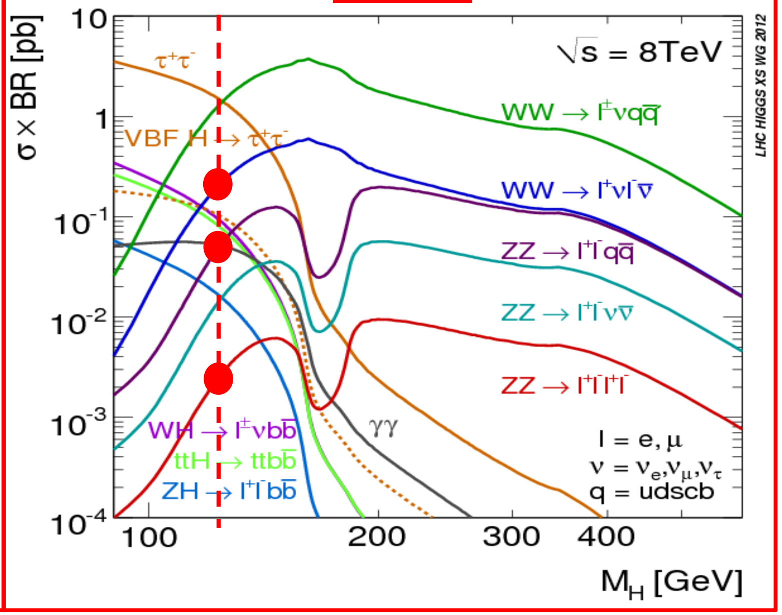

➔ **3 out of 5 main decay modes exploited at low mass are to dibosons** [γγ, ZZ(*)→4l, WW(*) →lνlν]

➔ **Analyses further optimised for increased sensitivity to VBF and VH productions**

LHC & ATLAS detector performance

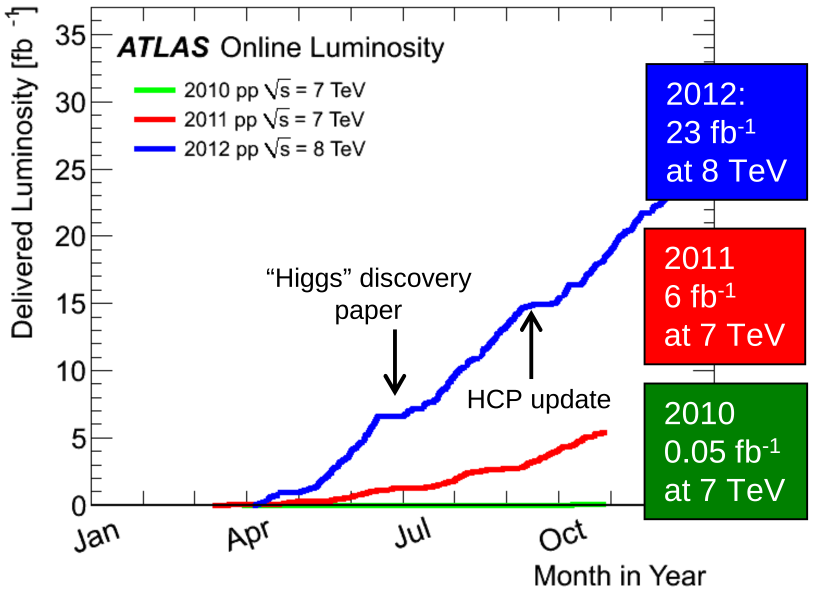

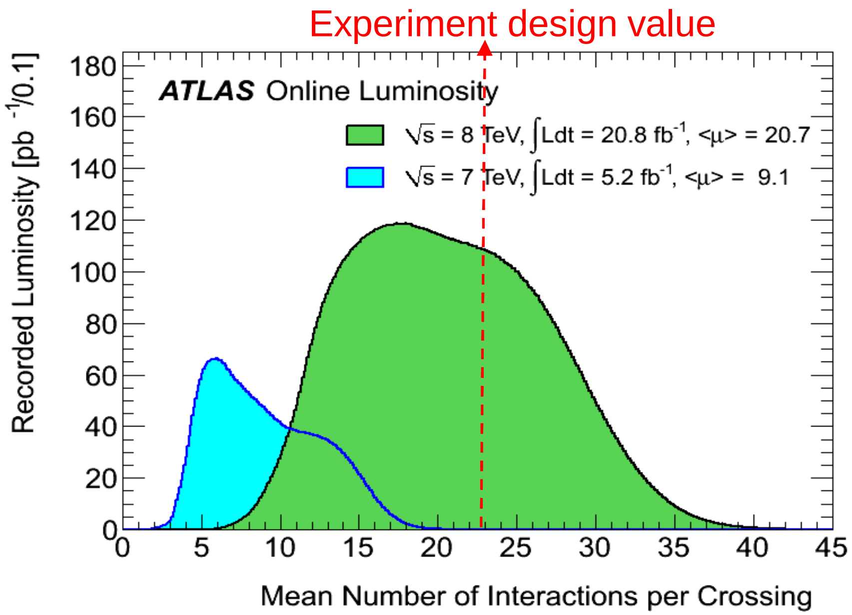

Outstanding LHC and detector performance

- L_{peak} up to $7.7 \cdot 10^{33}$ $cm^{-2} \cdot s^{-1}$ in 2012 at 8 TeV
- $L_{delivered}$ ~23 fb^{-1} (8 TeV) + 6 fb^{-1} (7 TeV)
- ~90% of delivered collisions are used in ATLAS physics analyses

Price to pay is large pile-up

- Pile-up level above design value (50 ns bunch crossing)
- Many challenges to mitigate its impact at all levels: trigger, computing, reco/identification of physics objects, …

➔ Most analyses shown in this talk use the full 2011+2012 statistics

H→γγ : Overview

ATLAS-CONF-2013-012

Main production mode and decay through loops → sensitive to t / W couplings and to New Physics

Background reduction

- Tight pile-up robust identification associated with isolation criteria [ε_{event}~40%]
- Reducible γ-jet and jet-jet background reduced below [~25%] irreducible γγ-continuum [~75%]
- Background extrapolated from side-bands in data

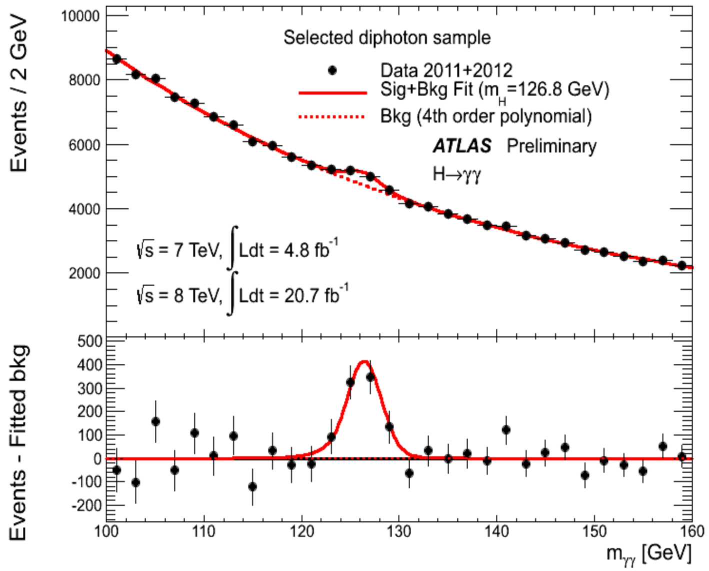

Simple topology: two high-E_T (>40,30 GeV) isolated photons

142681 events in 100<$m_{\gamma\gamma}$ [GeV]<160

→ S/B~3% in mass window ~125 GeV with 90% signal

Invariant mass resolution

$m^2_{\gamma\gamma} = 2\, E_{\gamma 1}\, E_{\gamma 2}\, (1-\cos\alpha)$

- Negligible vertex uncertainty contribution [<1.5 cm] thanks to "calorimeter pointing"
  [included in a BDT using track information to reject fake jets from pile-up in 2-jets/VBF category]
- Overall mass resolution ~1.7 GeV. Very stable with time and pile-up.

Photon energy scale and identification efficiencies (+ systematics) determined from MC and Z→ee, Z→llγ data

H→γγ : Overview

ATLAS-CONF-2013-012

Main production mode and decay through loops → sensitive to t / W couplings and to New Physics

Background reduction

Data-driven background decomposition

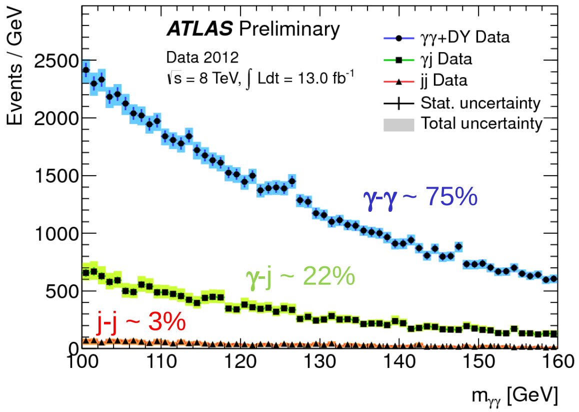

Fraction of photon candidates per conversion status

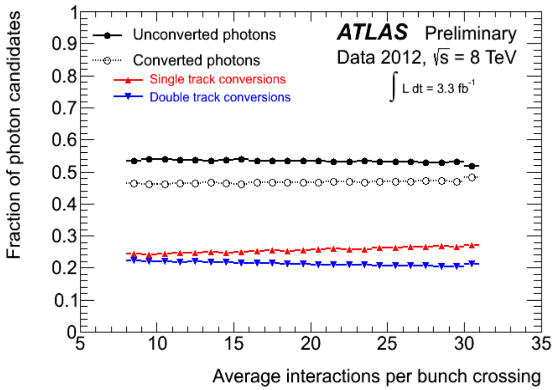

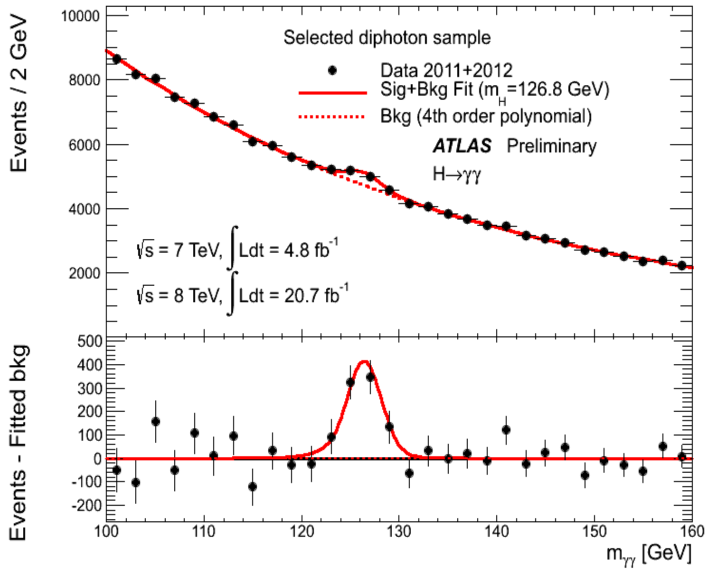

Simple topology: two high-E_T (>40,30 GeV) isolated photons

142681 events in $100<m_{\gamma\gamma}$ [GeV]<160

→ S/B~3% in mass window ~125 GeV with 90% signal

Invariant mass resolution

Stability of EM calorimeter response vs time (and pile-up) <0.1%

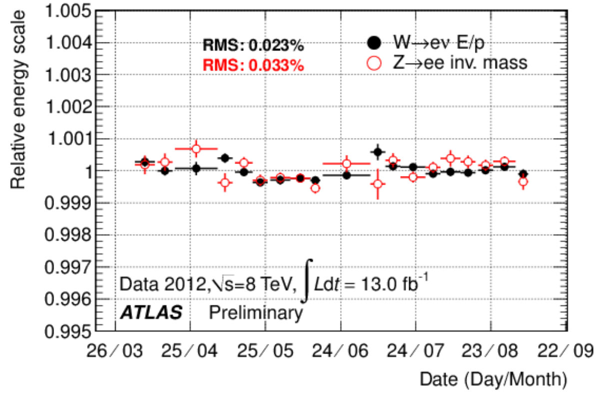

Mass resolution is pile-up robust

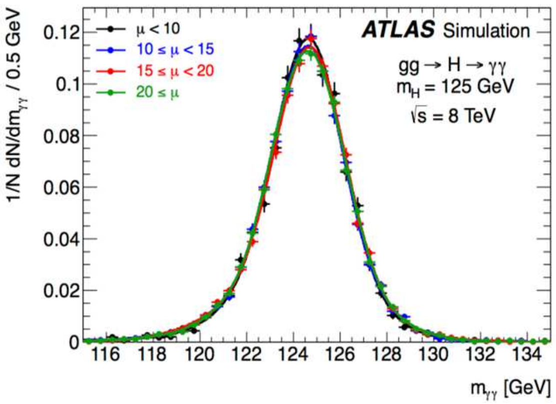

$H \rightarrow \gamma\gamma$: Categorisation

ATLAS-CONF-2013-012

- To increase signal sensitivity - overall and to specific production processes - 14 exclusive categories are built → different S/B (1-60%) and resolution (1.4-2.5 GeV)

➔ re-optimised categorisation (wrt last public results) to favor coupling measurements

(7 TeV data analysis unchanged)

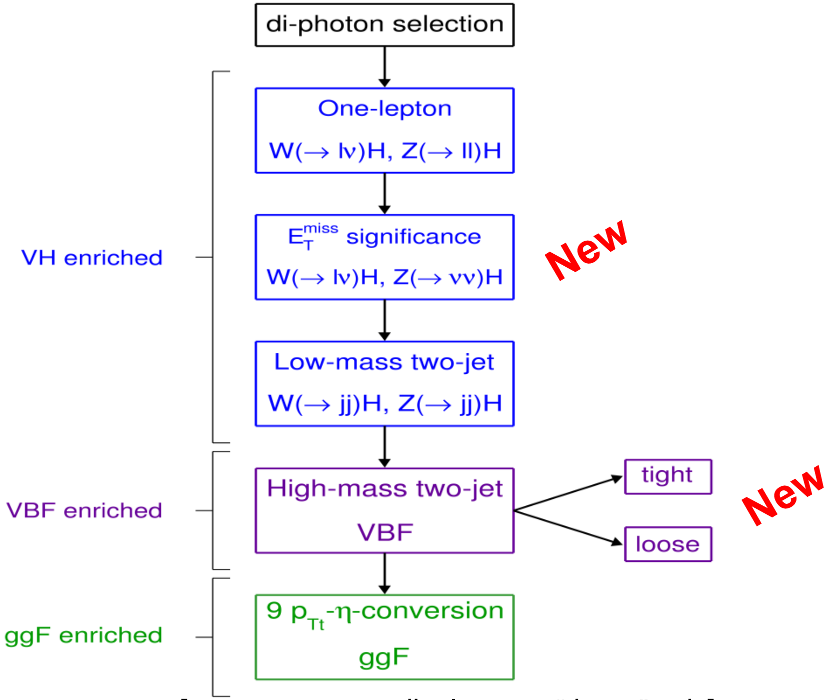

[p_{Tt} = $p_T^{\gamma\gamma}$ perpendicular to $\gamma\gamma$ "thrust" axis]

- None of the categories targeting a particular production mode are 100% pure and all have an admixture of other production mechanisms
- For instance, category targeting VBF production built on a MVA discriminant ➔ VBF purity ~75% (was 68% in last public results), 8.1 signal events expected

- Signal extracted by fit to $m_{\gamma\gamma}$ in each category. Background model carefully chosen with MC to minimize biases → largest bias (0.1-11.4 events / category) as systematics on signal yield

H→γγ : mass and signal strength

ATLAS-CONF-2013-012

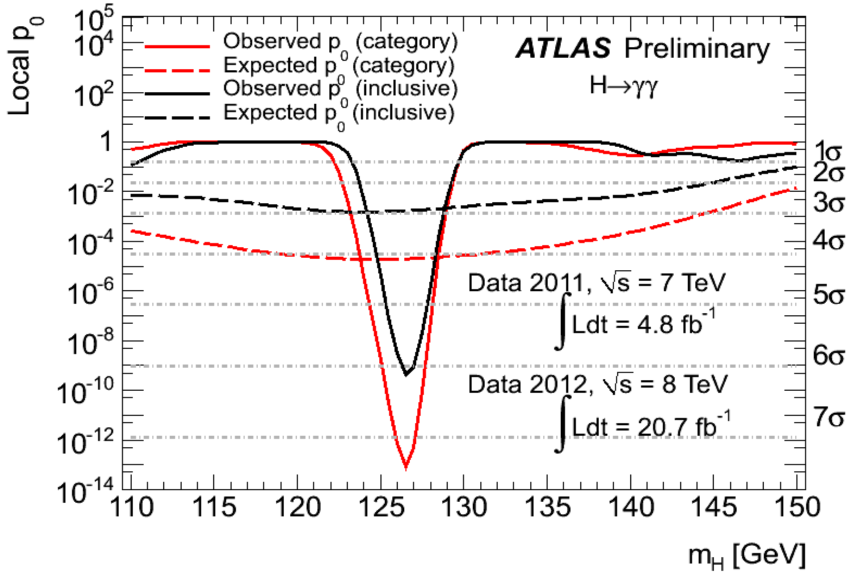

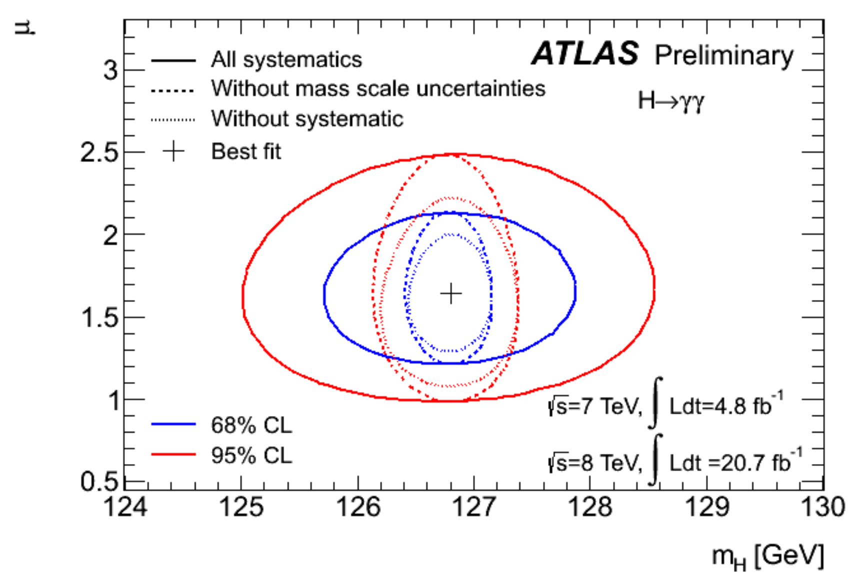

- Observed local significance of the excess: **7.4σ** (4.1σ expected for SM Higgs)
- Best mass fit: **126.8 ± 0.2 (stat) ± 0.7 (syst) GeV** → Systematics fully dominated by γ-energy scale
- Best fit of signal strength @ this mass **$\mu=1.65^{+0.34}_{-0.30}$ = 1.65 ± 0.24 (stat) $^{+0.25}_{-0.18}$ (syst)**
  [consistent across various categories]

➔ 2.3σ from SM Higgs + background hypothesis

- Inclusive fiducial cross-section of observed particle: **$\sigma_{fid}\cdot BR=56.2 \pm 12.5$ fb**
  [particle level acceptance cuts: $|\eta^\gamma|<2.37$, $E_T^\gamma>40/30$ GeV] [±10.5(stat) ± 6.5(syst) ± 2.0(lumi)]

H→γγ : coupling studies

ATLAS-CONF-2013-012

Production mechanisms associated with either top (ggF+ttH) or gauge (VBF+VH) couplings:

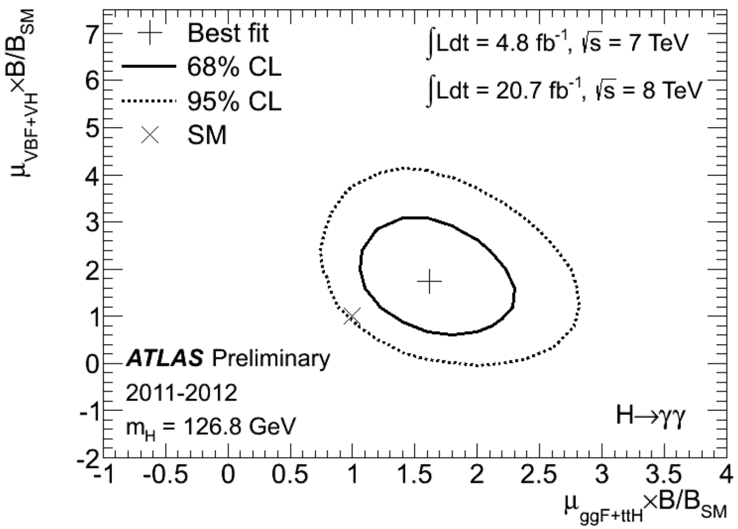

Further split of VBF and VH production:

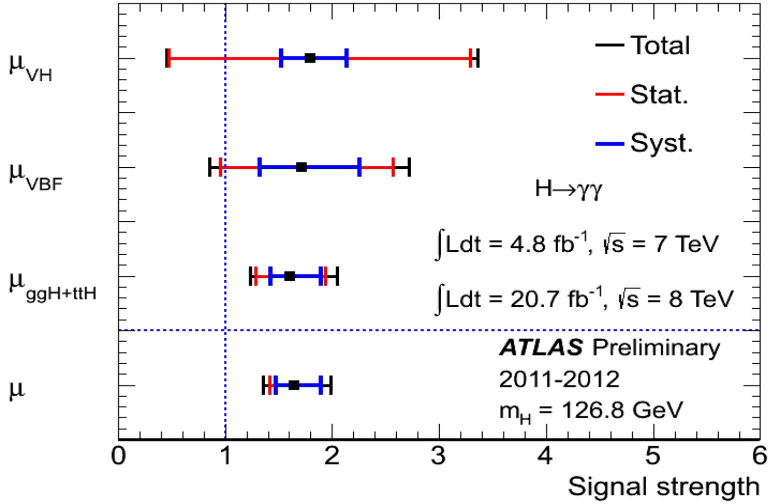

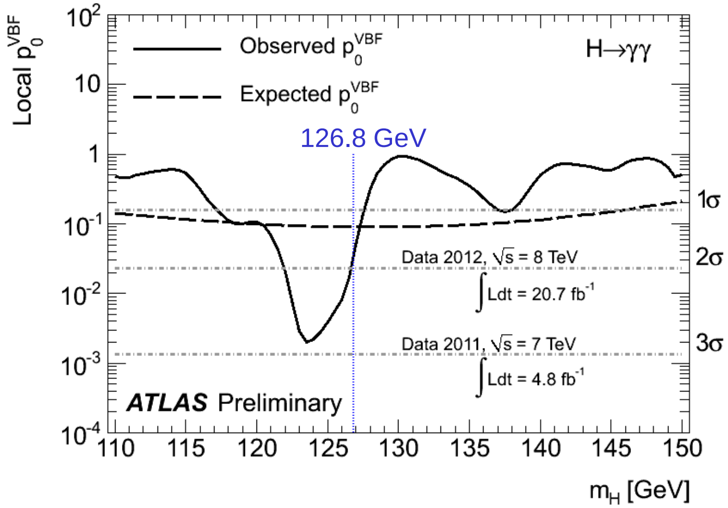

➔ **Agreement with SM expectations at 2σ level**

➔ **Uncertainties improved by ~30% (45%) for VBF (VH) production signal strengths** w.r.t. last public results
[statistics + systematics thanks to re-optimised categorisation]

➔ **Excess at ~2σ level for VBF production at 126.8 GeV**

Spin studies with H→γγ

[analysis using 13 fb^{-1} of 8 TeV data]

ATLAS-CONF-2012-168

- From distribution of polar angle θ* of the photons in the resonance rest frame
  - Compare dN/d|cosθ*| for:
    - spin-0$^+$ hypothesis: flat before cuts
    - spin-2$^+$ hypothesis: ~ $1+6\cos^2\theta^* + \cos^4\theta^*$ for G-like gg production [minimal coupling model]
  - Signal region: events within ±1.5σ around the peak (m_H=126.5 GeV)
  - Normalisation and distribution of dN/d|cosθ*| for background from data (side-bands)

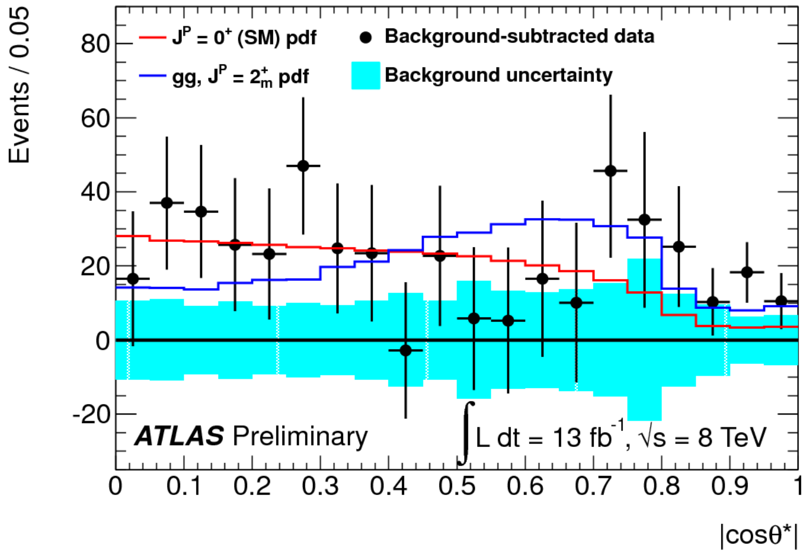

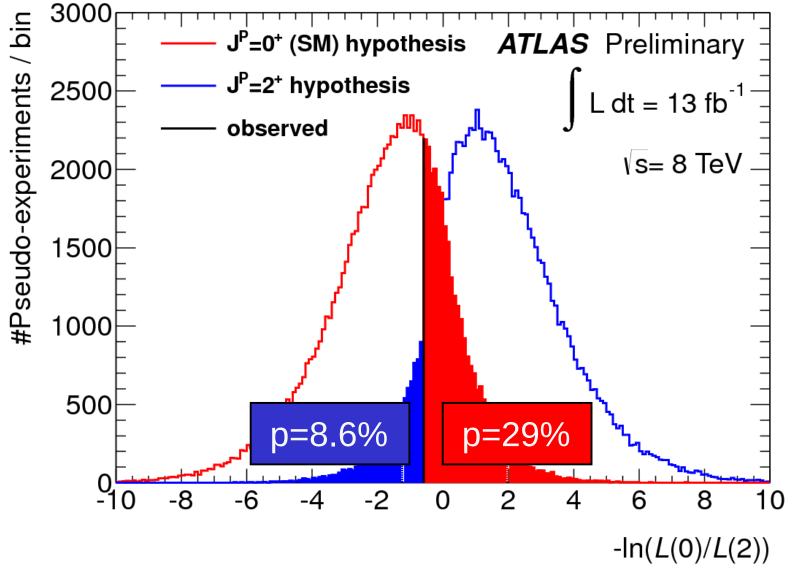

- **Spin-2$^+$ hypothesis expected exclusion CL_s at 93%** [for 100% gg spin-2 production]
- **Observation compatible with spin-0$^+$, slightly favored over spin-2$^+$ hypothesis**

H→ZZ$^{(*)}$→4l (l=e,μ) : Overview

ATLAS-CONF-2013-013

The golden channel, with small cross-section but very good S/B ratio and fully-reconstructed mass

Signal reconstruction

- Maximise acceptance → high reco/ID efficiency down to low-p_T 6/7 GeV μ/e [ε_{event}~40/20% 4μ/4e]
- FSR γ candidate (E_T>1 GeV) added if $66<M_{12}^{\mu\mu}$ [GeV] <89 - ~4% of events
- Mass resolution 1.3/1.9% for 4μ/4e @125 GeV using Z-mass constraint on leading lepton pair

[Improved selection w.r.t last results: lepton pairing, tighter electron ID, relaxed m_{34} cut]

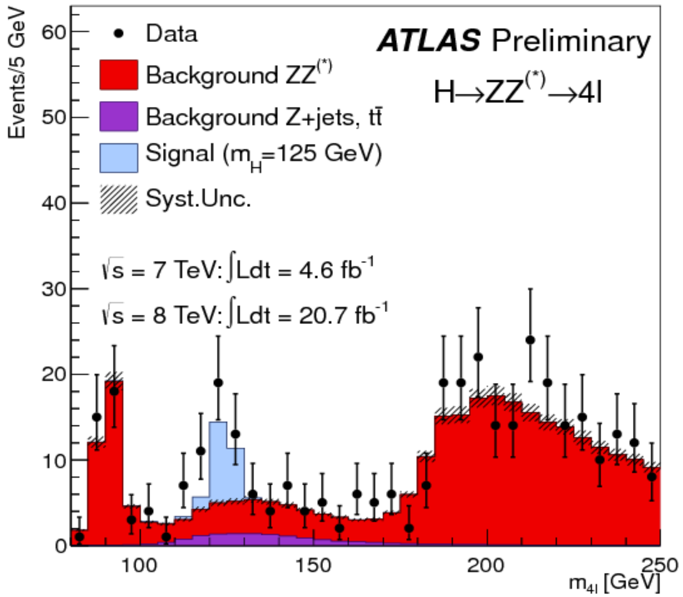

Two pairs of opposite-sign same-flavor isolated leptons

➔ In region 125±5 GeV: 32 events observed [11.1±1.3 expected from bknd & 15.9±2.1 from SM Higgs]

Background control

- Irreducible background: continuum ZZ$^{(*)}$ (from MC)
- Reducible bknd @ low mass: Z+bb/jets, ttbar

▸ reduced using isolation and impact parameter cuts

▸ measured using various background-enriched control regions in data & transfer factors from MC (+checks)

In region m_{4l}>160 GeV: 376 events observed, 348±26 expected from bknd (mainly ZZ)

Lepton energy scale & linearity and identification efficiencies (+ systematics) measured on data down to low p_T

H→ZZ$^{(*)}$→4l (l=e,μ) : Overview

ATLAS-CONF-2013-013

The golden channel, with small cross-section but very good S/B ratio and fully-reconstructed mass

Signal reconstruction

Electron reco ε measured with Z→ee

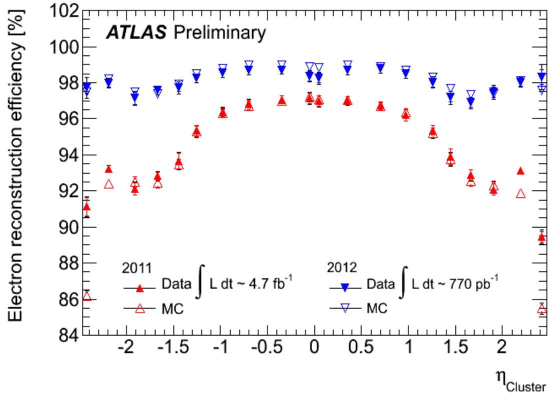

Mass resolution in 4-μ channel

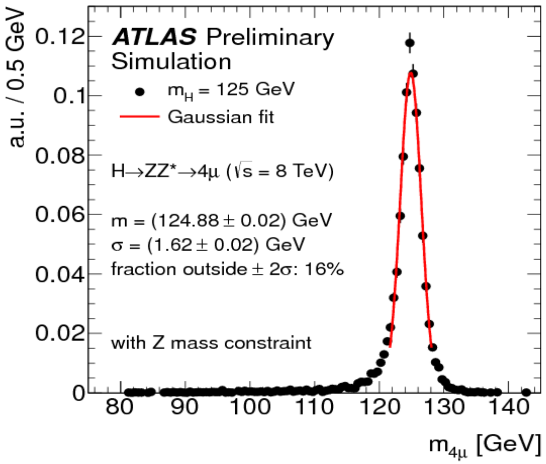

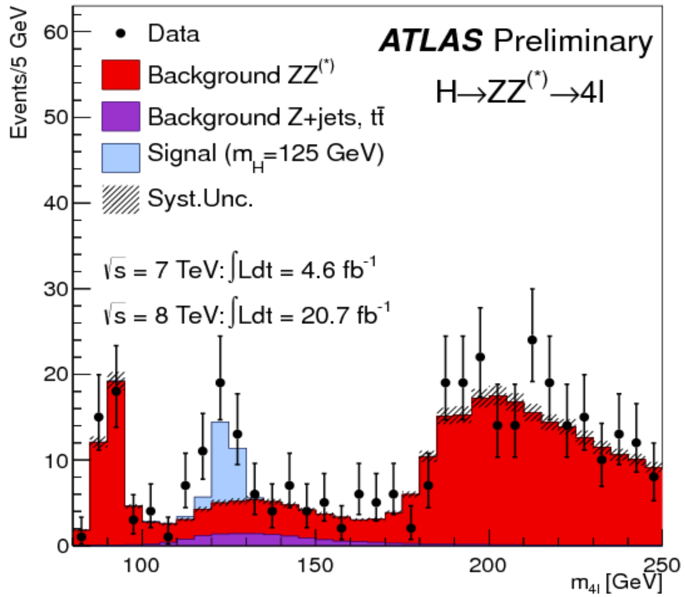

Two pairs of opposite-sign same-flavor isolated leptons

➔ In region 125±5 GeV: 32 events observed [11.1±1.3 expected from bknd & 15.9±2.1 from SM Higgs]

Background control

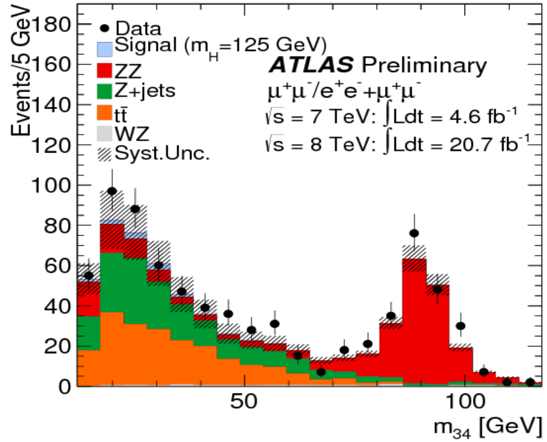

Example of control regions: no isolation nor IP cuts on softest leptons

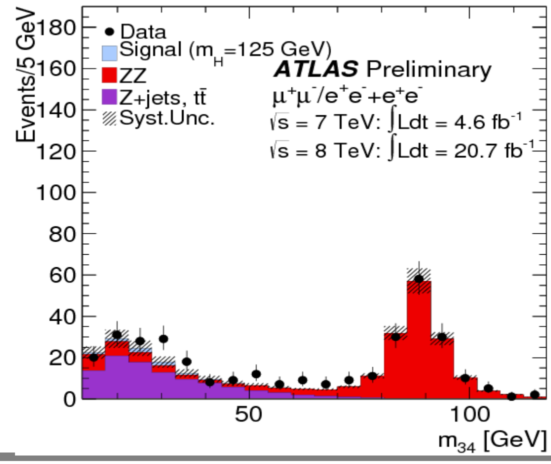

H→ZZ(*)→4l (l=e,μ) : Results

ATLAS-CONF-2013-013

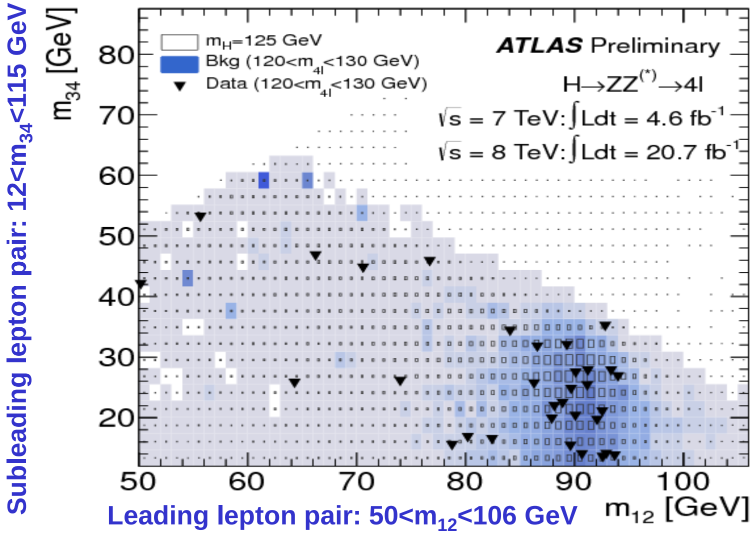

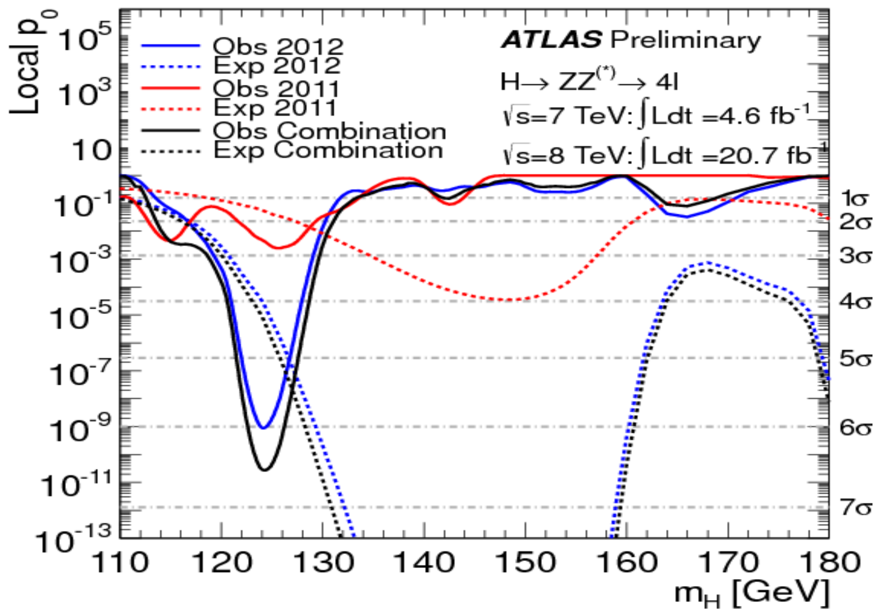

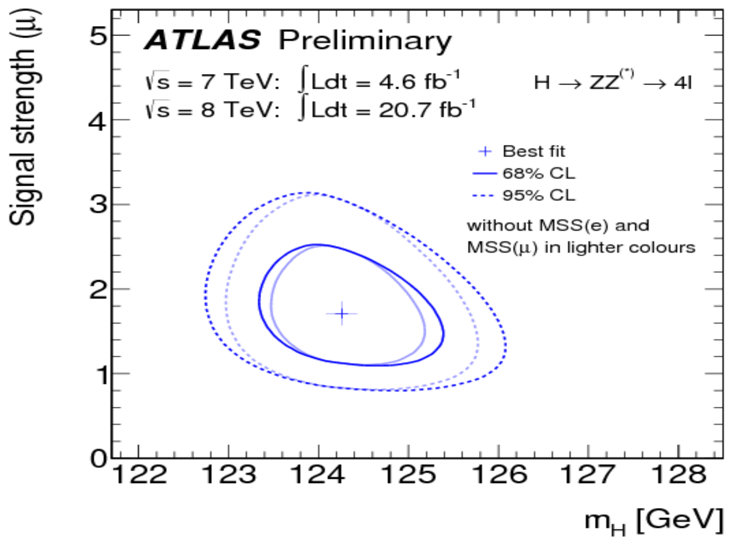

- Observed local significance of the excess: **6.6σ**
  (4.4σ expected for SM Higgs)
- Best mass fit **$124.3^{+0.6}_{-0.5}$ (stat) $^{+0.5}_{-0.3}$ (syst) GeV**
  [measurement dominated by 4μ – 0.2% systematics from p_T-scale]
- Signal strength @ this mass: **$\mu=1.7^{+0.5}_{-0.4}$**
  [@ 125.5 GeV: μ =1.5 ± 0.4]

$H \rightarrow ZZ^{(*)} \rightarrow 4l$ ($l=e,\mu$) : coupling studies

ATLAS-CONF-2013-013

- First analysis with dedicated VBF- and VH-production enriched categories
  [gauge coupling in both production and decay]

VBF category

Selection: 2 jets $|\Delta\eta_{jj}|>3$ and $m_{jj}>350$ GeV

For $m_{4l}>160$ GeV: 6 events observed, 3.8±1.3 expected from background (mainly ZZ)

In m_{4l} region 125±5 GeV: 1 event observed [0.71±0.10 expected from SM Higgs with 60% VBF purity, with S/B~5]

➔ Measurement of signal strengths for production mechanisms associated with either top (ggF+ttH) or gauge (VBF+VH) couplings

➔ Agreement with SM at <2σ level

➔ Further coupling interpretations in B. Mansoulié's talk

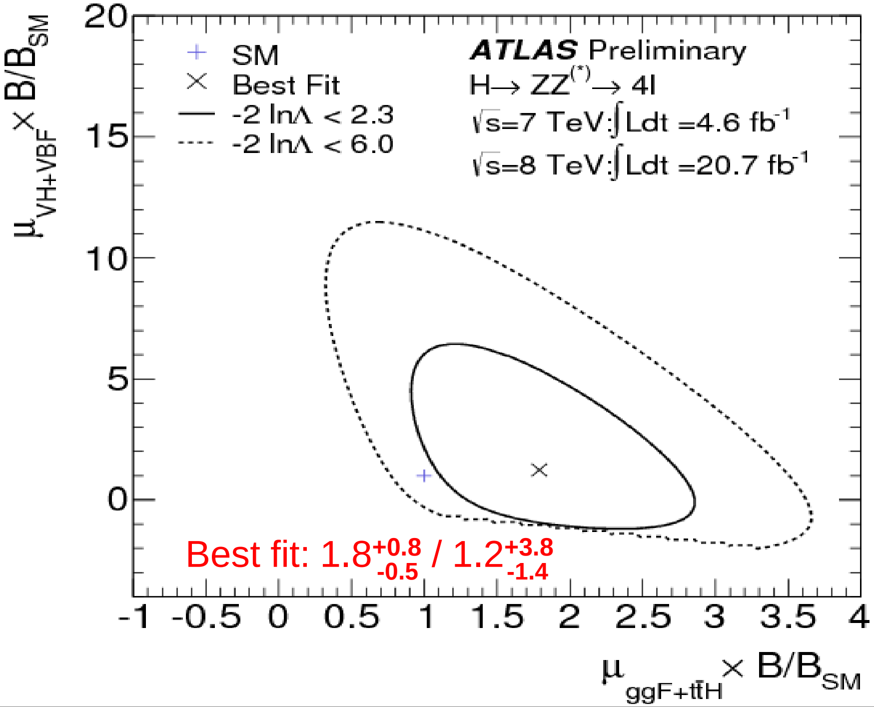

H→ZZ$^{(*)}$→4l : spin-parity studies

ATLAS-CONF-2013-013

- Discriminant combining kinematics of production and decay [5 angles, Z masses], sensitive to new boson spin/parity ➔ 43 events in region 115 GeV <m_{4l}<130 GeV are used

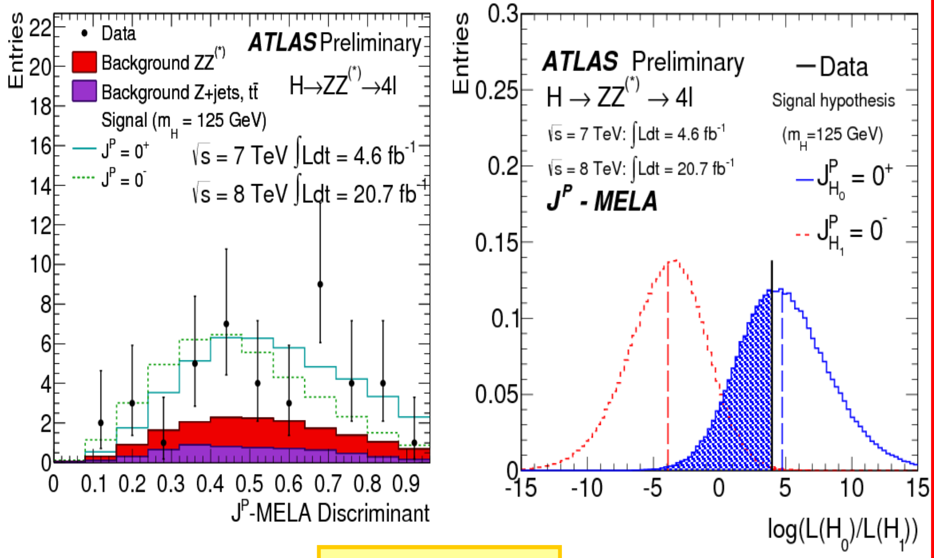

0⁺ vs 0⁻

Expected exclusion of 0^- at 3σ level
Observation fully compatible with 0^+
Observed exclusion CL_s of 0^- at 99.6%

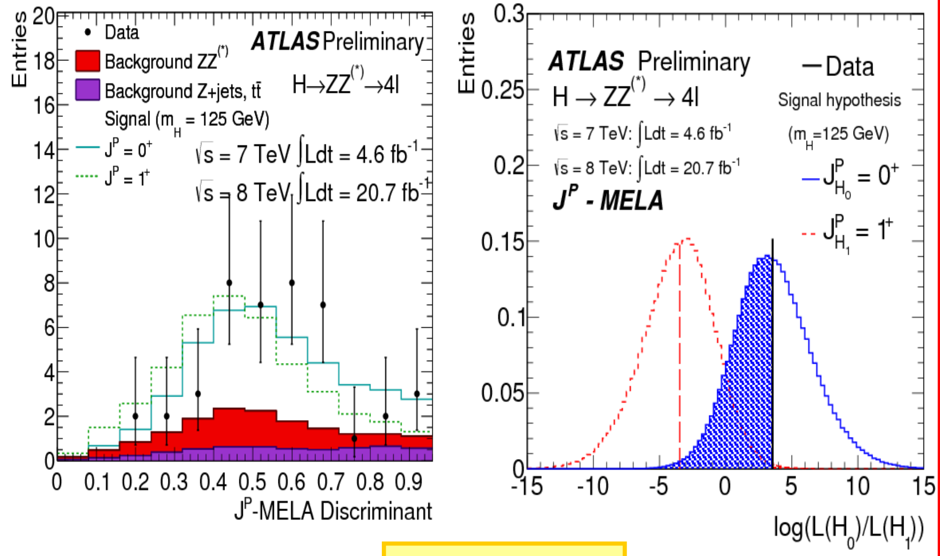

0⁺ vs 1⁺

Expected exclusion of 1^+ at 3σ level
Observation fully compatible with 0^+
Observed exclusion CL_s of 1^+ at 99.4%

Results for spin-1^- hypothesis and gg/qq admixtures for spin-2^+ production in backup

➔ 0^+ state favoured over tested hypotheses 0^-, 1^+, 1^- and 2^+

H→WW(*)→lνl'ν (l=e,μ)

ATLAS-CONF-2012-158

Results using different lepton-flavor final states with 0/1-jet and 13 fb⁻¹ of 8 TeV data

Transverse mass in Signal region

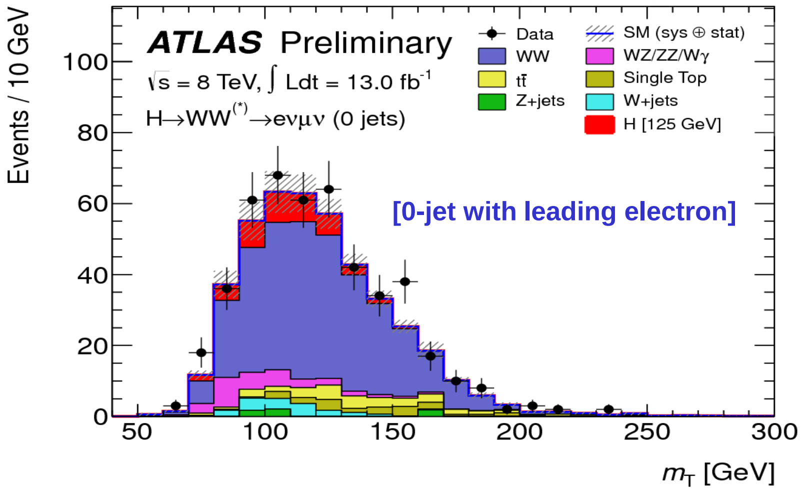

Background-subtracted data and signal MC

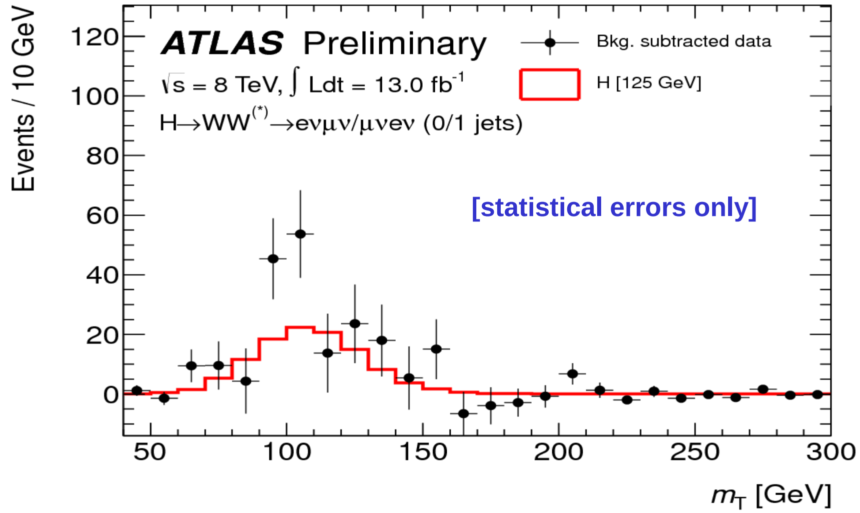

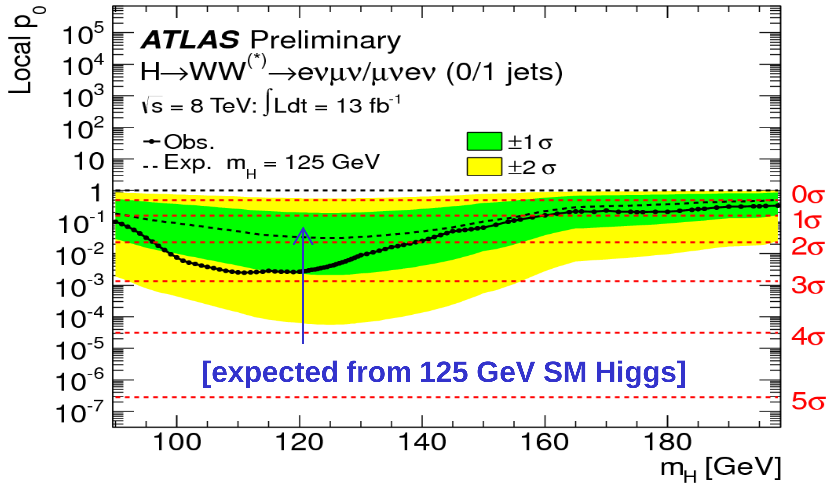

- Main backgrounds estimated from signal-free control regions in data
- Observed local significance of the broad excess @ 125 GeV: **2.6σ** (1.9σ expected for SM Higgs)
- Signal strength @ 125GeV **μ=1.5±0.6**

[dominated by systematic uncertainties]

H→Zγ : First results

ATLAS-CONF-2013-009

- Decay through loops ➔ BSM particles can affect Br(H→γγ) and Br(H→Zγ) in different ways
- In SM, σ(H→Z(ll)γ)~2 fb @125 GeV ➔ expect ~15 events in whole LHC dataset [ε_{event}~30%]
- Analysis using full 2011+2012 dataset, with event selection: 2 SF-OS isolated leptons p_T>10 GeV and $m_{ll}>m_Z$-10 GeV - 1 isolated photon E_T>15 GeV and $\Delta R_{l\gamma}$>0.3. Categories: e^+e^- / $\mu^+\mu^-$
- Main backgrounds: SM Z+γ (~82%) and Z+jets (~17%) – obtained from fit in sidebands (similar to H→γγ) of discriminating variable $\Delta m = m_{ll\gamma} - m_{ll}$ (+ data-driven checks of background composition)
- No excess observed ➔ limit at m_H=125 GeV: 18.2×SM cross section (expected 13.5×SM)

Example of Δm distribution: muon channel - 8 TeV data

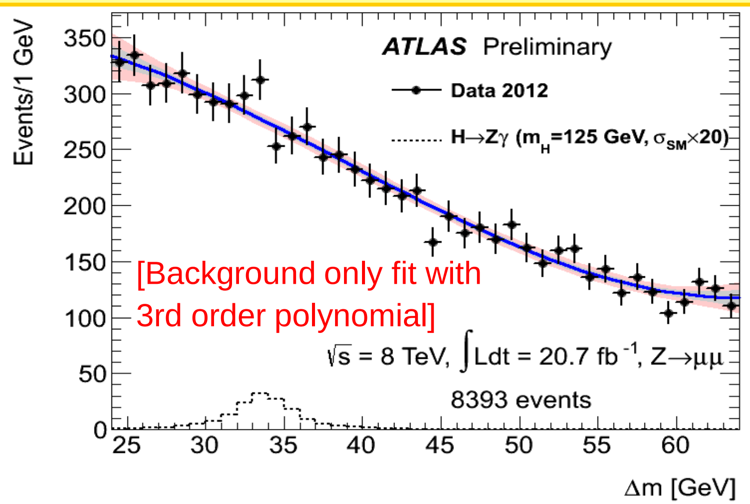

Production cross section limits

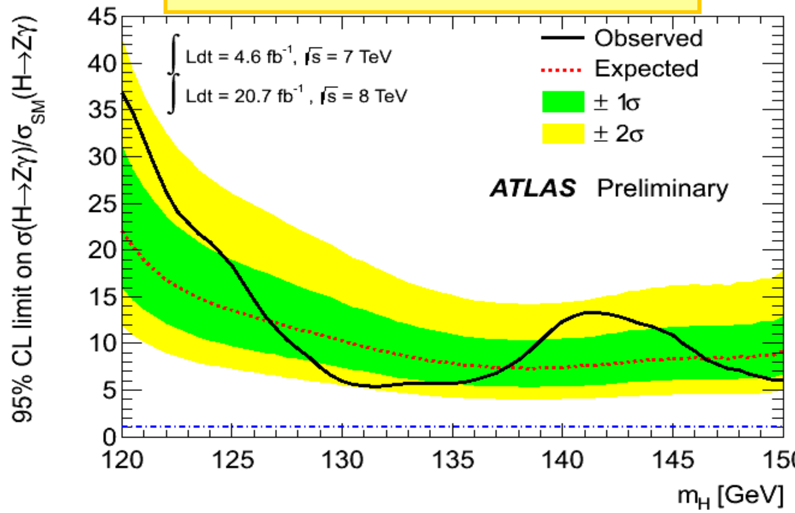

High-mass BSM Higgs searches

- Analyses published with full 2011 dataset (4.7 fb^{-1} @ $\sqrt{s}$=7 TeV) → no excess above SM

H→ZZ→llνν (l=e,μ)	H→ZZ→llqq (l=e,μ)	H→WW→lνlν (l=e,μ)	H→WW→lνqq (l=e,μ)
PLB 717 (2012) 29	PLB 717 (2012) 70	PLB 716 (2012) 62	PLB 718 (2012) 391

➔ **Need to be re-interpreted in light of the new boson discovery**

- Complement the analyses made with ZZ→4l final state at high-mass

► updated H→ZZ→4l analysis in mass range [200-1000] GeV with full LHC dataset, assuming signal with SM-like width [Complex-Pole-Scheme] ATLAS-CONF-2013-013

➔ **Upper limits on production cross section × branching ratio**

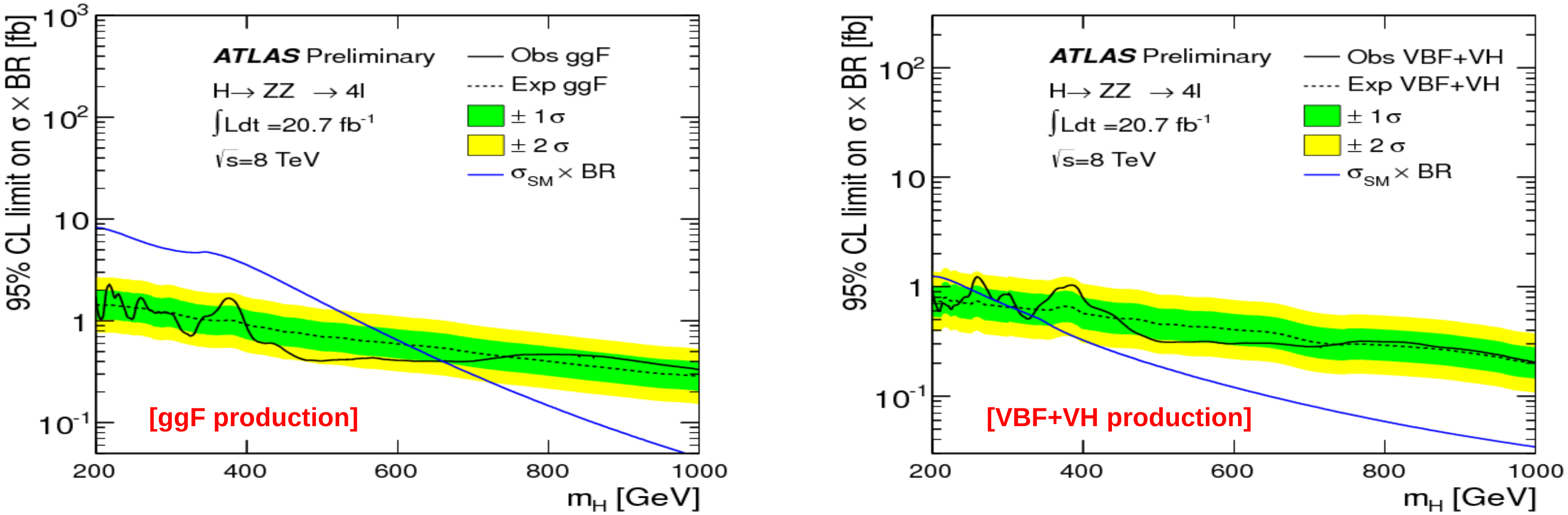

Conclusions

- **Preliminary analyses of the Higgs-like boson in $\gamma\gamma$ and $ZZ^{(*)} \rightarrow 4l$ channels with full LHC dataset** [20.7 fb^{-1} (8 TeV) + 4.7 fb^{-1} (7 TeV)] **→ refined property measurements**

  - Observation with a >6σ signal significance in both individual channels
  - Mass measurement at ~0.5% level in both channels - compatibility and combination discussed in B. Mansoulié's talk
  - Signal strengths: consistency with SM expectations within at most 2.3σ [$H \rightarrow \gamma\gamma$ channel]. Analyses reoptimised for increased sensitivity to VBF and VH production modes
  - Spin-parity: SM 0^+ state favoured over all tested hypotheses in both channels

- **Analysis in $H \rightarrow WW^{(*)} \rightarrow l\nu l\nu$ channel with 13 fb^{-1} of 8 TeV data**

- **First analysis on $H \rightarrow Z\gamma$ decay channel and high-mass searches in $H \rightarrow ZZ \rightarrow 4l$**

- **2 other ATLAS Higgs talks**
  - **Higgs to fermion pairs → Victoria Martin's talk**
  - **Channel combination → Bruno Mansouliés talk**

SPARES


~2900 authors
(1000 students)
38 countries
174 institutes
ATLAS
Collaboration

The ATLAS detector

L ~ 46 m, ∅ ~ 22 m, 7000 tons
~10^8 electronic channels

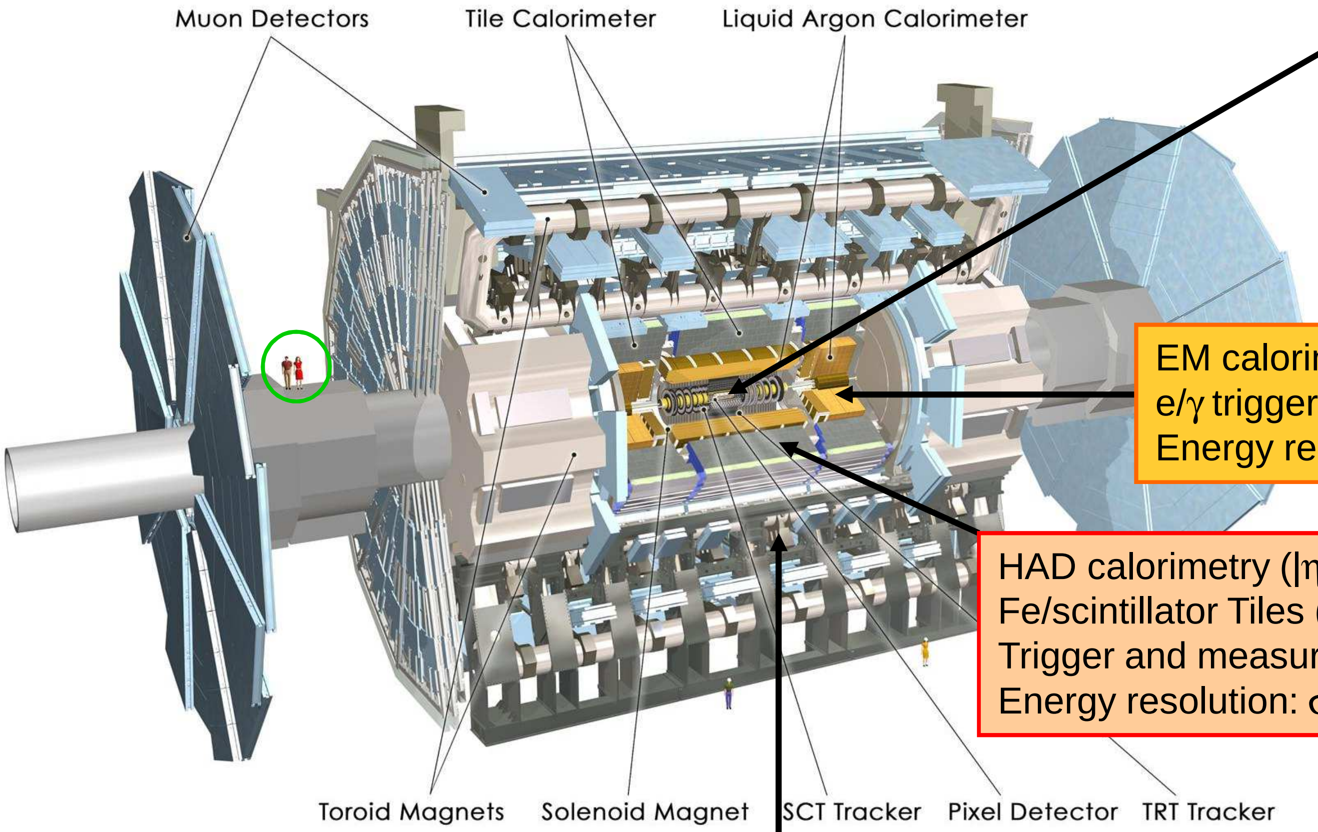

Inner Tracker ($|\eta|<2.5$, B=2T):
Si Pixels, Si strips, Transition Radiation detector (straws).
Precise tracking and vertexing, e/π separation.
Momentum resolution:
$\sigma/p_T \sim 0.04\%\ p_T\,(\mathrm{GeV}) \oplus 1.5\%$

EM calorimeter: Pb-LAr Accordion.
e/γ trigger, identification and measurement
Energy resolution: $\sigma/E \sim 10\%/\sqrt{E} \oplus 0.7\%$

HAD calorimetry ($|\eta|<5$): segmentation, hermeticity.
Fe/scintillator Tiles (central), Cu/W-LAr (forward).
Trigger and measurement of jets and missing E_T.
Energy resolution: $\sigma/E \sim 50\%/\sqrt{E} \oplus 3\%$

Muon Spectrometer ($|\eta|<2.7$) : air-core toroids with gas-based muon chambers.
Muon trigger and measurement with momentum resolution < 10% up to $E_\mu \sim 1$ TeV

3-level trigger reducing the rate from 40 MHz to ~200 Hz

Trigger

- Optimization of selections (e.g. object isolation) to maintain low un-prescaled thresholds (e.g. for inclusive leptons) in spite of higher luminosity and pile-up than in 2011
- Pile-up robust algorithms developed (~flat performance vs pile-up, minimize CPU usage, ...)

→ Results from 2012 operation show trigger is coping very well (in terms of rates, efficiencies, robustness, ..) with harsh conditions while meeting physics requirements

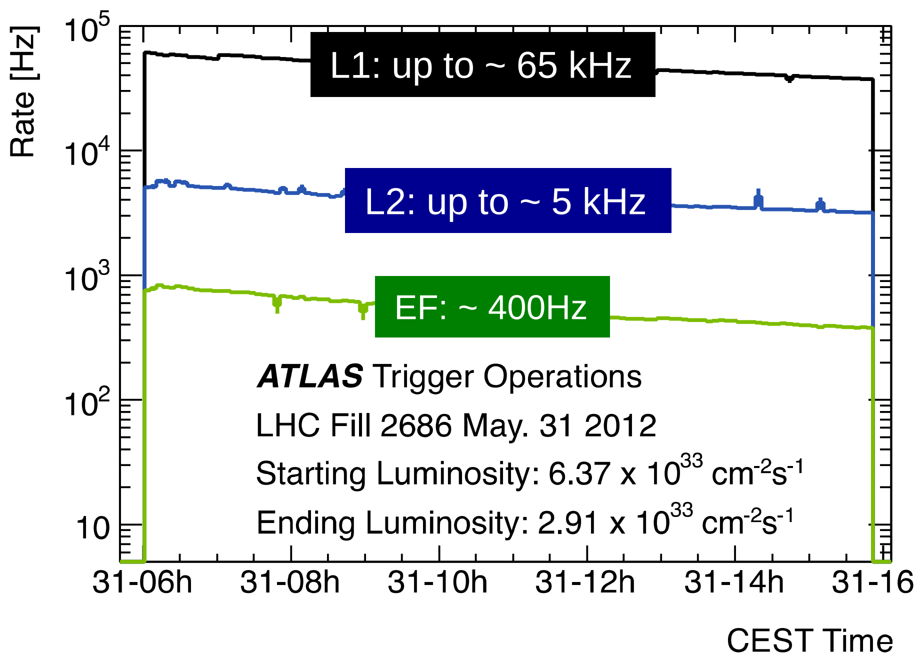

Note: ~ 500 items in trigger menu

Lowest un-prescaled thresholds (examples)

Item	p_T threshold (GeV)	Rate (Hz) 5×10^{33}
Incl. e	24	70
Incl. μ	24	45
ee	12	8
μμ	13	5
ττ	29,20	12
γγ	35,25	10
E_T^{miss}	80	17

Managed to keep inclusive un-prescaled lepton thresholds within ~ 5 GeV over last two years in spite factor ~ 70 peak lumi increase

Spin-2 model

Spin 2 model for X→VV:

$$
\begin{aligned}
A(X \to VV) = \Lambda^{-1} \Big[& 2g_1 t_{\mu\nu} f^{*1,\mu\alpha} f^{*2,\nu\alpha} + 2g_2 t_{\mu\nu} \frac{q_\alpha q_\beta}{\Lambda^2} f^{*1,\mu\alpha} f^{*2,\nu\alpha} \\
& + g_3 \frac{\tilde{q}^\beta \tilde{q}^\alpha}{\Lambda^2} t_{\beta\nu} (f^{*1,\mu\nu} f^{*2}_{\mu\alpha} + f^{*2,\mu\nu} f^{*1}_{\mu\alpha}) + g_4 \frac{\tilde{q}^\nu \tilde{q}^\mu}{\Lambda^2} t_{\mu\nu} f^{*1,\alpha\beta} f^{*(2)}_{\alpha\beta} \\
& + m_V^2 \left(2g_5 t_{\mu\nu} \epsilon_1^{*\mu} \epsilon_2^{*\nu} + 2g_6 \frac{\tilde{q}^\mu q_\alpha}{\Lambda^2} t_{\mu\nu} (\epsilon_1^{*\nu} \epsilon_2^{*\alpha} - \epsilon_1^{*\alpha} \epsilon_2^{*\nu}) + g_7 \frac{\tilde{q}^\mu \tilde{q}^\nu}{\Lambda^2} t_{\mu\nu} \epsilon_1^* \epsilon_2^* \right) \\
& + g_8 \frac{\tilde{q}_\mu \tilde{q}_\nu}{\Lambda^2} t_{\mu\nu} f^{*1,\alpha\beta} \tilde{f}^{*(2)}_{\alpha\beta} + g_9 t_{\mu\alpha} \tilde{q}^\alpha \epsilon_{\mu\nu\rho\sigma} \epsilon_1^{*\nu} \epsilon_2^{*\rho} q^\sigma \\
& + \frac{g_{10} t_{\mu\alpha} \tilde{q}^\alpha}{\Lambda^2} \epsilon_{\mu\nu\rho\sigma} q^\rho \tilde{q}^\sigma (\epsilon_1^{*\nu} (q\epsilon_2^*) + \epsilon_2^{*\nu} (q\epsilon_1^*)) \Big],
\end{aligned}
$$

General interaction of spin-2 particle with gauge bosons pair has 10 independent tensor couplings

- Excluding generic spin-2 model is impossible at this stage
- Start with model with minimal couplings (g1=g5=1)
- Two production modes allowed: gg and qqbar
- Study 5 different gg fractions from 0% to 100%

Uncertainties on mass measurements

$H \rightarrow \gamma\gamma$ mass systematic uncertainties

Absolute energy scale **from Z→ee**	0.3%
Uncertainties on upstream material simulation	0.3%
Pre-sampler energy scale	0.1%
Non-linearity of EM calo electronics	0.15%
Conversion fraction	0.1%
Relative calibration of first and second sampling	0.2%
Lateral leakage corrections	0.1%

+other smaller effects
Total systematic error is 0.55% (0.7 GeV)

4l mass measurement
dominated by the 4μ channel

Muon momentum scale	0.2%
Electron energy scale (4e)	0.4%
Low E_T electrons	0.1%

Possible local detector biases checked event by event

ID and MS measurements also checked separately

$H \rightarrow \gamma\gamma$

$\sigma \times BR \sim 50$ fb for $m_H \sim 125$ GeV

H→γγ : photon reco / identification

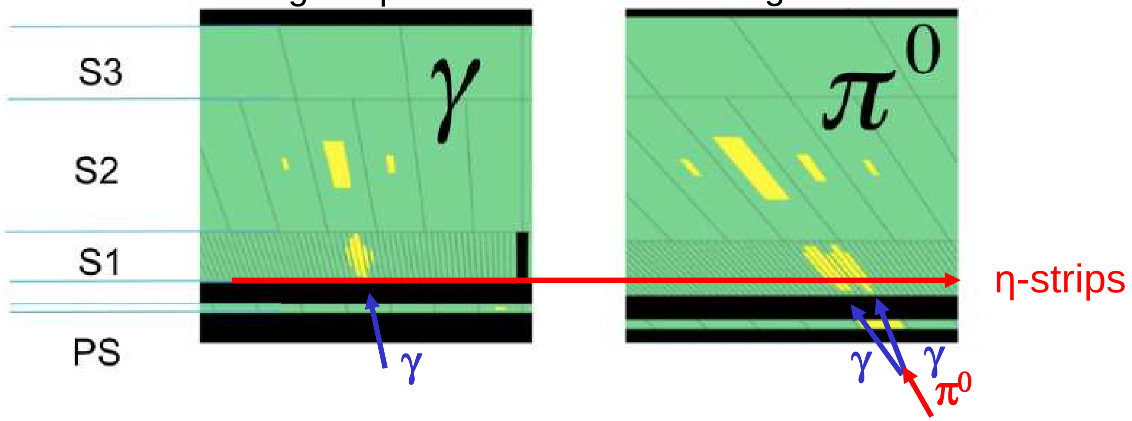

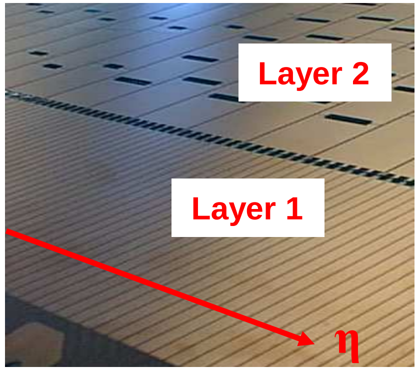

Identification efficiency (unconverted photons) vs pile-up

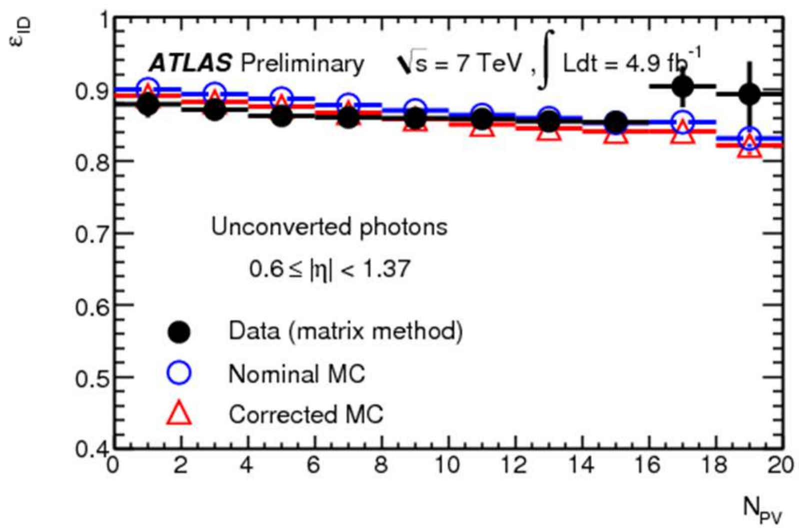

Fraction of converted photons vs pile-up

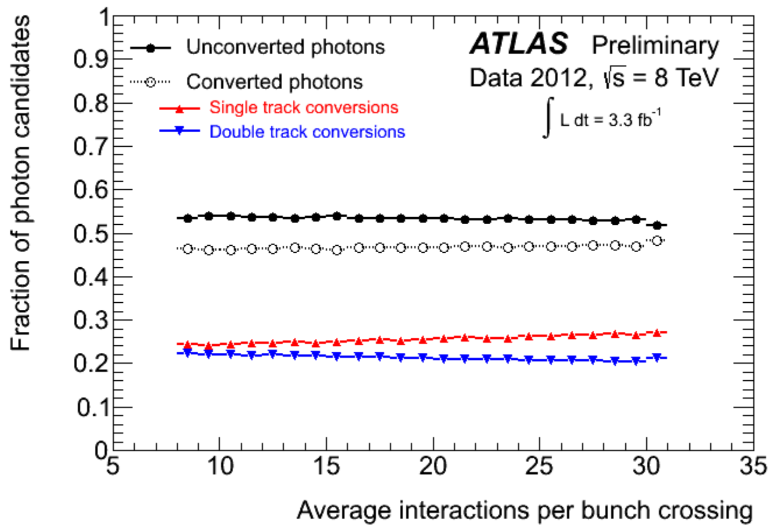

H→γγ : background rejection

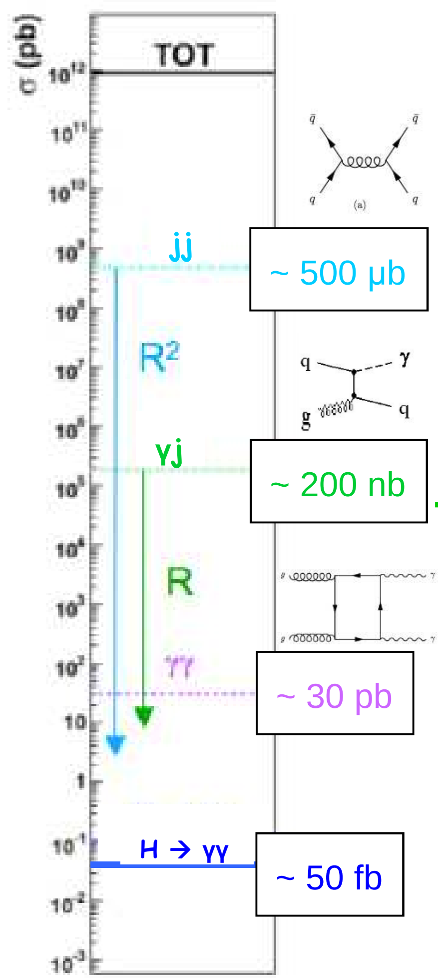

Data-driven background decomposition

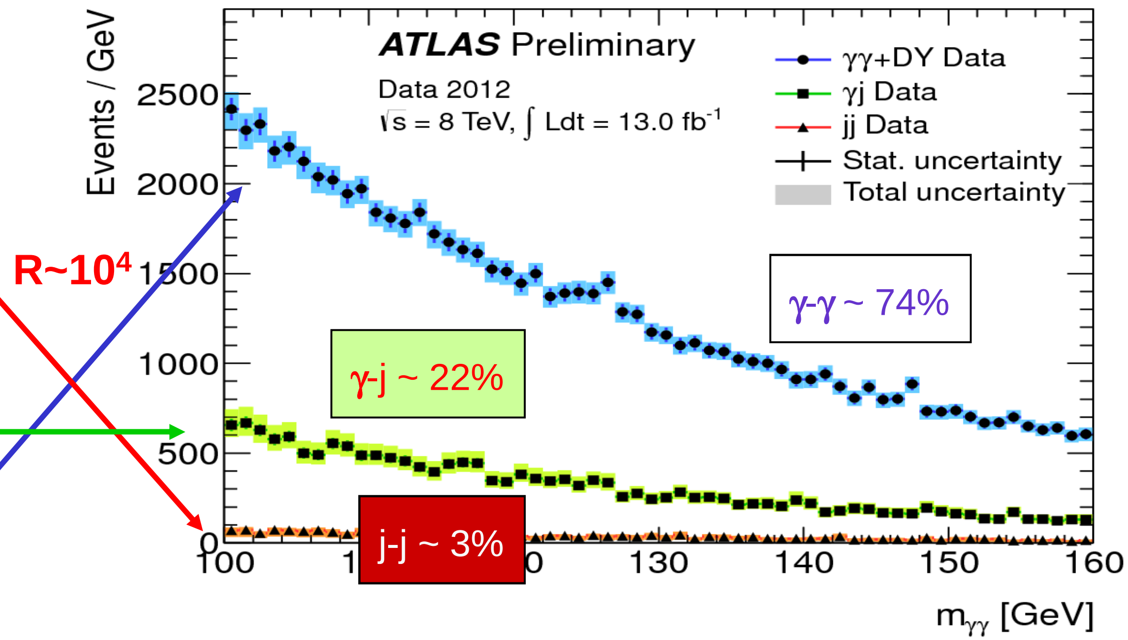

➔ Reducible background γ-jet and jet-jet largely below irreducible background γ-γ

► Remark 1: this decomposition is not directly used in the Higgs search: the background is extrapolated from data sidebands

► Remark 2: Drell-Yan ~negligible for $m_{\gamma\gamma}$>100 GeV (~1%)

Background decomposition (2D sidebands extension)

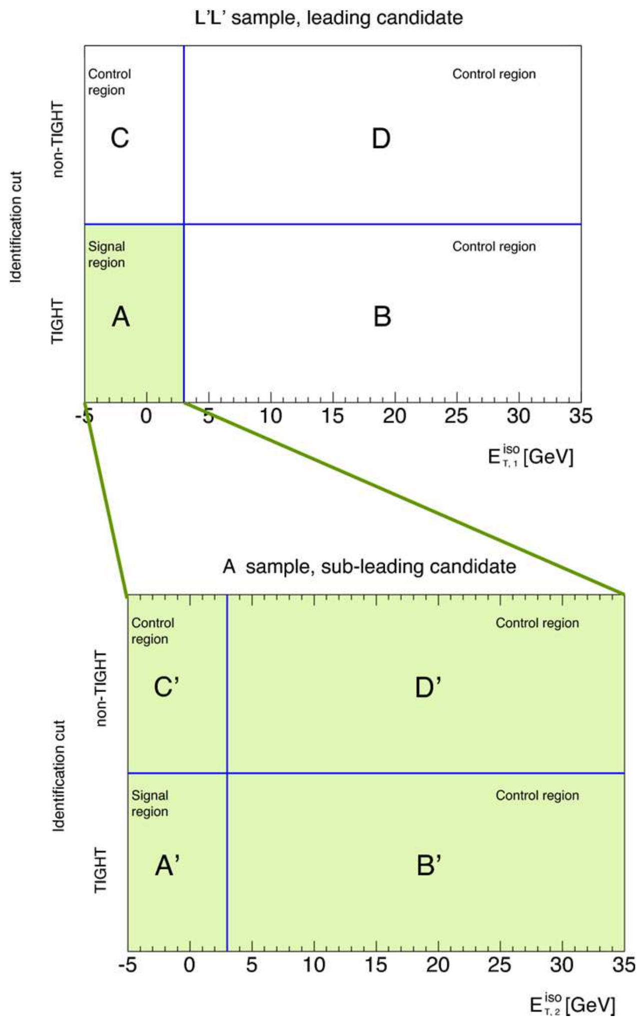

Extend the 2D sidebands method to the case of 2 photon candidates :

- preselect events with 2 candidates passing a loose photon definition.
- As for the inclusive analysis the number of signal candidates in region A of the first matrix is

$$N_A^{\mathrm{sig}} = N_A - \left[(N_B - c_1 N_A^{\mathrm{sig}}) \frac{N_C - c_2 N_A^{\mathrm{sig}}}{N_D - c_1 c_2 N_A^{\mathrm{sig}}} \right] R^{\mathrm{bkg}}$$

- For events with the leading candidates in A region a second 2D matrix is used for the second candidate
- After a bit of algebra (α has to be taken from MC while the other parameters from data)

$$N_{\gamma\gamma}^{\mathbf{TITI}} = \frac{\epsilon' \left(\alpha f' N_A^{\mathrm{sig}} + (\alpha - 1) N_A'^{\,\mathrm{sig}} \right)}{(\alpha - 1)\epsilon' + \alpha f'}$$

H→γγ : background modelling

- **Choice of analytical functional form to describe background per category**
  - Based on high-stat MC samples → Signal+background fit to background $m_{\gamma\gamma}$ spectrum
  - Accept model if fitted number of signal events is <10% of expected signal or <20% of the background statistical uncertainty
  - Among model left, choose the one with smallest number of degrees of freedom
  - Normalisation and parameter sets left free in final fit to $m_{\gamma\gamma}$ distribution
  - Systematic uncertainty on background model = largest absolute signal component fitted anywhere in full mass range 100-150 GeV

Table 4: Systematic uncertainty on the number of fitted signal events due to the background model for the $\sqrt{s}$ = 7 TeV (10 categories) and $\sqrt{s}$ = 8 TeV (14 categories) analyses. Three different background models are used depending on the category; an exponential function, a fourth order polynomial and the exponential of a second order polynomial.

Category	Parametrisation	Uncertainty [N_{evt}] $\sqrt{s}$ = 7 TeV	Uncertainty [N_{evt}] $\sqrt{s}$ = 8 TeV
Inclusive	4th order pol.	7.3	12.0
Unconverted central, low p_{Tt}	Exp. of 2nd order pol.	2.1	4.6
Unconverted central, high p_{Tt}	Exponential	0.2	0.8
Unconverted rest, low p_{Tt}	4th order pol.	2.2	11.4
Unconverted rest, high p_{Tt}	Exponential	0.5	2.0
Converted central, low p_{Tt}	Exp. of 2nd order pol.	1.6	2.4
Converted central, high p_{Tt}	Exponential	0.3	0.8
Converted rest, low p_{Tt}	4th order pol.	4.6	8.0
Converted rest, high p_{Tt}	Exponential	0.5	1.1
Converted transition	Exp. of 2nd order pol.	3.2	9.1
Loose high-mass two-jet	Exponential	0.4	1.1
Tight high-mass two-jet	Exponential	-	0.3
Low-mass two-jet	Exponential	-	0.6
E_T^{miss} significance	Exponential	-	0.1
One-lepton	Exponential	-	0.3

Calorimeter pointing

Use 2 layers from calo to reconstruct γ direction

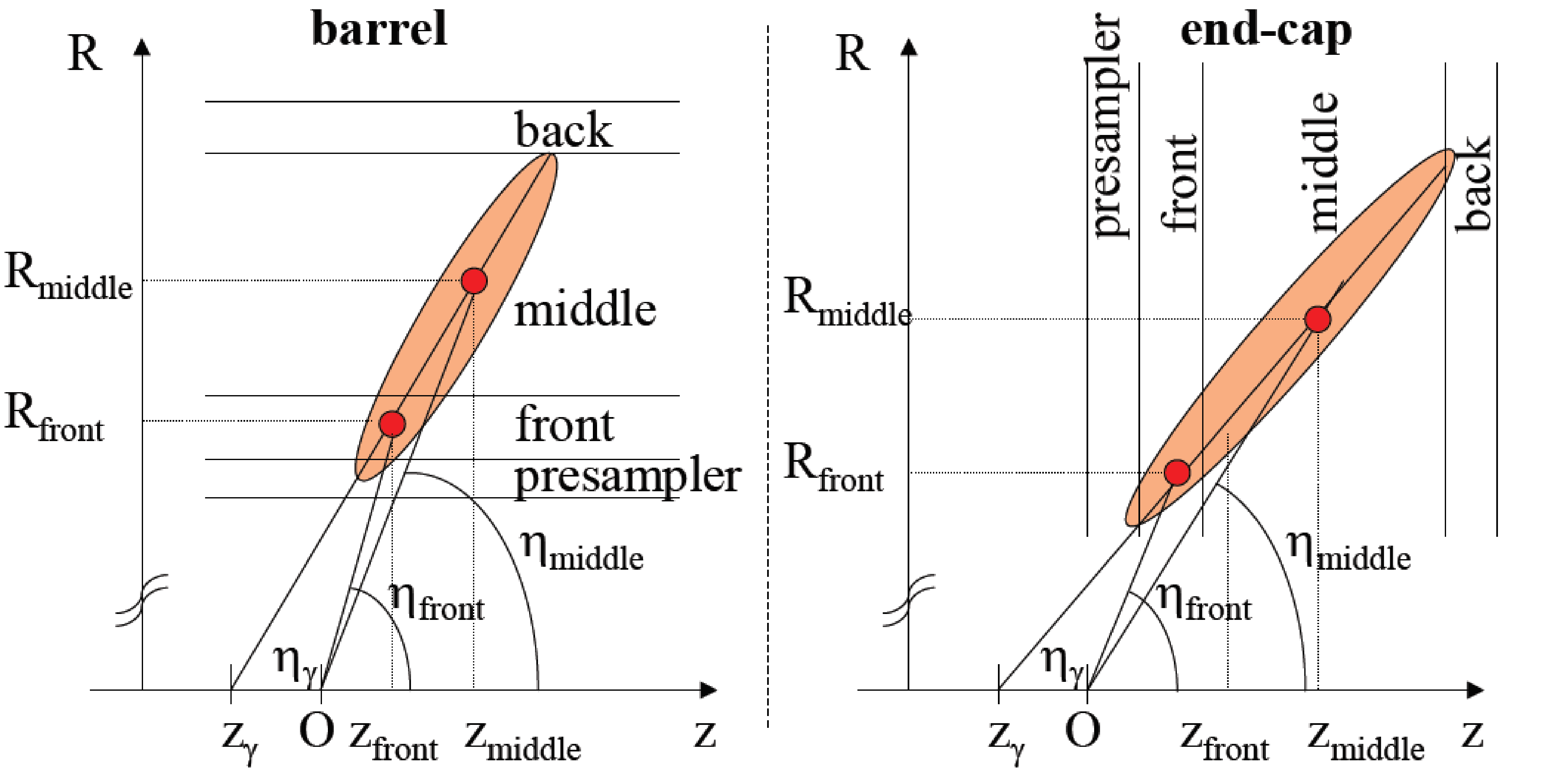

$H \rightarrow \gamma\gamma$: mass resolution

$m^2_{\gamma\gamma} = 2 E_1 E_2 (1-\cos\theta)$

- **Precise location of di-photon primary vertex necessary**
  - For invariant mass reconstruction and computation of track-based quantities (e.g. isolation, jet selection for VBF category to associate jets from hard scattering)
  - Calo pointing alone allows to reduce uncertainty on vertex position to 1.5 cm and makes angle contribution to mass resolution negligible. It is pile-up robust
  - NN-based diphoton vertex selection, combining photon pointing, position of conversion vertex (if any), Σp_T^2, Σp_T, $\Delta\Phi(\Sigma \vec{p}_T, \gamma\gamma)$

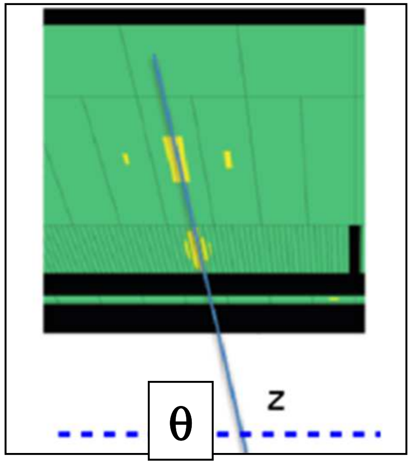

Z(vertex) measurement with calo pointing for γ–γ events

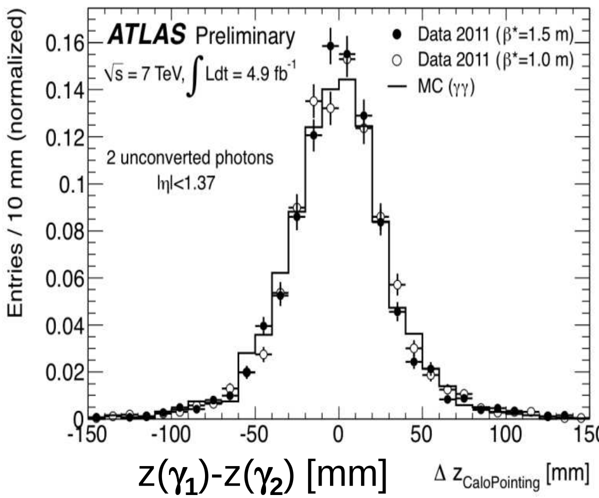

Efficiency to select PV within $|\Delta z|<0.2$ mm from truth

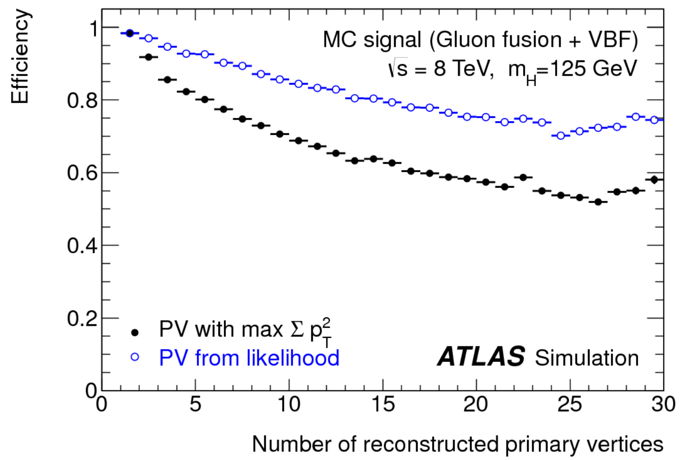

$H \rightarrow \gamma\gamma$: categorisation

14 exclusive categories:

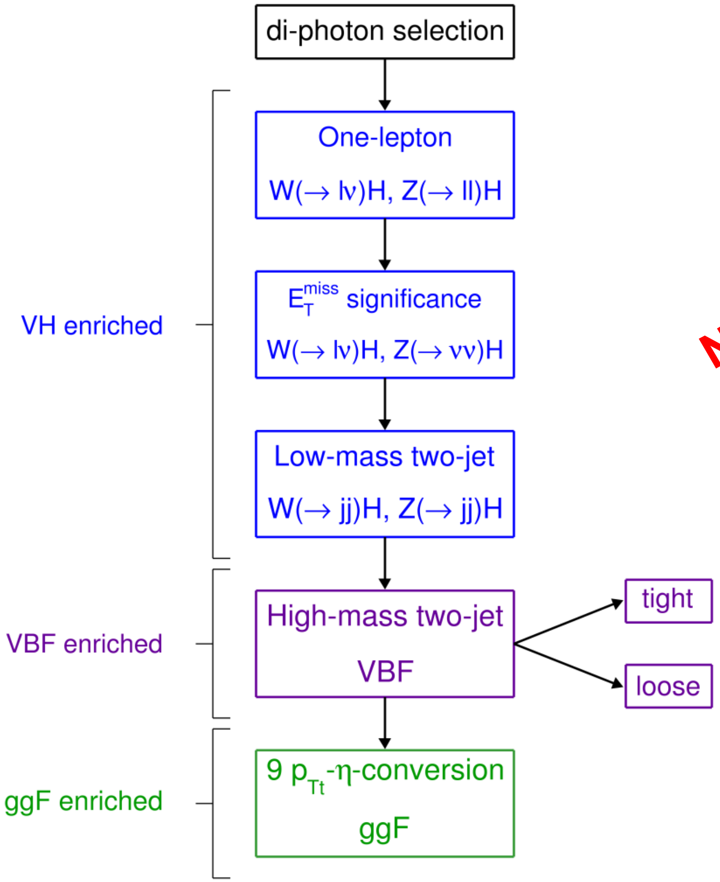

- 1 isolated muon/electron p_T>10/15 GeV
- !(84<$m_{e\gamma}$<94 GeV) ($Z \rightarrow ee\gamma$ bknd)

New

- Missing E_T significance $\frac{E_T^{miss}}{0.67 \times \Sigma E_T} > 5$

- 60<m_{jj}<110 GeV and $|\Delta\eta_{jj}|$<3.5
- p_{Tt}>70 GeV and $|\eta_{\gamma\gamma}-\eta_{jj}|$<1

New

See next to next slide

See next slide

H→γγ : categorisation

Both unconverted:

- Central
- Rest

At least one converted:

- Central
- Transition
- Rest

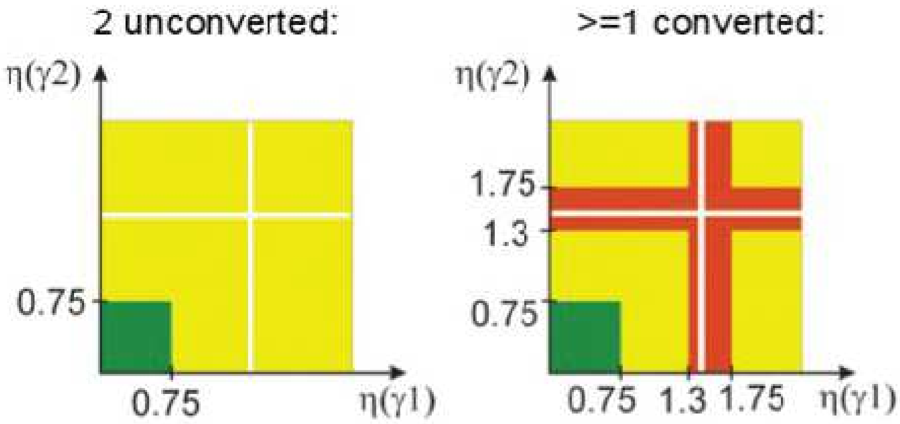

Resolution:

Good
Medium
Poor

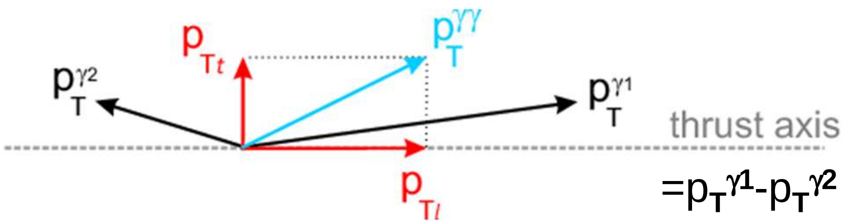

$=p_T^{\gamma 1}-p_T^{\gamma 2}$

Variable p_{Tt} is strongly correlated with diphoton p_T but has better detector resolution and retains a monotically falling invariant mass for background

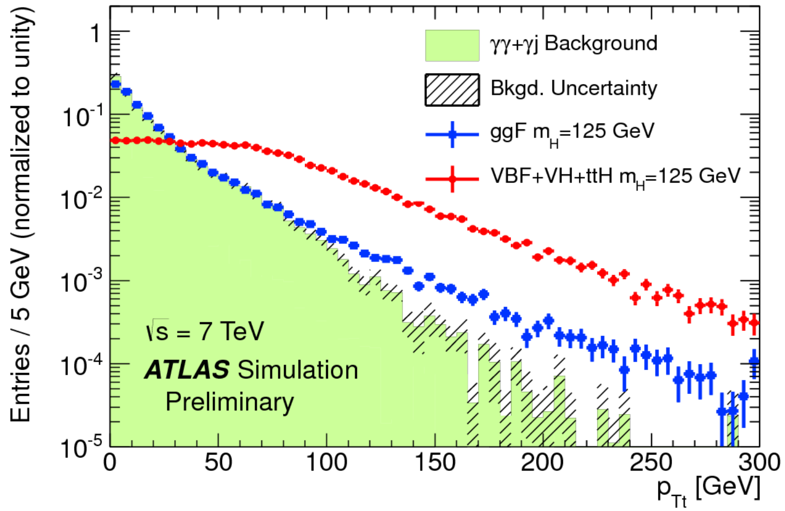

H→γγ : VBF category

❑ BDT using following 8 variables

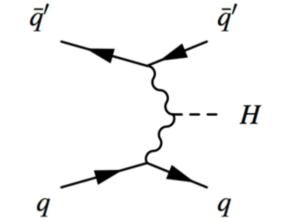

- 2 jets with p_T>25-30 GeV, |η|<4.5 and |JVF|*>0.25 (for |η|<2.4)
  → Leading jet eta, sub-leading jet eta, $|\Delta\eta_{jj}|$, m_{jj} ,diphoton p_{Tt}
  → $\Delta\varphi(\gamma\gamma;jj)$, $\eta^* = |\eta_{\gamma\gamma} - (\eta_{j1}+\eta_{j2})/2|$ = diphoton η in frame of tagging jets
  → ΔRmin: minimal ΔR between leading/subleading photon and leading/subleading jet
- BDT trained to optimise separation between signal (VBF) and background (γγ, γj, jj) – γγ from SHERPA MC and γj+jj from data with one or both photon(s) not isolated
- 2 categories defined from BDT output, maximising VBF signal significance
- Check of BDT output with data sidebands and with high statistics Z→ee+jet sample
- Check that no correlation with $m_{\gamma\gamma}$ → mass spectrum steeply falling after BDT cuts
- Main systematics from ggF+2 jets QCD scale uncertainty (48%/28%)

❑ Previous analysis was cut-based

- $|\Delta\eta_{jj}|$>2.8, m_{jj}>400 GeV and $\Delta\varphi(\gamma\gamma;jj)$>2.6

* Jet-vertex fraction: sum of the p_T carried by tracks in the jet and associated to selected vertex divided by the total p_T carried by all tracks associated to the jet

$$\mathrm{JVF}(\mathrm{jet}_i, \mathrm{PV}_j) = \frac{\sum_k p_\mathrm{T}(\mathrm{track}_k^{\mathrm{jet}_i}, \mathrm{PV}_j)}{\sum_n \sum_l p_\mathrm{T}(\mathrm{track}_l^{\mathrm{jet}_i}, \mathrm{PV}_n)}$$

H→γγ : VBF category

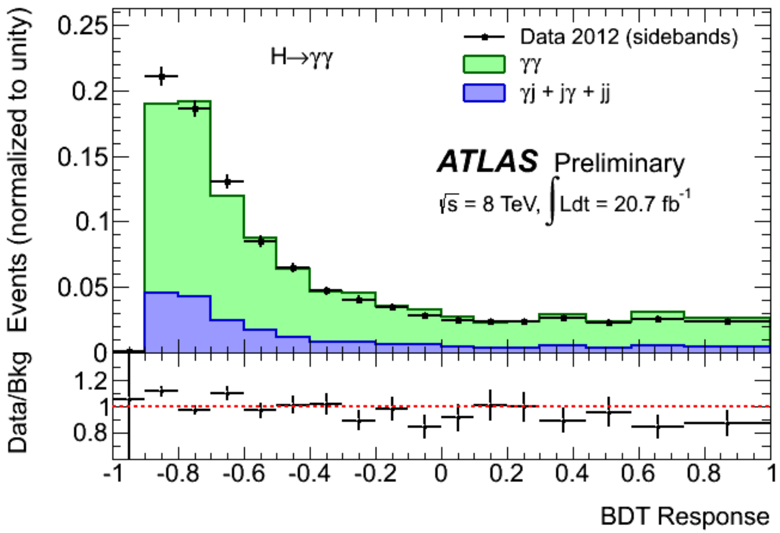

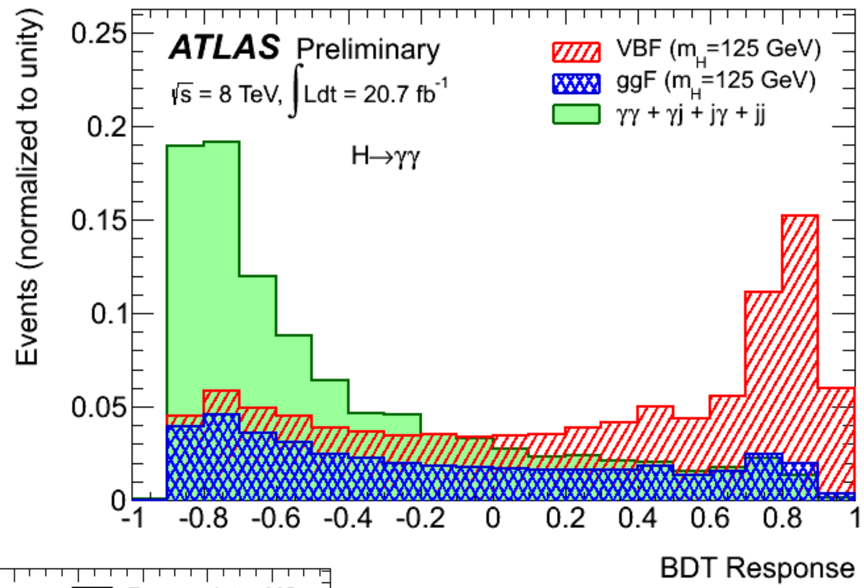

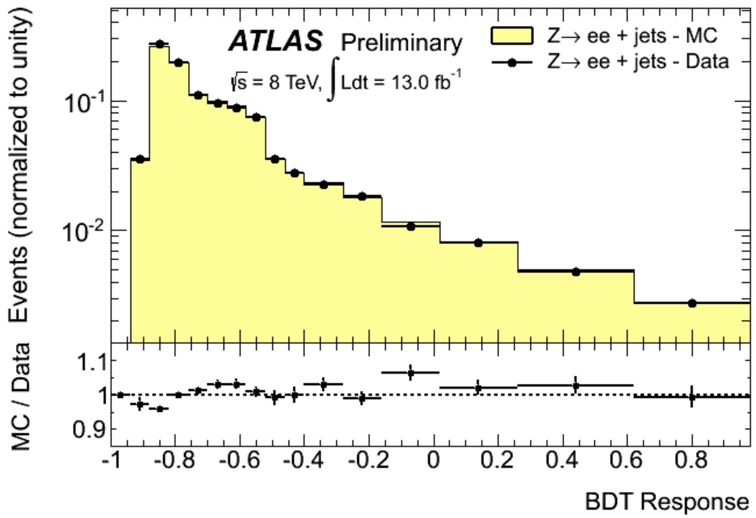

H→γγ : categorisation

Table 1: Number of events in the data (N_D) and expected number of SM Higgs signal events (N_S) for m_H = 126.5 GeV from the $H \to \gamma\gamma$ analysis, for each category in the mass range 100-160 GeV at $\sqrt{s}$ = 8 TeV. Numbers for the 7 TeV analysis can be found in Ref. [4]. The statistical uncertainties in N_S are less than 1%. The fractions of expected signal events from the $gg \to H$, VBF, WH, ZH, ttH processes are detailed.

$\sqrt{s}$	8 TeV						
Category	N_D	N_S	$gg \to H$ [%]	VBF [%]	WH [%]	ZH [%]	ttH [%]
Unconv. central, low p_{Tt}	10900	51.8	93.7	4.0	1.4	0.8	0.2
Unconv. central, high p_{Tt}	553	7.9	79.3	12.6	4.1	2.5	1.4
Unconv. rest, low p_{Tt}	41236	107.9	93.2	4.0	1.6	1.0	0.1
Unconv. rest, high p_{Tt}	2558	16.0	78.1	13.3	4.7	2.8	1.1
Conv. central, low p_{Tt}	7109	33.1	93.6	4.0	1.3	0.9	0.2
Conv. central, high p_{Tt}	363	5.1	78.9	12.6	4.3	2.7	1.5
Conv. rest, low p_{Tt}	38156	97.8	93.2	4.1	1.6	1.0	0.1
Conv. rest, high p_{Tt}	2360	14.4	77.7	13.0	5.2	3.0	1.1
Conv. transition	14864	40.1	90.7	5.5	2.2	1.3	0.2
Loose high-mass two-jet	276	5.3	45.0	54.1	0.5	0.3	0.1
Tight high-mass two-jet	136	8.1	23.8	76.0	0.1	0.1	0.0
Low-mass two-jet	210	3.3	48.1	3.0	29.7	17.2	1.9
E_T^{miss} significance	49	1.3	4.1	0.5	35.7	47.6	12.1
One-lepton	123	2.9	2.2	0.6	63.2	15.4	18.6
All categories (inclusive)	118893	395.0	88.0	7.3	2.7	1.5	0.5

H→γγ : categorisation

Table 2: Signal mass resolution (σ_{CB}), number of observed events, number of expected signal events (N_S), number of expected background events (N_B) and signal to background ratio (N_S/N_B) in a mass window around m_H = 126.5 GeV containing 90% of the expected signal for each of the 14 categories of the 8 TeV data analysis. The numbers of background events are obtained from the background + signal fit to the $m_{\gamma\gamma}$ data distribution.

$\sqrt{s}$	8 TeV				
Category	σ_{CB}(GeV)	Observed	N_S	N_B	N_S/N_B
Unconv. central, low p_{Tt}	1.50	911	46.6	881	0.05
Unconv. central, high p_{Tt}	1.40	49	7.1	44	0.16
Unconv. rest, low p_{Tt}	1.74	4611	97.1	4347	0.02
Unconv. rest, high p_{Tt}	1.69	292	14.4	247	0.06
Conv. central, low p_{Tt}	1.68	722	29.8	687	0.04
Conv. central, high p_{Tt}	1.54	39	4.6	31	0.15
Conv. rest, low p_{Tt}	2.01	4865	88.0	4657	0.02
Conv. rest, high p_{Tt}	1.87	276	12.9	266	0.05
Conv. transition	2.52	2554	36.1	2499	0.01
Loose High-mass two-jet	1.71	40	4.8	28	0.17
Tight High-mass two-jet	1.64	24	7.3	13	0.57
Low-mass two-jet	1.62	21	3.0	21	0.14
E_T^{miss} significance	1.74	8	1.1	4	0.24
One-lepton	1.75	19	2.6	12	0.20
Inclusive	1.77	14025	355.5	13280	0.03

H→γγ : categorisation

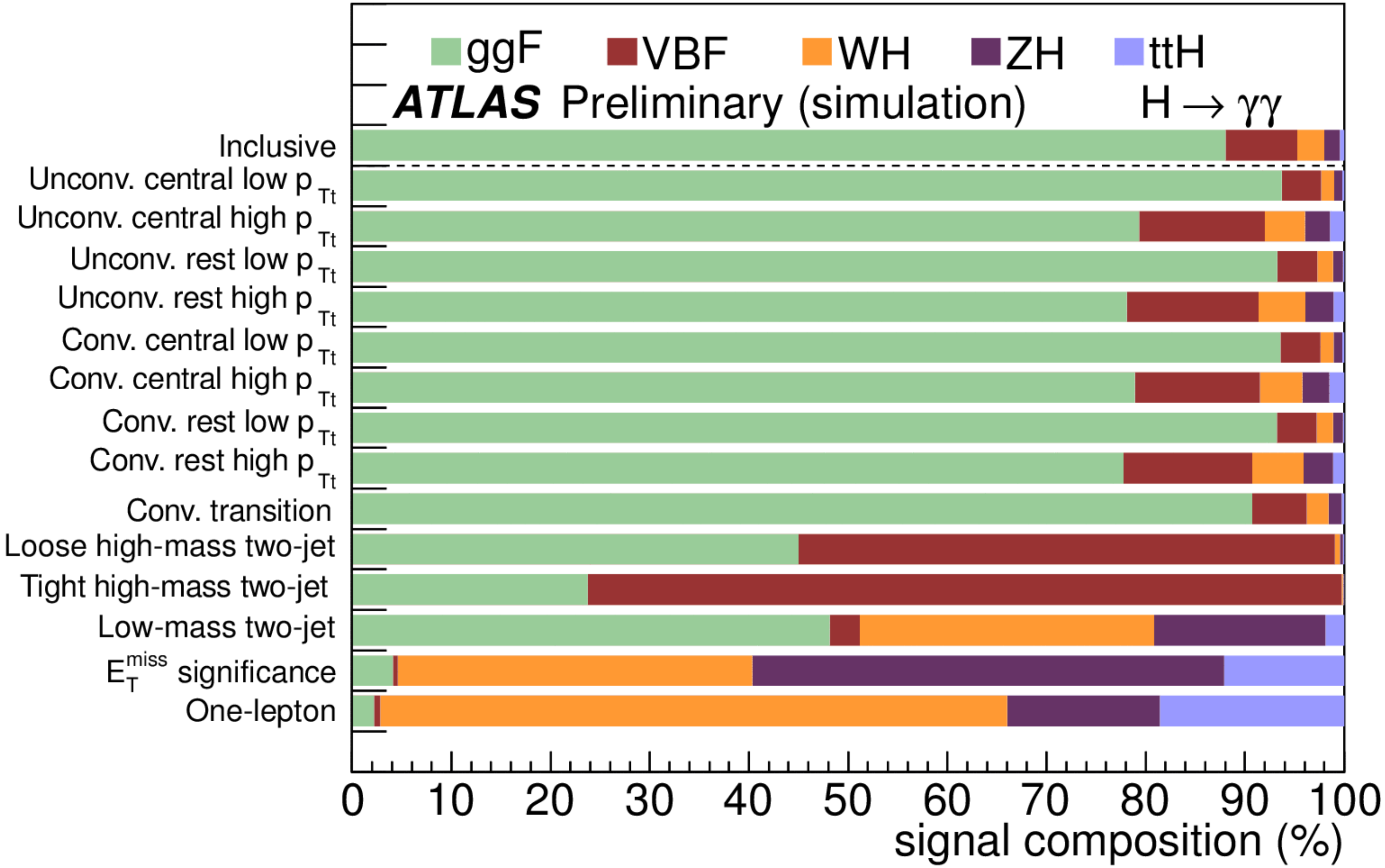

H→γγ : Results

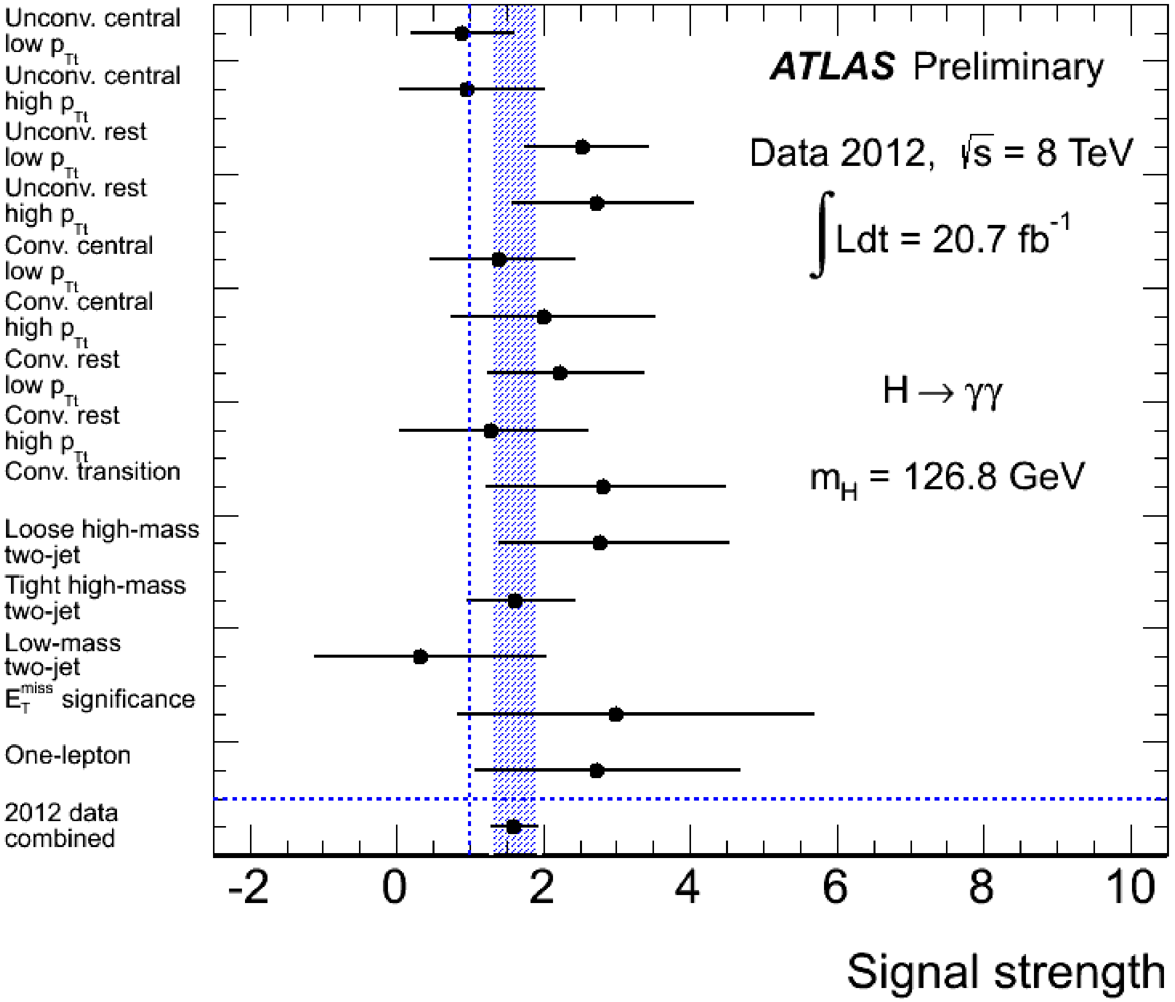

Unconv. central low p_{Tt}
Unconv. central high p_{Tt}
Unconv. rest low p_{Tt}
Unconv. rest high p_{Tt}
Conv. central low p_{Tt}
Conv. central high p_{Tt}
Conv. rest low p_{Tt}
Conv. rest high p_{Tt}
Conv. transition
Loose high-mass two-jet
Tight high-mass two-jet
Low-mass two-jet
E_T^{miss} significance
One-lepton
2012 data combined
ATLAS Preliminary
Data 2012, $\sqrt{s}$ = 8 TeV
$\int Ldt = 20.7\ fb^{-1}$
$H \rightarrow \gamma\gamma$
m_H = 126.8 GeV
-2
0
2
4
6
8
10
Signal strength

H→γγ : Results

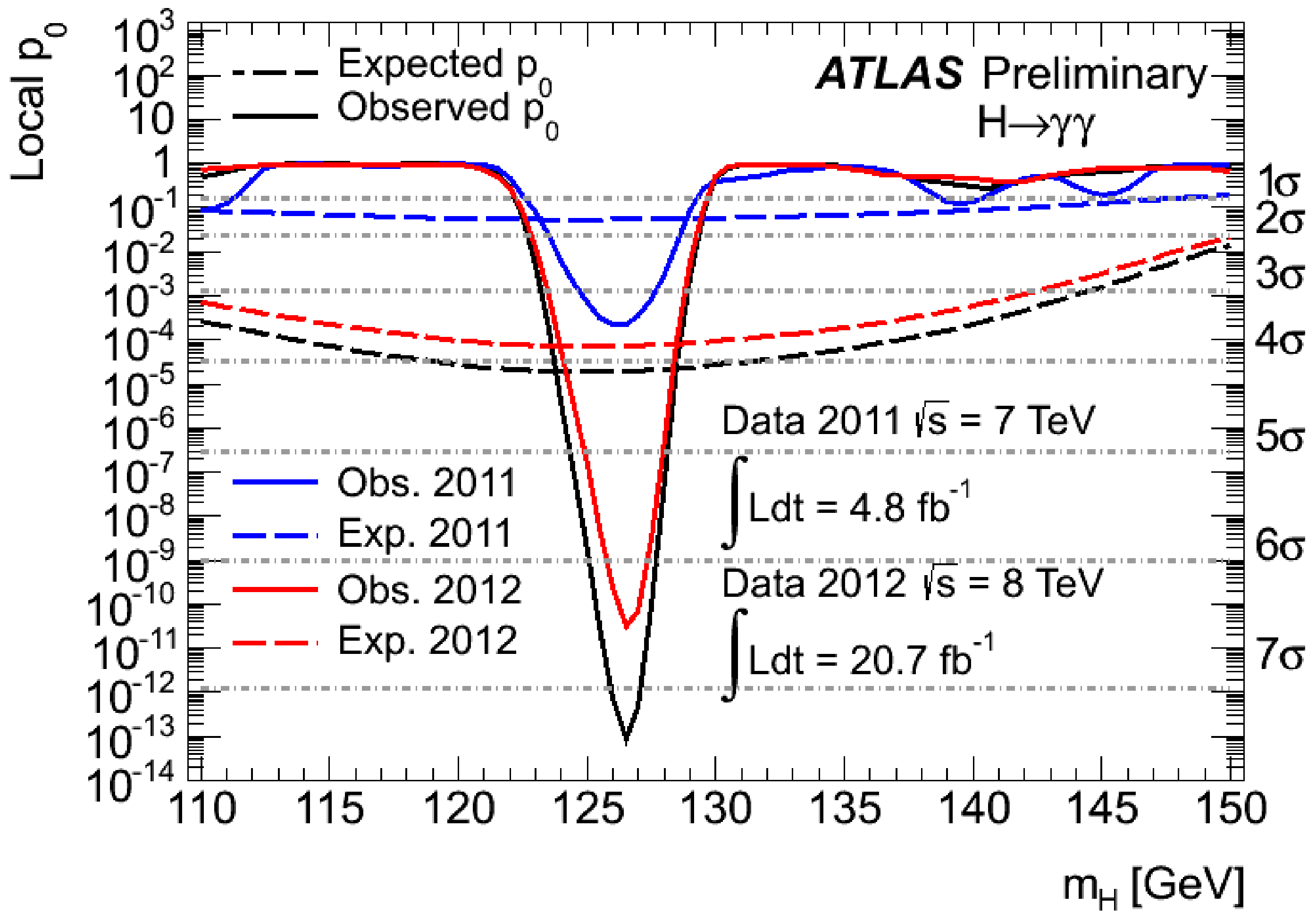

Local p_0
10^3
10^2
10
1
10^{-1}
10^{-2}
10^{-3}
10^{-4}
10^{-5}
10^{-6}
10^{-7}
10^{-8}
10^{-9}
10^{-10}
10^{-11}
10^{-12}
10^{-13}
10^{-14}
Expected p_0
Observed p_0
ATLAS Preliminary
$H\rightarrow\gamma\gamma$
1σ
2σ
3σ
4σ
5σ
6σ
7σ
Obs. 2011
Exp. 2011
Obs. 2012
Exp. 2012
Data 2011 $\sqrt{s}$ = 7 TeV
$\int Ldt = 4.8\ fb^{-1}$
Data 2012 $\sqrt{s}$ = 8 TeV
$\int Ldt = 20.7\ fb^{-1}$
110
115
120
125
130
135
140
145
150
m_H [GeV]

H→γγ : Results

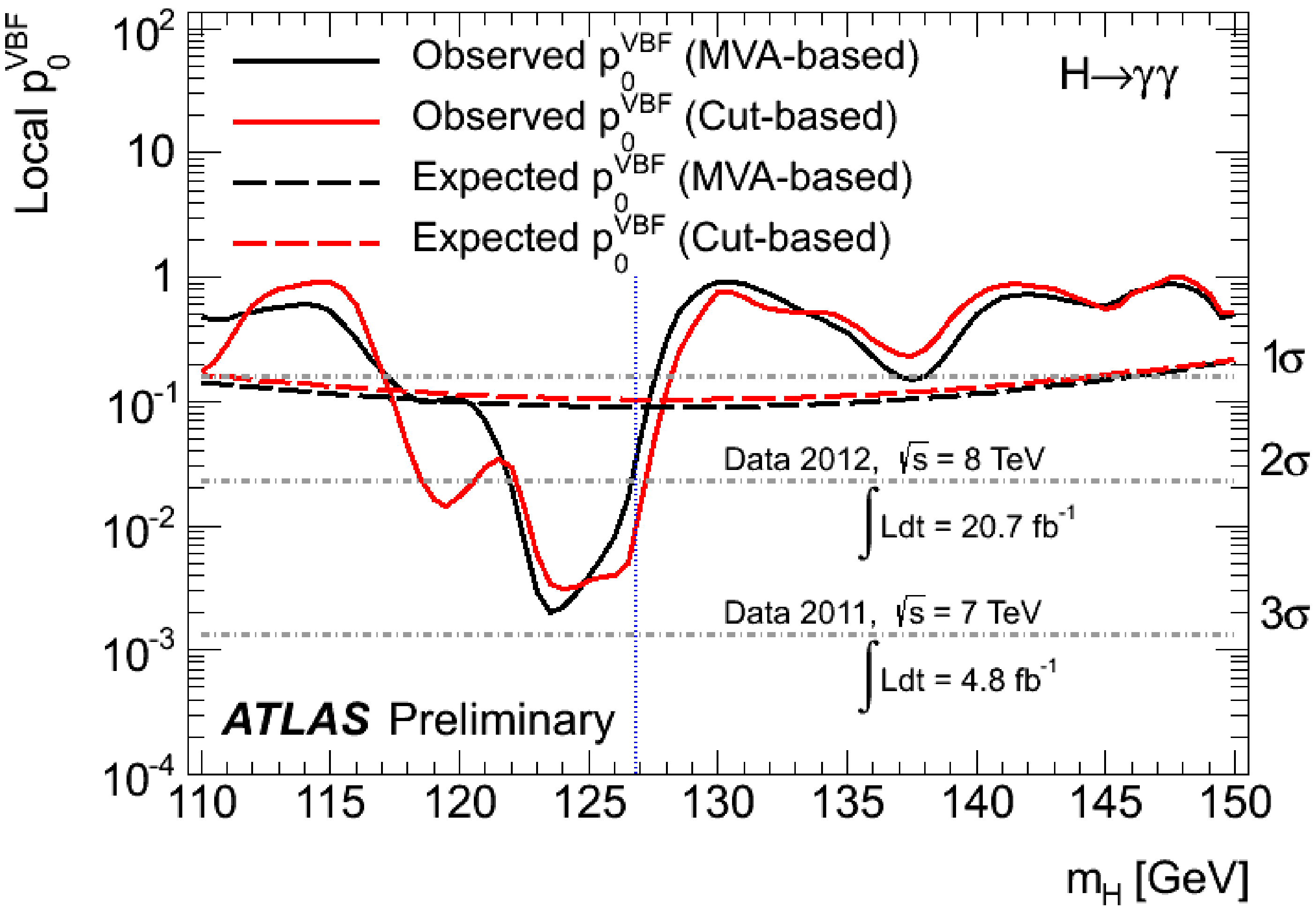

Observed p_0^{VBF} (MVA-based)
Observed p_0^{VBF} (Cut-based)
Expected p_0^{VBF} (MVA-based)
Expected p_0^{VBF} (Cut-based)
H→γγ
Data 2012, √s = 8 TeV
∫Ldt = 20.7 fb⁻¹
Data 2011, √s = 7 TeV
∫Ldt = 4.8 fb⁻¹
ATLAS Preliminary
1σ
2σ
3σ
Local p_0^{VBF}
m_H [GeV]

H→γγ : signal strengths

$$\mu_{\mathrm{ggF+ttH}} \times B/B_{\mathrm{SM}} = 1.6^{+0.3}_{-0.3}(\mathrm{stat})^{+0.3}_{-0.2}(\mathrm{syst})$$

$$\mu_{\mathrm{VBF}} \times B/B_{\mathrm{SM}} = 1.7^{+0.8}_{-0.8}(\mathrm{stat})^{+0.5}_{-0.4}(\mathrm{syst})$$

$$\mu_{\mathrm{VH}} \times B/B_{\mathrm{SM}} = 1.8^{+1.5}_{-1.3}(\mathrm{stat})^{+0.3}_{-0.3}(\mathrm{syst})$$

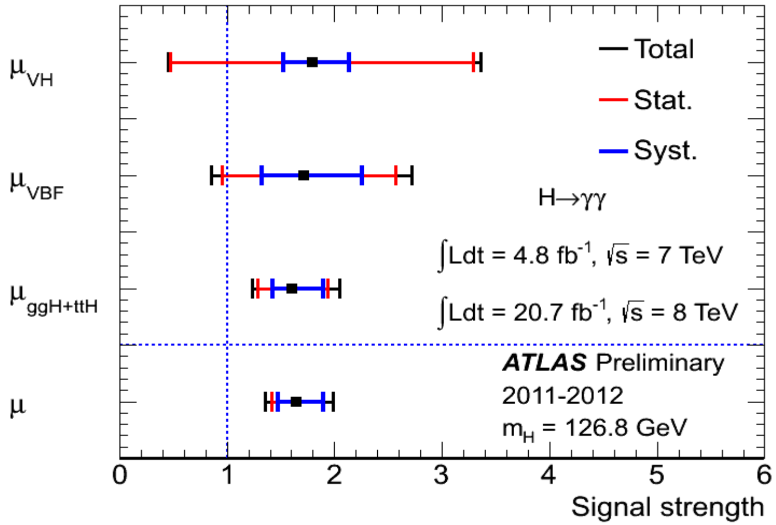

➔ **Agreement with SM expectations at better than 2σ**

➔ **Uncertainties improved by ~30% (45%) for VBF (VH) production signal strengths**

w.r.t. last public results

[statistics + systematics thanks to re-optimised categorisation]

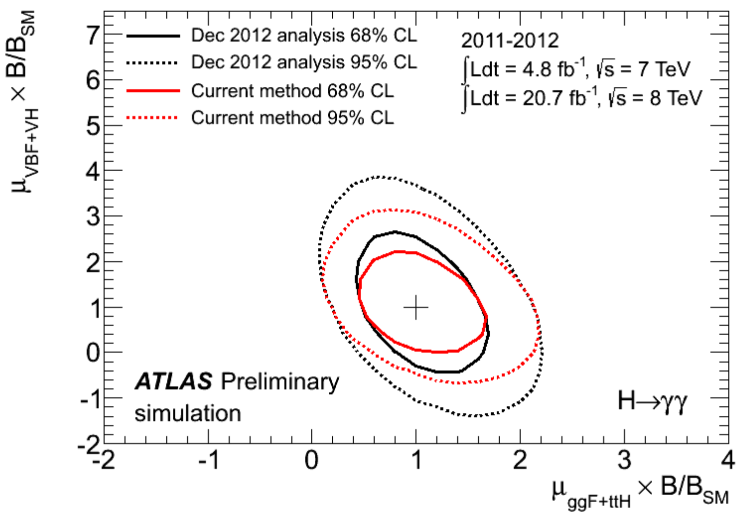

H→γγ : systematics

Main systematics on signal yield:

Theory (PDF, scales, αs)	~12% (overall), up to 50% (2-jets)
γ-efficiency	2.4%
Background model	~3%
Luminosity	3.6%

Table 5: Summary of the impact of systematic uncertainties on the signal yields for the analysis of the 8 TeV data.

Systematic uncertainties	Value(%)	Constraint
Luminosity	±3.6	Log-normal
Trigger	±0.5	Log-normal
Photon Identification	±2.4	Log-normal
Isolation	±1.0	Log-normal
Photon Energy Scale	±0.25	Log-normal
Branching ratio	±5.9% – ±2.1% (m_H = 110 - 150 GeV)	Asymmetric Log-normal
Scale	ggF: $^{+7.2}_{-7.8}$ VBF: $^{+0.2}_{-0.2}$ WH: $^{+0.2}_{-0.6}$ ZH: $^{+1.6}_{-1.5}$ ttH: $^{+3.8}_{-9.3}$	Asymmetric Log-normal
Pdf+α_s	ggF: $^{+7.5}_{-6.9}$ VBF: $^{+2.6}_{-2.7}$ WH: ±3.5 ZH: ±3.6 ttH: ±7.8	Asymmetric Log-normal
Theory cross section on ggF	Tight high-mass two-jet: ±48 Loose high-mass two-jet: ±28 Low-mass two-jet: ±30	Log-normal

H→γγ : systematics

Main systematics on categories migration:

Higgs pTt modelling	Up to 10%
Jet energy scale	Up to 20%
Underlying event	Up to 13%
Material mismodelling	~4%

Table 6: Systematic uncertainties on the signal assignment to categories (migration) for the analysis of the 8 TeV data.

Systematic uncertainties	Category	Value(%)			Constraint
Underlying Event	Tight high-mass two-jet	ggF: ±8.8	VBF: ±2.0	VH, ttH: ±8.8	Log-normal
	Loose high-mass two-jet	ggF: ±12.8	VBF: ±3.3	VH, ttH: ±12.8	
	Low-mass two-jet	ggF: ±12	VBF: ±3.9	VH, ttH: ±12	
Jet Energy Scale	Low p_{Tt}	ggF: −0.1	VBF: −1.0	Others: −0.1	Gaussian
	High p_{Tt}	ggF: −0.7	VBF: −1.3	Others: +0.4	
	Tight high-mass two-jet	ggF: +11.8	VBF: +6.7	Others: +20.2	
	Loose high-mass two-jet	ggF: +10.7	VBF: +4.0	Others: +5.7	
	Low-mass two-jet	ggF: +4.7	VBF: +2.6	Others: 1.4	
	E_T^{miss} significance	ggF: 0.0	VBF: 0.0	Others: 0.0	
	one-lepton	ggF: 0.0	VBF: 0.0	Others: −0.1	
Jet Energy Resolution	Low p_{Tt}	ggF: 0.0	VBF: 0.2	Others: 0.0	Gaussian
	High p_{Tt}	ggF: −0.2	VBF: 0.2	Others: 0.6	
	Tight high-mass two-jet	ggF: 3.8	VBF: −1.3	Others: 7.0	
	Loose high-mass two-jet	ggF: 3.4	VBF: −0.7	Others: 1.2	
	Low-mass two-jet	ggF: 0.5	VBF: 3.4	Others: −1.3	
	E_T^{miss} significance	ggF: 0.0	VBF: 0.0	Others: 0.0	
	one-lepton	ggF: −0.9	VBF: −0.5	Others: −0.1	
η^* modelling		Tight high-mass two-jet: +7.6			Gaussian
		Loose high-mass two-jet: +6.2			
Dijet angular modelling		Tight high-mass two-jet: +12.1			Gaussian
		Loose high-mass two-jet: +8.5			
Higgs p_T		Low p_{Tt}: +1.3			Gaussian
		High p_{Tt}: −10.2			
		Tight high-mass two-jet: −10.4			
		Loose high-mass two-jet: −8.5			
		Low-mass two-jet: −12.5			
		E_T^{miss} significance: −2.0			
		one-lepton : −4.0			
Material Mismodelling		Unconv: −4.0	Conv: +3.5		Gaussian
JVF	Loose High-mass two-jet	ggF: −1.2	VBF: −0.3	Others: −1.2	Gaussian
	Low-mass two-jet	ggF: −2.3	VBF: −2.4	Others: −2.3	
E_T^{miss}	E_T^{miss} significance	ggF: +66.4	VBF: +30.7	VH, ttH: +1.2	Gaussian
e reco and identification		one-lepton: < 1			Gaussian
e Escale and resolution		one-lepton: < 1			Gaussian
μ reco, ID resolution		one-lepton: < 1			Gaussian
μ spectrometer resolution		one-lepton: 0			Gaussian

H→γγ : fiducial cross-section

❑ Inclusive fiducial cross-section measurement of the observed state

$$\sigma_{fid} \times BR = \frac{N^{signal}}{C_H \times L_{int}}$$

- Computed from the inclusive 2012 sample (analysis without categories)
- N^{signal} : number of signal events (748) extracted from a signal-plus-background fit on the inclusive $m_{\gamma\gamma}$ distribution - uncertainties: stat 18.5% and syst 11.2%(resolution, bknd model)
- L_{int} : integrated luminosity (3.6% uncertainty in 2012)
- C_H : correction factor for detector effects for events falling within the acceptance
  → uncertainty 2.7% (trigger, photon reconstruction, identification, isolation, theory)

  → compatible within a few % for each production mode, except ttH (photons less isolated)
- Model independent (at first order): extrapolation to full phase space not needed
- Particle level acceptance cuts: $|\eta^{\gamma}|<2.37$, $E_T^{\gamma}>40/30$ GeV

$\sigma_{fid} \cdot BR = 56.2 \pm 12.5$ fb

[±10.5(stat) ± 6.5(syst) ± 2.0(lumi)]

H→γγ : Spin studies

Simulations, after analysis selection cuts

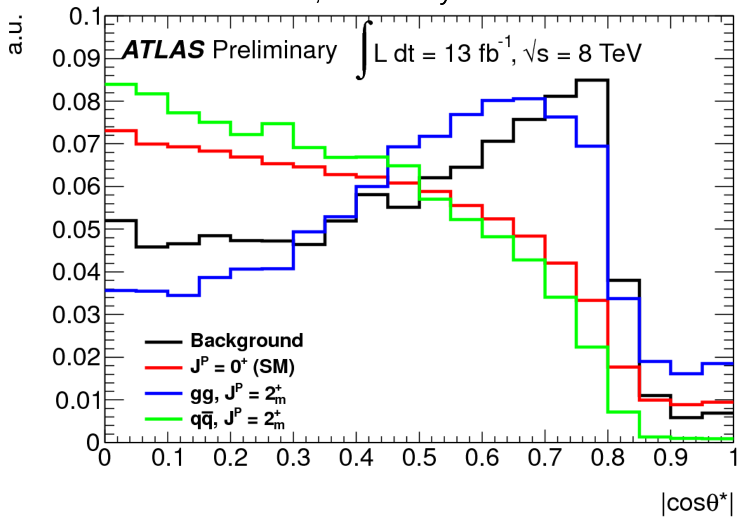

Fit to data for SM signal + background hypothesis

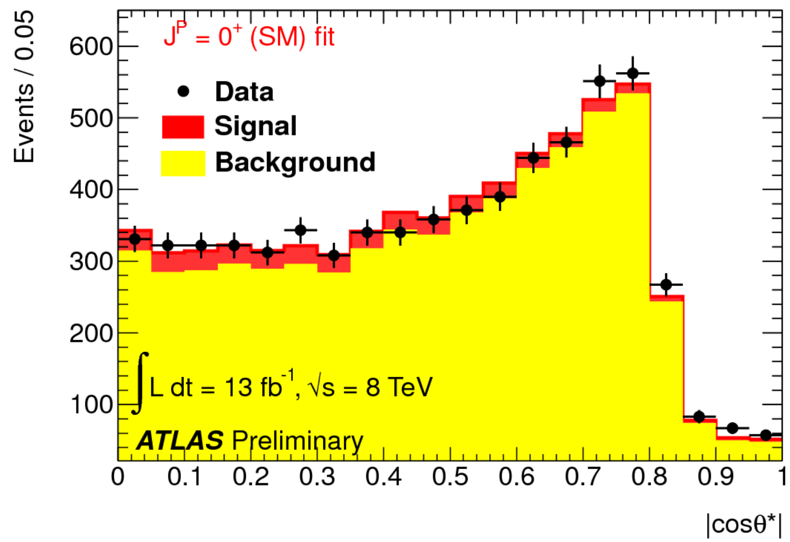

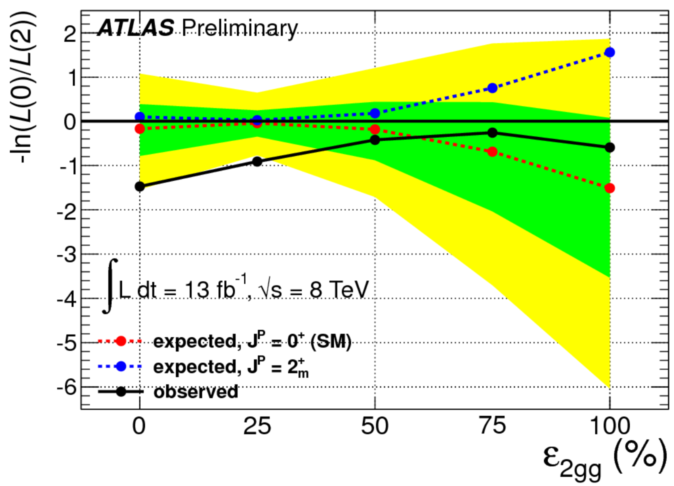

Results with 5 different fractions of gluon initiated process for spin-2 resonance production

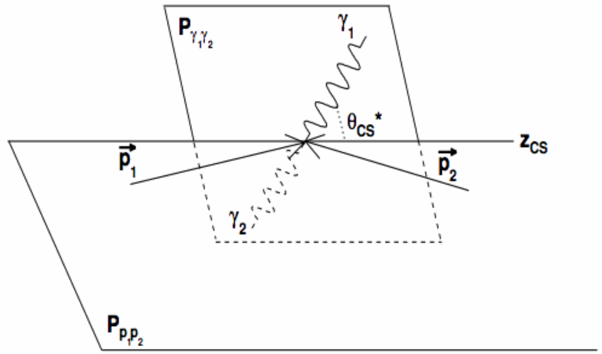

Event displays

Candidate H→$\gamma\gamma$, $m_{\gamma\gamma}$=126.6 GeV

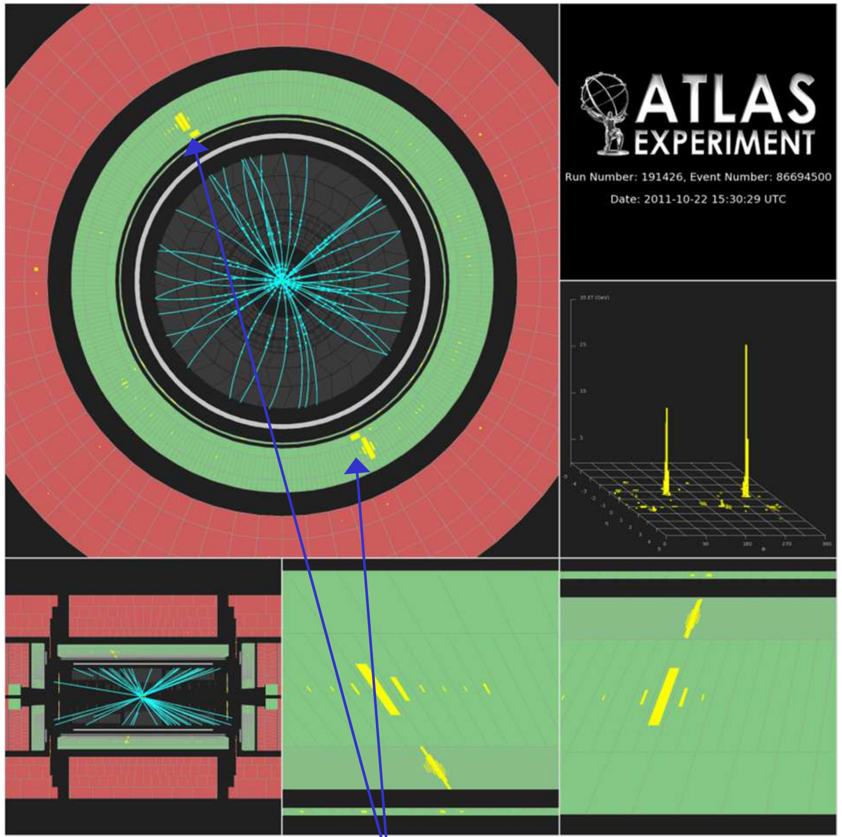

Candidate H→4e, m_{eeee}=124.6 GeV

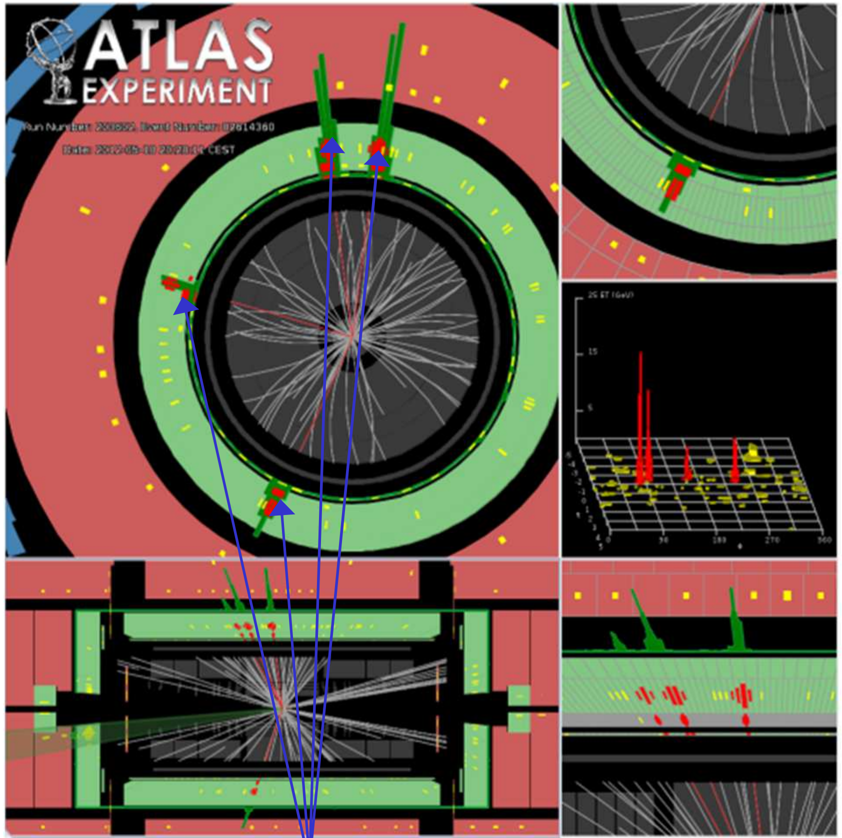

EM calorimeter energy deposits

$H \rightarrow ZZ^{(*)} \rightarrow 4l$ ($l=e,\mu$)

$\sigma \times BR \sim 2.5$ fb for $m_H \sim 125$ GeV

$H \rightarrow ZZ^{(*)} \rightarrow 4l$ ($l=e,\mu$) : Background

- **Background composition depends on flavor of sub-leading leptons → $ll+\mu\mu$**
  - Main reducible backgrounds: tt and Z+jets (Zbb and π/K in-flight decays) → ~20% of total bknd
  - Control region: no isolation cut on sub-leading pair + fail IP significance cut (to remove ZZ) → bb contribution enhanced: tt and Z+jets estimated simultaneously through fit to m_{12}
  - Extrapolation to signal region through MC transfer factor (IP cut and isolation efficiencies with bb MC) – systematics from comparison of transfer factor with data-driven Z+μ
  - Various checks of background estimates with other control regions (e.g. fail track isolation, $e\mu+\mu\mu$, SS pair, …) → all yield compatible results

Example: tt & Z+jets control region in 2e2μ channel

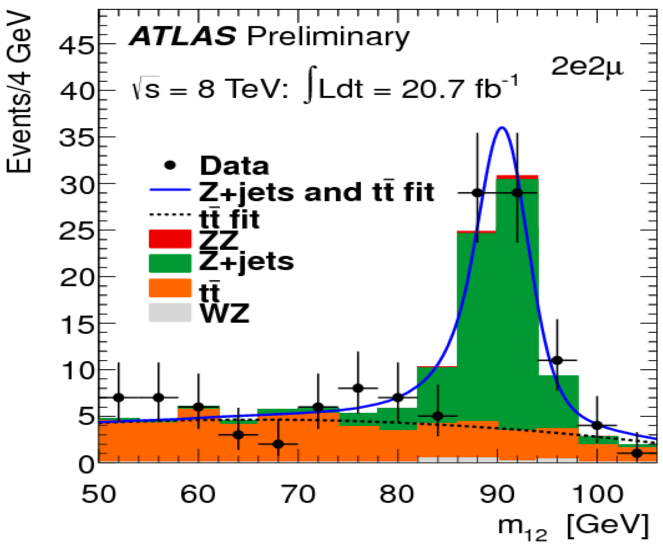

$H \rightarrow ZZ^{(*)} \rightarrow 4l$ ($l=e,\mu$) : Background

- **Background composition depends on flavor of sub-leading leptons → ll+ee**
  - Main reducible backgrounds: tt and Z+jets (hadrons mis-identified as electrons, electrons from photon conversions and non-prompt electrons from heavy flavor decay) → ~25% of total bknd
  - Control region: relaxed identification criteria on sub-leading electrons → sum of tt and Z+jets
  - Use detector strengths (e.g. transition radiation, b-layer, shower shapes) to constrain composition
  - Extrapolation to signal region through MC transfer factor
  - Various checks of background estimates with other control regions (e.g. Same-Sign sub-leading di-electron pair) → all yield compatible results

$H \to ZZ^{(*)} \to 4l$ ($l=e,\mu$) : Background

Table 3: Summary of the estimated numbers of Z + jets and $t\bar{t}$ background events for the 20.7 fb^{-1} of $\sqrt{s}$ = 8 TeV data and for the 4.6 fb^{-1} of $\sqrt{s}$ = 7 TeV data for the full mass range of the analysis after the kinematic selections described in the text. Except for the sub-leading same sign full analysis events are given only for $m_{4\ell} < 160$ GeV to avoid contamination from the irreducible $ZZ^{(*)}$ background with an incorrect charge measurement. Approximately 80% of the reducible background has $m_{4\ell} < 160$ GeV. The "†" symbol indicates the estimates used for the background normalisation, the others being cross-checks. The first uncertainty is statistical, the second is systematic.

method	estimate at $\sqrt{s} = 8$ TeV	estimate at $\sqrt{s} = 7$ TeV
	4μ	4μ
m_{12} fit: Z + jets contribution	$2.4 \pm 0.5 \pm 0.6^{\dagger}$	$0.22 \pm 0.07 \pm 0.02^{\dagger}$
m_{12} fit: $t\bar{t}$ contribution	$0.14 \pm 0.03 \pm 0.03^{\dagger}$	$0.03 \pm 0.01 \pm 0.01^{\dagger}$
$t\bar{t}$ from $e\mu + \mu\mu$	$0.10 \pm 0.05 \pm 0.004$	-
	$2e2\mu$	$2e2\mu$
m_{12} fit: Z + jets contribution	$2.5 \pm 0.5 \pm 0.6^{\dagger}$	$0.19 \pm 0.06 \pm 0.02^{\dagger}$
m_{12} fit: $t\bar{t}$ contribution	$0.10 \pm 0.02 \pm 0.02^{\dagger}$	$0.03 \pm 0.01 \pm 0.01^{\dagger}$
$t\bar{t}$ from $e\mu + \mu\mu$	$0.12 \pm 0.07 \pm 0.005$	-
	$2\mu 2e$	$2\mu 2e$
$\ell\ell + e^{\pm}e^{\mp}$ relaxed cuts	$5.2 \pm 0.4 \pm 0.5^{\dagger}$	$1.8 \pm 0.3 \pm 0.4$
$\ell\ell + e^{\pm}e^{\mp}$ inverted cuts	$3.9 \pm 0.4 \pm 0.6$	-
$3\ell + \ell$ (same-sign)	$4.3 \pm 0.6 \pm 0.5$	$2.8 \pm 0.4 \pm 0.5^{\dagger}$
sub-leading same sign full analysis events	4	0
	$4e$	$4e$
$\ell\ell + e^{\pm}e^{\mp}$ relaxed cuts	$3.2 \pm 0.5 \pm 0.4^{\dagger}$	$1.4 \pm 0.3 \pm 0.4$
$\ell\ell + e^{\pm}e^{\mp}$ inverted cuts	$3.6 \pm 0.6 \pm 0.6$	-
$3\ell + \ell$ (same-sign)	$4.2 \pm 0.5 \pm 0.5$	$2.5 \pm 0.3 \pm 0.5^{\dagger}$
sub-leading same sign full analysis events	3	2

H→ZZ$^{(*)}$→4l (l=e,μ) : Background

Control regions with no isolation nor IP cuts on softest leptons [muons (left) and electrons (right)]

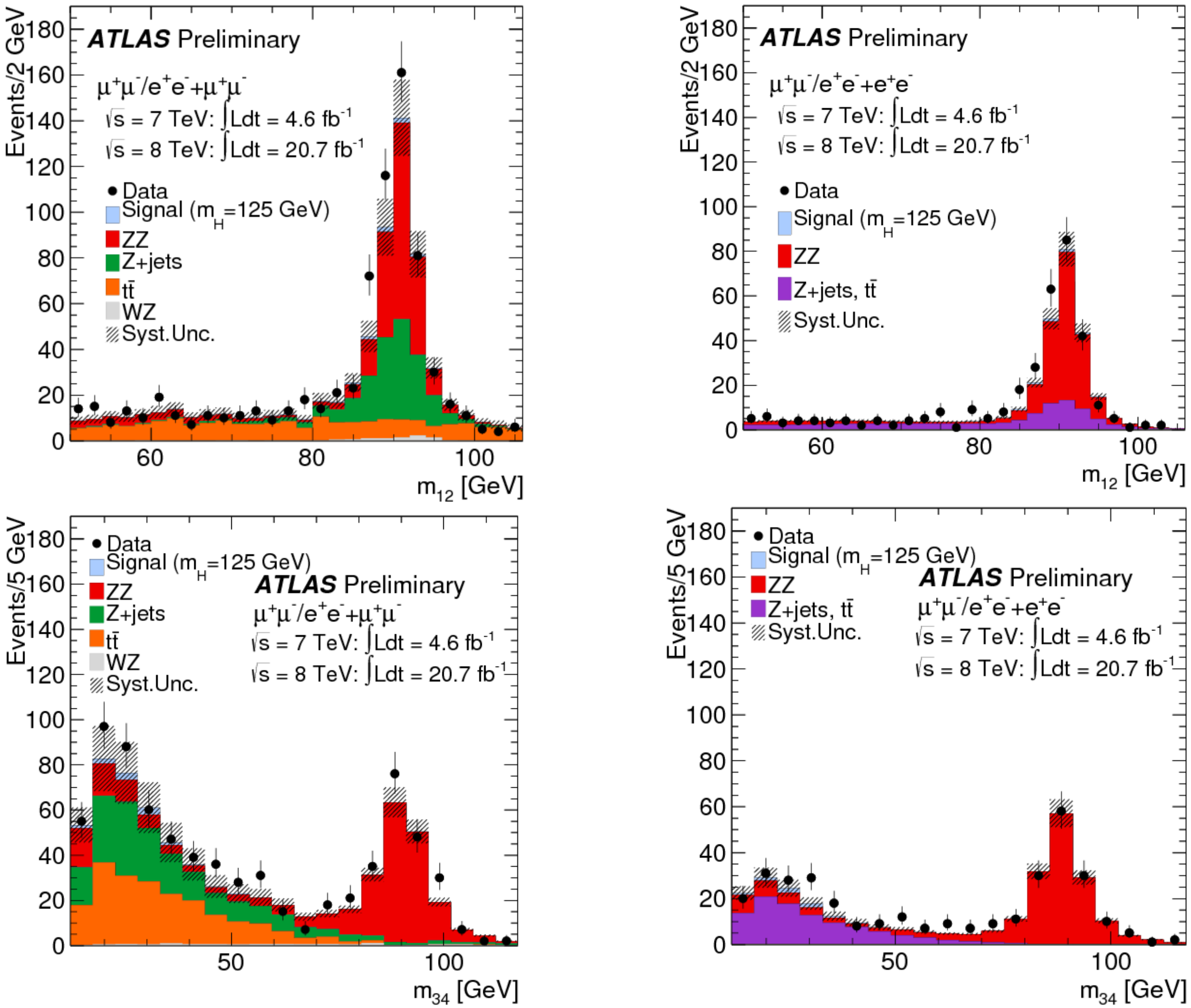

H→ZZ$^{(*)}$→4l (l=e,μ) : single resonance

❑ Single resonance pp→Z→4l

- Cuts relaxed wrt standard analysis to improve acceptance
- 20 GeV<m_{12}<106 GeV, 1 GeV<m_{34}<115 GeV, p_T(softest muon)>4 GeV

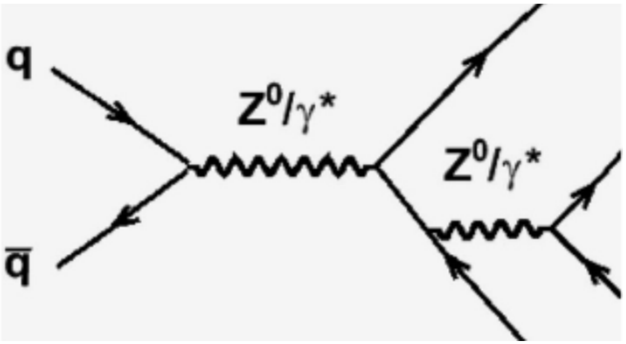

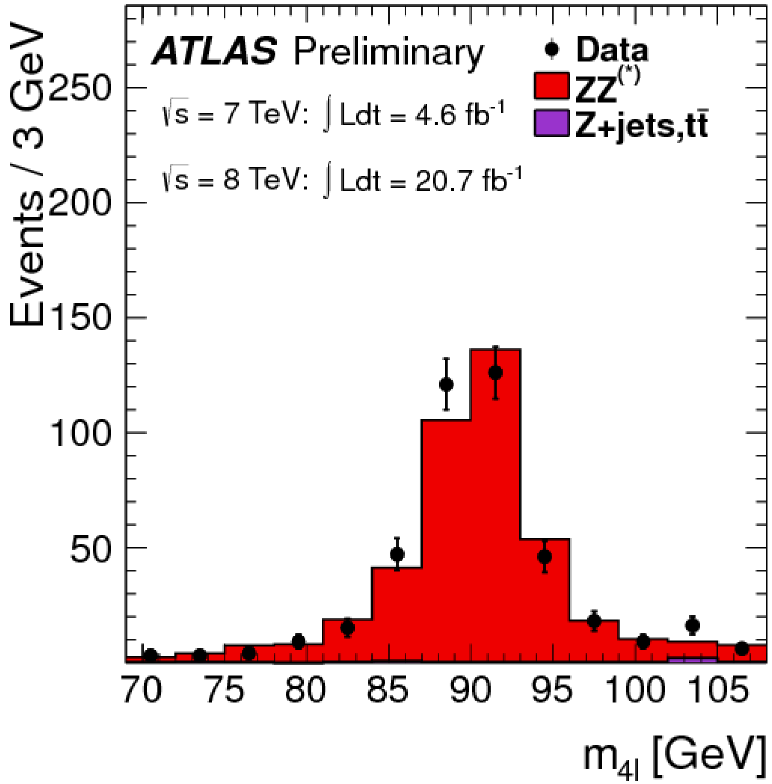

H→ZZ$^{(*)}$→4l (l=e,μ) : electrons

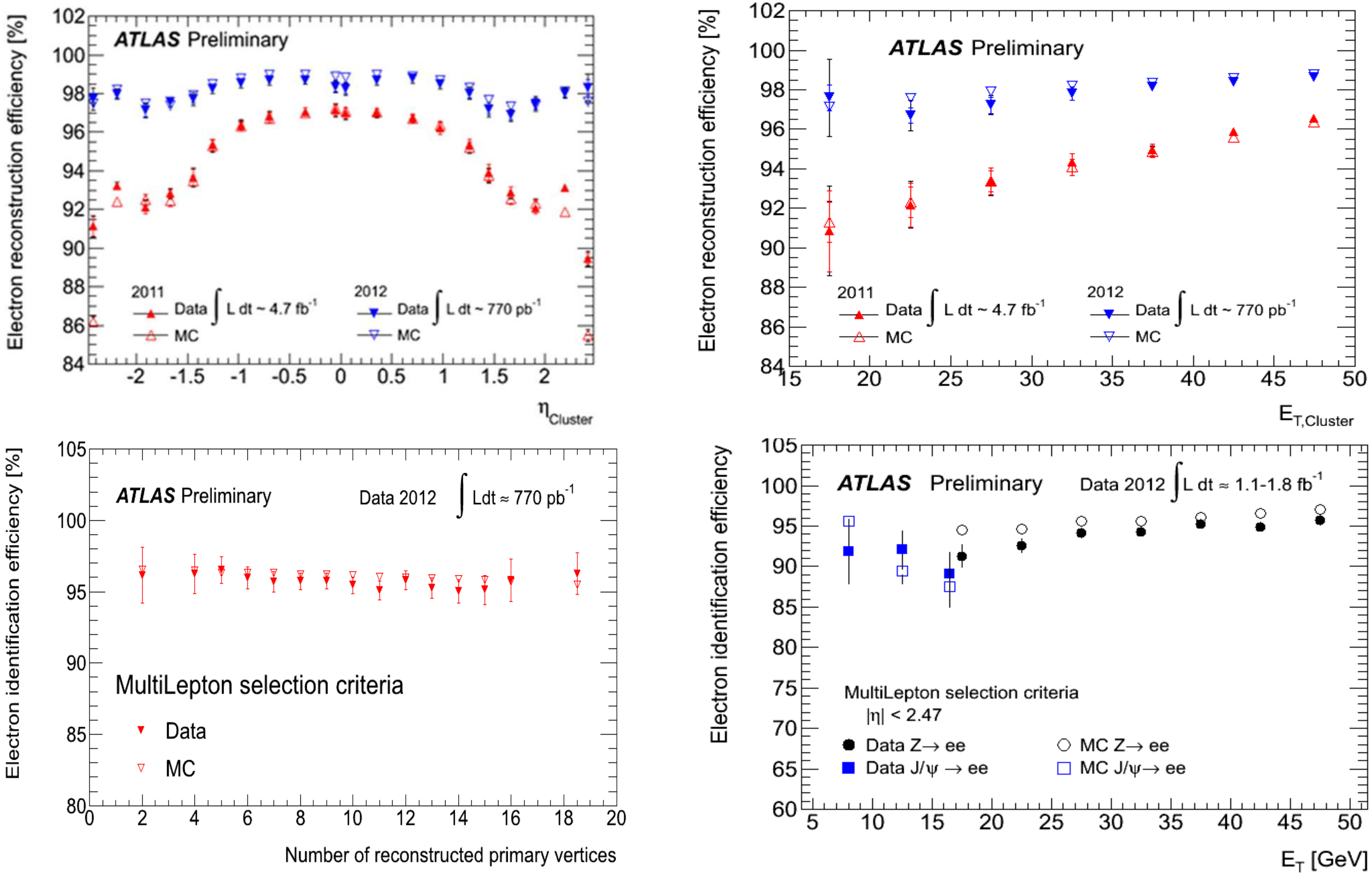

H→ZZ(*)→4l (l=e,μ) : signal

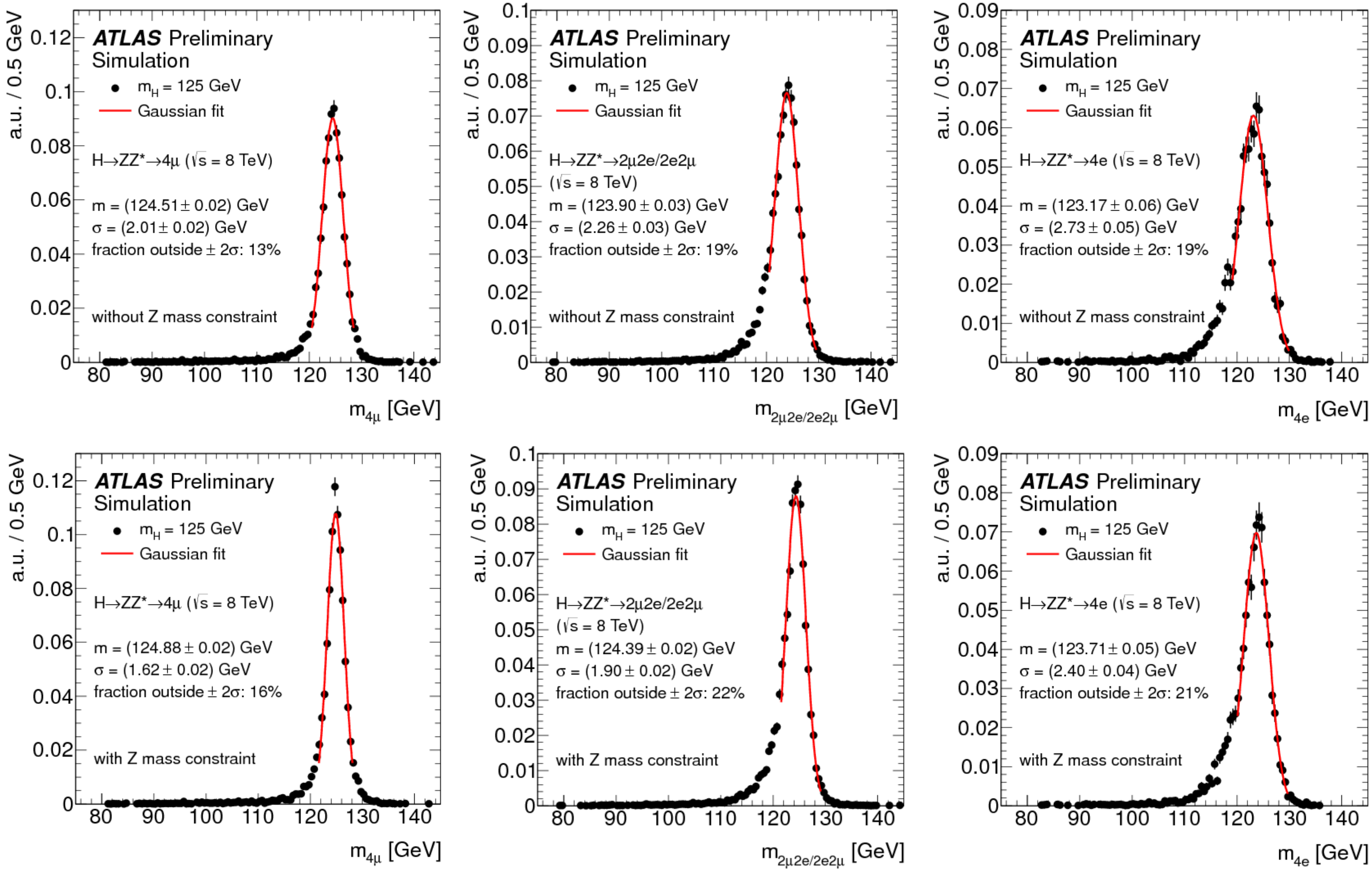

H→ZZ$^{(*)}$→4l (l=e,μ) : results

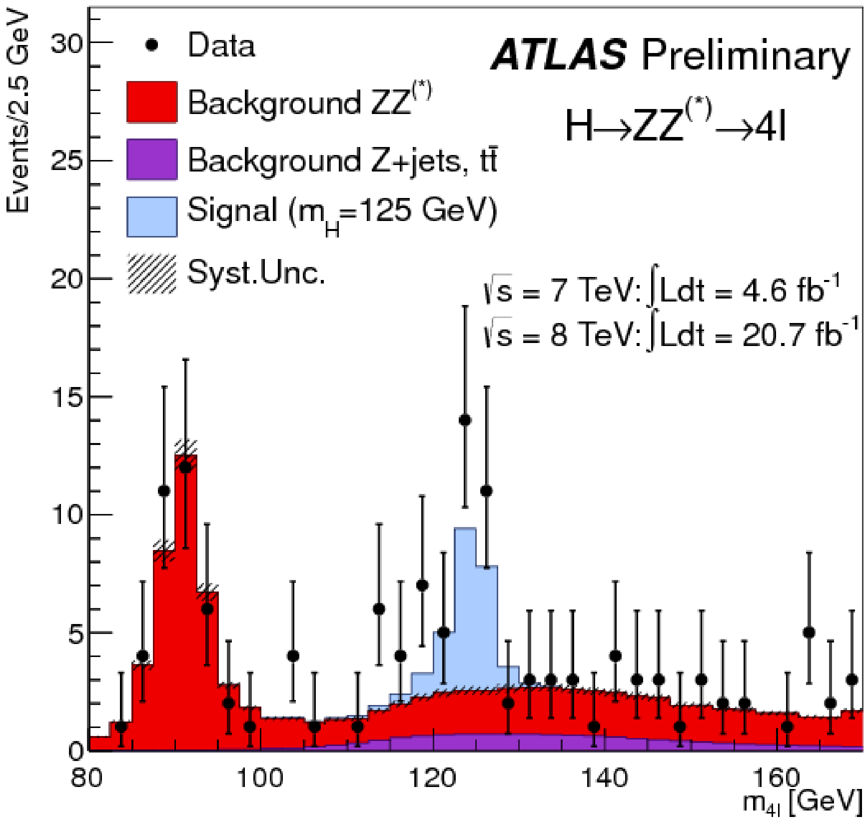

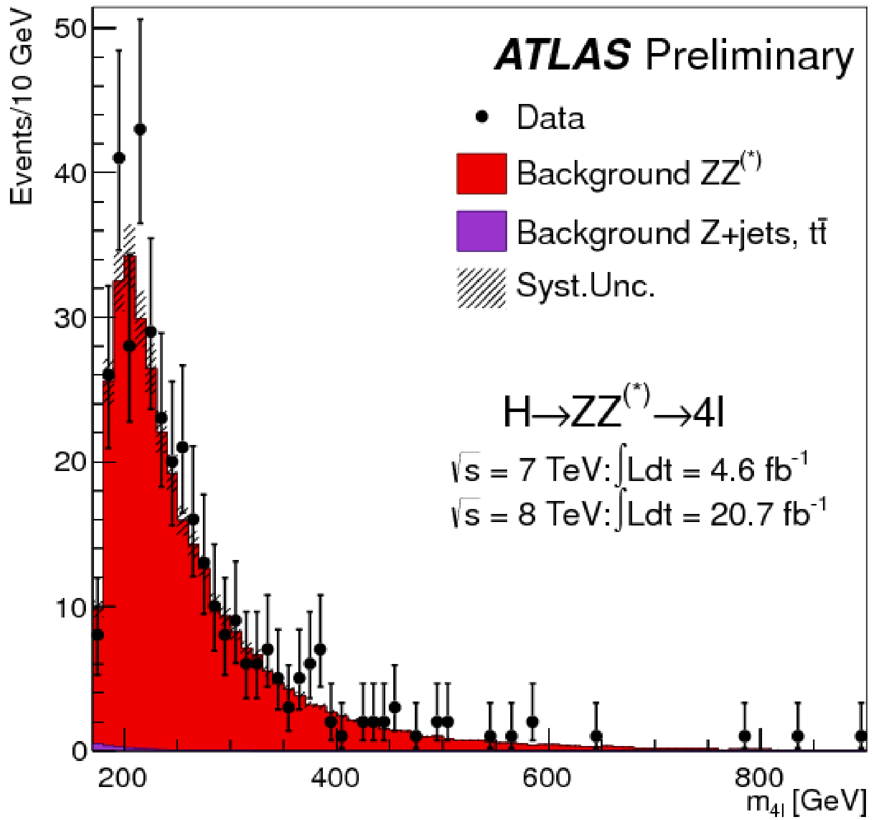

H→ZZ$^{(*)}$→4l (l=e,μ) : results

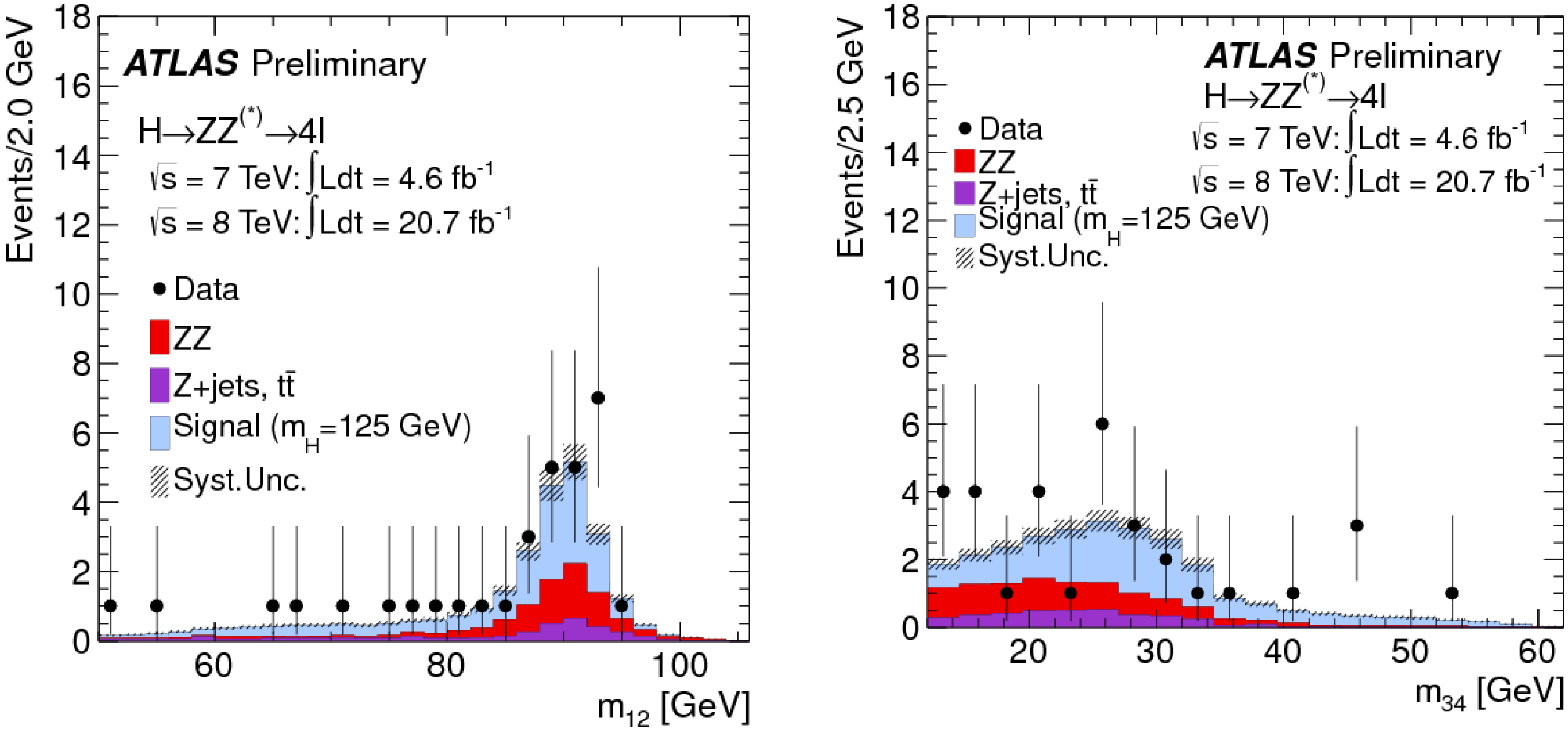

$H \rightarrow ZZ^{(*)} \rightarrow 4l$ ($l=e,\mu$) : results

Table 6: The observed numbers of events and the final estimates for the expected backgrounds, separated into "low mass" ($100 < m_{4\ell} < 160$ GeV) and "high mass" ($m_{4\ell} \geq 160$ GeV) regions. The expected numbers of signal events are also shown for various Higgs boson mass hypotheses. For the signal and background estimates the corresponding total uncertainties are given.

	4μ		$2\mu 2e/2e2\mu$		$4e$	
	low mass	high mass	low mass	high mass	low mass	high mass
$\sqrt{s} = 8$ TeV integrated luminosity 20.7 fb^{-1}						
$ZZ^{(*)}$	12.4 ± 0.6	92.6 ± 6.7	14.7 ± 0.9	144 ± 11	5.4 ± 0.5	55.9 ± 4.5
Z, $Zb\bar{b}$, and $t\bar{t}$	1.9 ± 0.6	0.5 ± 0.2	6.1 ± 1.5	1.5 ± 0.4	2.5 ± 0.6	0.6 ± 0.2
total background	14.3 ± 0.8	93.1 ± 6.7	20.8 ± 1.8	145 ± 11	8.0 ± 0.8	56.5 ± 4.5
data	27	93	28	169	13	55
$m_H = 123$ GeV	4.4 ± 0.6		5.4 ± 0.8		2.2 ± 0.4	
$m_H = 125$ GeV	5.8 ± 0.7		7.0 ± 0.9		2.9 ± 0.4	
$m_H = 127$ GeV	6.7 ± 0.9		8.4 ± 1.2		3.4 ± 0.5	
$\sqrt{s} = 7$ TeV integrated luminosity 4.6 fb^{-1}						
$ZZ^{(*)}$	2.2 ± 0.1	16.8 ± 1.2	2.5 ± 0.2	26.6 ± 2.0	0.8 ± 0.1	9.4 ± 0.8
Z, $Zb\bar{b}$, and $t\bar{t}$	0.2 ± 0.1	0.05 ± 0.02	2.4 ± 0.5	0.6 ± 0.1	2.0 ± 0.5	0.48 ± 0.1
total background	2.4 ± 0.1	16.9 ± 1.2	4.9 ± 0.6	27.1 ± 2.0	2.8 ± 0.5	9.8 ± 0.8
data	8	23	5	23	2	13
$m_H = 123$ GeV	0.7 ± 0.1		0.8 ± 0.1		0.3 ± 0.1	
$m_H = 125$ GeV	1.0 ± 0.1		1.1 ± 0.2		0.4 ± 0.1	
$m_H = 127$ GeV	1.0 ± 0.2		1.2 ± 0.2		0.4 ± 0.1	

H→ZZ$^{(*)}$→4l (l=e,μ) : results

Table 7: The numbers of expected signal events for the m_H=125 GeV hypothesis and background events together with the numbers of observed events, in a window of ±5 GeV around 125 GeV for 20.7 fb^{-1} at $\sqrt{s}$ = 8 TeV and 4.6 fb^{-1} at $\sqrt{s}$ = 7 TeV as well as for their combination.

	total signal full mass range	signal	$ZZ^{(*)}$	Z + jets, $t\bar{t}$	S/B	expected	observed
$\sqrt{s}$ = 8 TeV							
4μ	5.8 ± 0.7	5.3 ± 0.7	2.3 ± 0.1	0.50 ± 0.13	1.9	8.1 ± 0.9	11
$2\mu 2e$	3.0 ± 0.4	2.6 ± 0.4	1.2 ± 0.1	1.01 ± 0.21	1.2	4.8 ± 0.7	4
$2e2\mu$	4.0 ± 0.5	3.4 ± 0.4	1.7 ± 0.1	0.51 ± 0.16	1.5	5.6 ± 0.7	6
$4e$	2.9 ± 0.4	2.3 ± 0.3	1.0 ± 0.1	0.62 ± 0.16	1.4	3.9 ± 0.6	6
total	15.7 ± 2.0	13.7 ± 1.8	6.2 ± 0.4	2.62 ± 0.34	1.6	22.5 ± 2.9	27
$\sqrt{s}$ = 7 TeV							
4μ	1.0 ± 0.1	0.97 ± 0.13	0.49 ± 0.02	0.05 ± 0.02	1.8	1.5 ± 0.2	2
$2\mu 2e$	0.4 ± 0.1	0.39 ± 0.05	0.21 ± 0.02	0.55 ± 0.12	0.5	1.2 ± 0.1	1
$2e2\mu$	0.7 ± 0.1	0.57 ± 0.08	0.33 ± 0.02	0.04 ± 0.01	1.5	0.9 ± 0.1	2
$4e$	0.4 ± 0.1	0.29 ± 0.04	0.15 ± 0.01	0.49 ± 0.12	0.5	0.9 ± 0.1	0
total	2.5 ± 0.4	2.2 ± 0.3	1.17 ± 0.07	1.12 ± 0.17	1.0	4.5 ± 0.5	5
$\sqrt{s}$ = 8 TeV and $\sqrt{s}$ = 7 TeV							
4μ	6.8 ± 0.8	6.3 ± 0.8	2.8 ± 0.1	0.55 ± 0.15	1.9	9.6 ± 1.0	13
$2\mu 2e$	3.4 ± 0.5	3.0 ± 0.4	1.4 ± 0.1	1.56 ± 0.33	1.0	6.0 ± 0.8	5
$2e2\mu$	4.7 ± 0.6	4.0 ± 0.5	2.1 ± 0.1	0.55 ± 0.17	1.5	6.6 ± 0.8	8
$4e$	3.3 ± 0.5	2.6 ± 0.4	1.2 ± 0.1	1.11 ± 0.28	1.1	4.9 ± 0.8	6
total	18.2 ± 2.4	15.9 ± 2.1	7.4 ± 0.4	3.74 ± 0.93	1.4	27.1 ± 3.4	32

Reminder: HCP analysis, 18 events observed [8.3±0.6 expected from bknd & 9.9±1.3 from SM higgs]

H→ZZ$^{(*)}$→4l (l=e,μ) : results

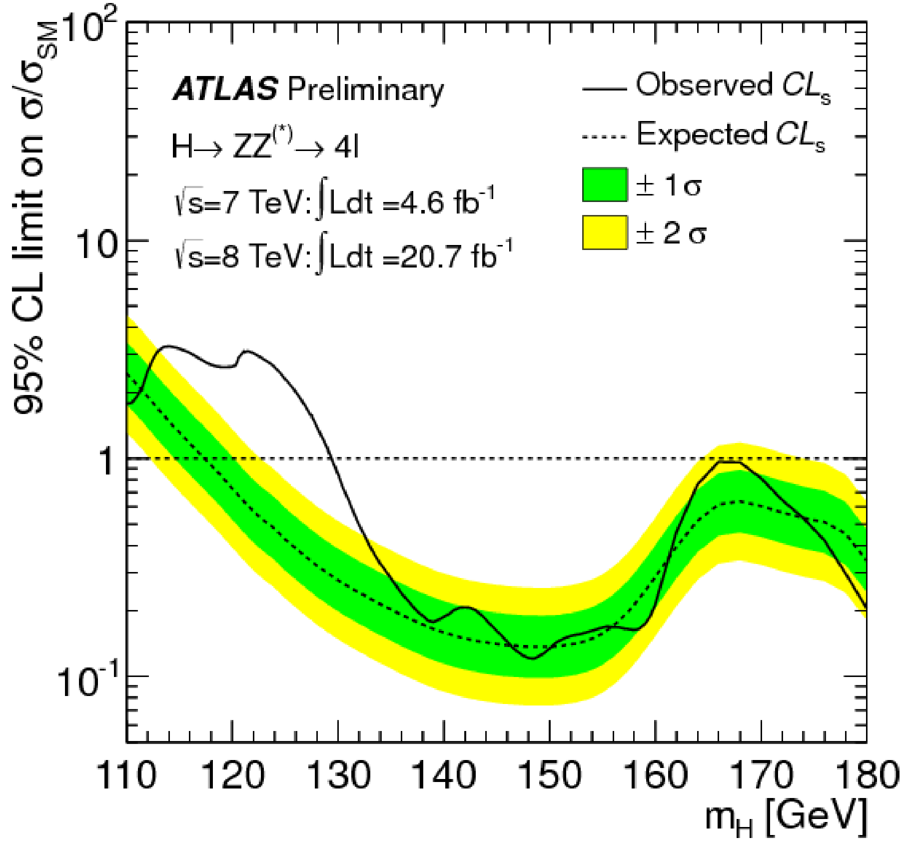

$H \to ZZ^{(*)} \to 4l$ ($l=e,\mu$) : results

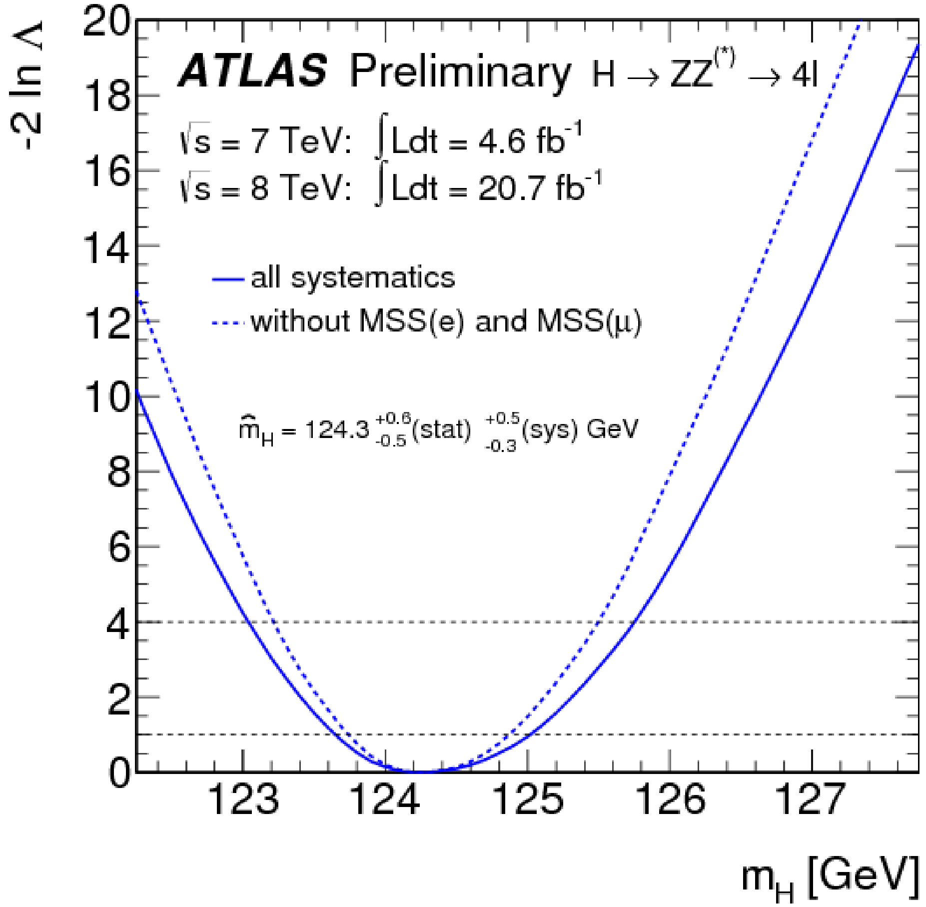

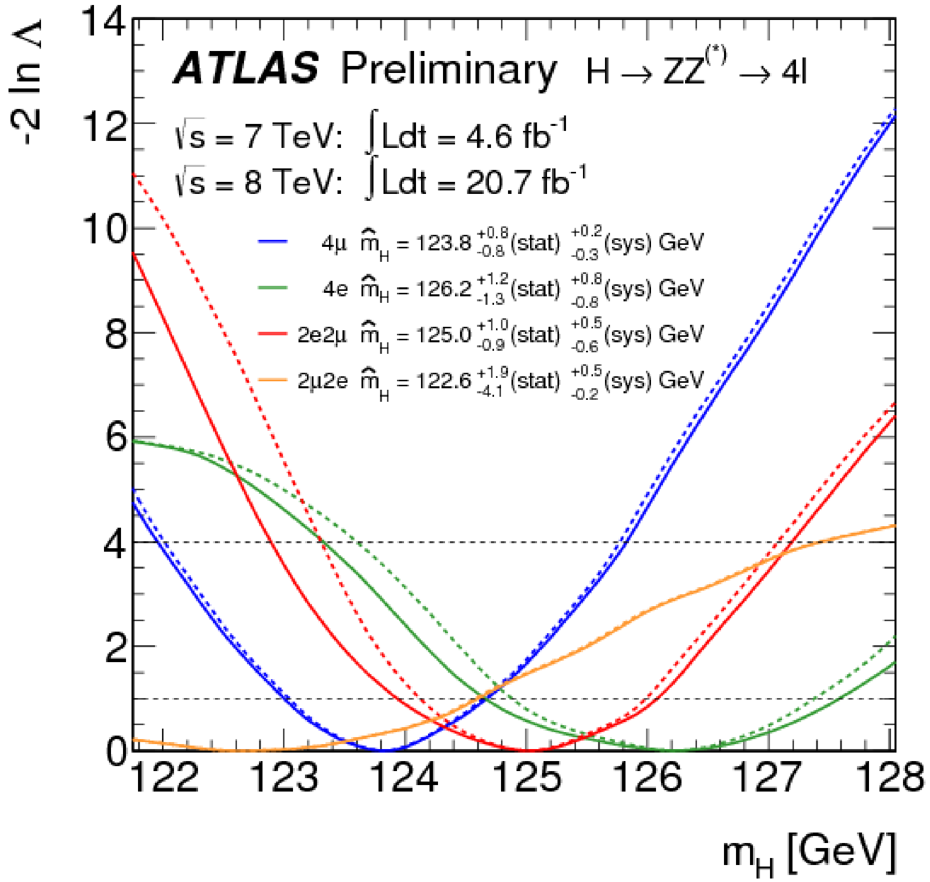

$H \to ZZ^{(*)} \to 4l$ ($l=e,\mu$) : FSR

- Include soft FSR photons in Higgs invariant mass calculation for leading-$Z \to \mu\mu$ events
- Photon selection for $E_T>1$ GeV, using $\Delta R_{\mu\gamma}$ and the fraction of energy deposited in the first calorimeter sampling ($f_1=E_{strips}/E_{cluster}$)

  For $1<E_T<3.5$ GeV: $f_1>0.2$ and $\Delta R_{\mu\gamma}<0.08$
  For $E_T>3.5$ GeV: $f_1>0.1$ and $\Delta R_{\mu\gamma}<0.15$

- Apply correction if $66<M_{12}$ [GeV]<89 and $M_{\mu\mu\gamma}<100$ GeV
- Recovers 70% of FSR photons in selected fiducial region, with a 85% purity
- Observe 3.5% affected events, in agreement with MC expectations
- 1 event affected in signal region 125±5 GeV

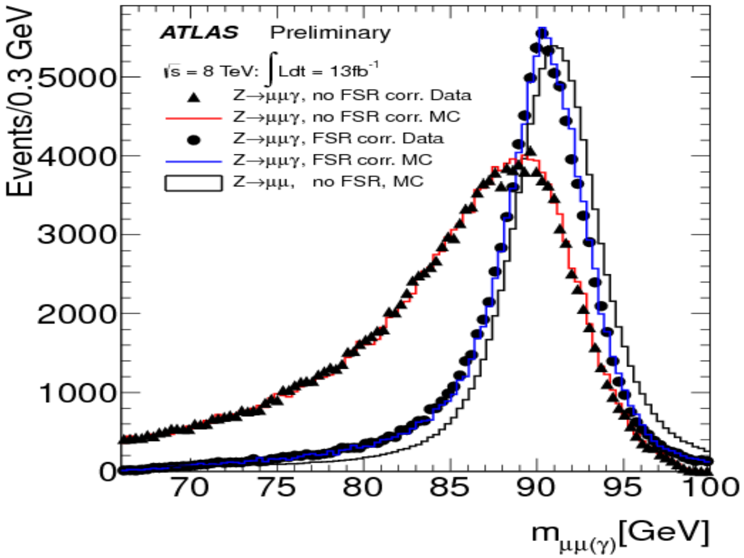

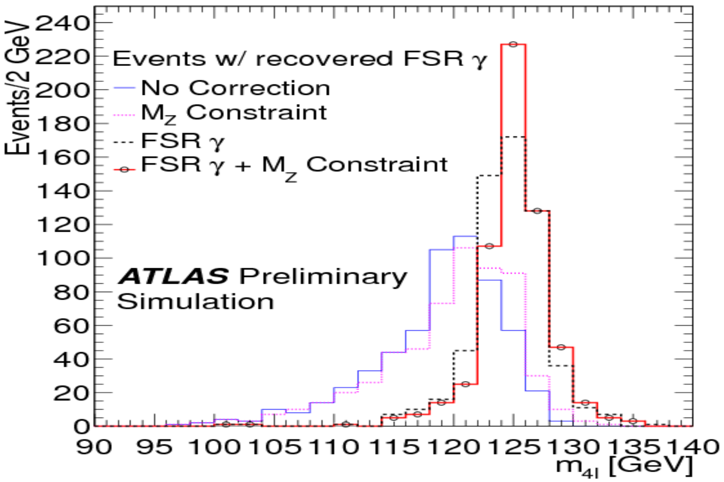

Remark: Z-mass constraint is applied after FSR correction → Improvement in Higgs mass resolution: 20% (12%) for 4μ (4e) channel

H→ZZ$^{(*)}$→4l (l=e,μ) : categorisation

❑ VBF-enriched category

$$\mathrm{JVF}(\mathrm{jet}_i, \mathrm{PV}_j) = \frac{\sum_k p_\mathrm{T}(\mathrm{track}_k^{\mathrm{jet}_i}, \mathrm{PV}_j)}{\sum_n \sum_l p_\mathrm{T}(\mathrm{track}_l^{\mathrm{jet}_i}, \mathrm{PV}_n)}$$

- 2 jets with p_T>25-30 GeV, |η|<4.5 and |JVF|*>0.5 (for |η|<2.4)
- Cuts on $|\Delta\eta_{jj}|$>3 and m_{jj}>350 GeV

* Jet-vertex fraction: sum of the p_T carried by tracks in the jet and associated to selected vertex divided by the total p_T carried by all tracks associated to the jet

❑ VH-renriched category

- Additional isolated lepton p_T>8 GeV

Table 2: The expected numbers of events in each category (ggF-like, VBF-like, VH-like), after all analysis criteria are applied, for each signal production mechanism (ggF/$t\bar{t}H$, VBF, VH) at m_H =125 GeV and the $ZZ^{(*)}$ background, for 20.7 fb^{-1} at $\sqrt{s}$ = 8 TeV and 4.6 fb^{-1} at $\sqrt{s}$ = 7 TeV. The requirement $m_{4\ell}$ > 100 GeV is applied.

category	$gg \to H, q\bar{q}/gg \to t\bar{t}H$	$qq' \to Hqq'$	$q\bar{q} \to W/ZH$	$ZZ^{(*)}$
		$\sqrt{s}$ = 8 TeV		
ggF-like	13.5	0.79	0.65	320.4
VBF-like	0.28	0.43	0.01	3.58
VH-like	0.06	-	0.14	0.69
		$\sqrt{s}$ = 7 TeV		
ggF-like	2.20	0.14	0.11	57.5
VBF-like	0.03	0.06	-	0.44
VH-like	0.01	-	0.03	0.25

VBF purity ~60%

VH purity ~70%

$H \rightarrow ZZ^{(*)} \rightarrow 4l$ ($l=e,\mu$) : Event display

Candidate $H \rightarrow 2e2\mu$ (VBF category) $m_{ee\mu\mu}$=123.5 GeV, m_{ee}=94 GeV, $m_{\mu\mu}$=27 GeV, m_{jj}~900 GeV, $\Delta\eta(j,j)$=3.4

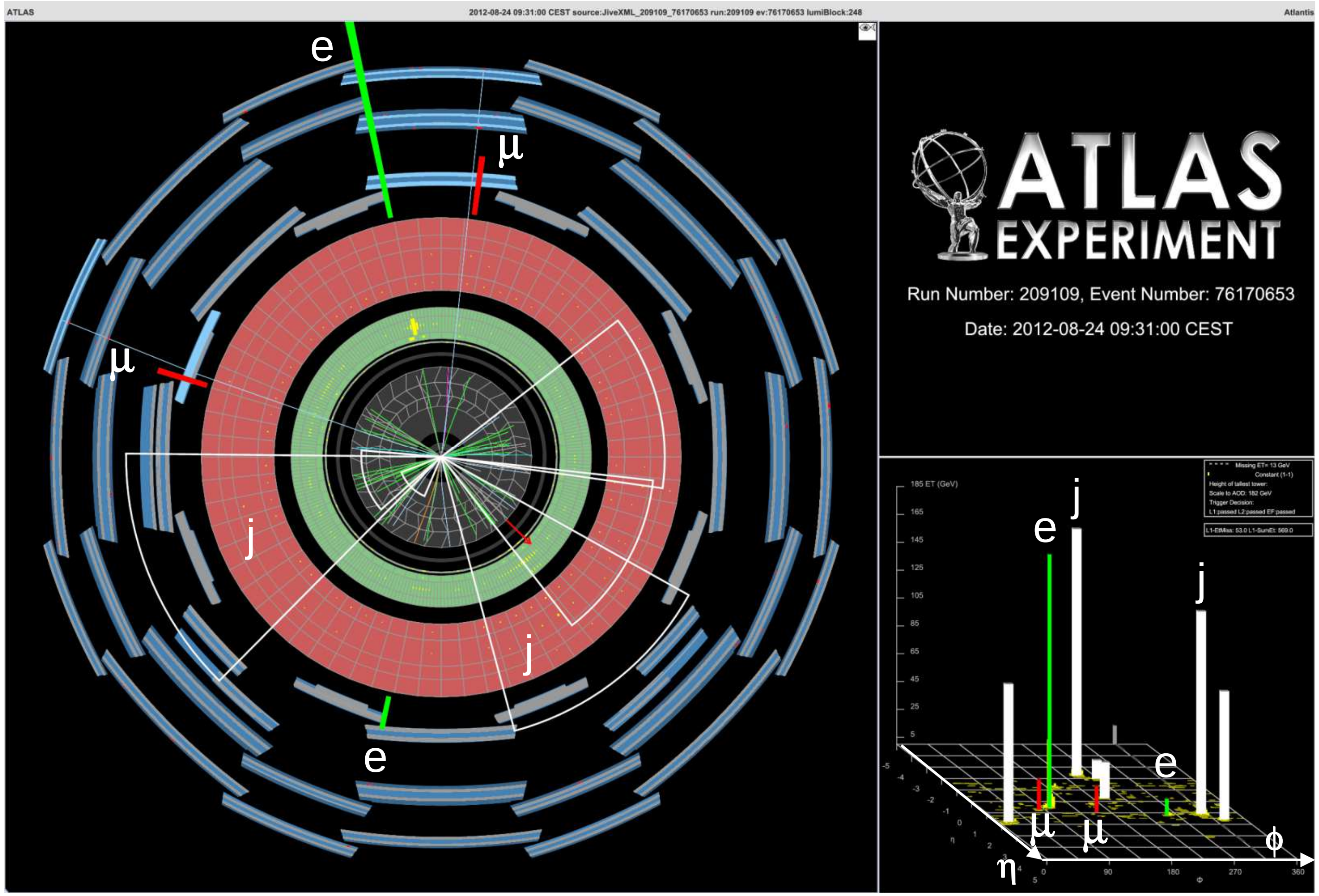

$p_T(e_1,e_2,m_1,m_2,j_1,j_2)$=180/12/22/19/140/110 GeV $\eta(e_1,e_2,m_1,m_2,j_1,j_2)$=0.6/1.2/0.8/1.0/-2.2/1.2

$H \rightarrow ZZ^{(*)} \rightarrow 4l$ ($l=e,\mu$) : Spin-Parity

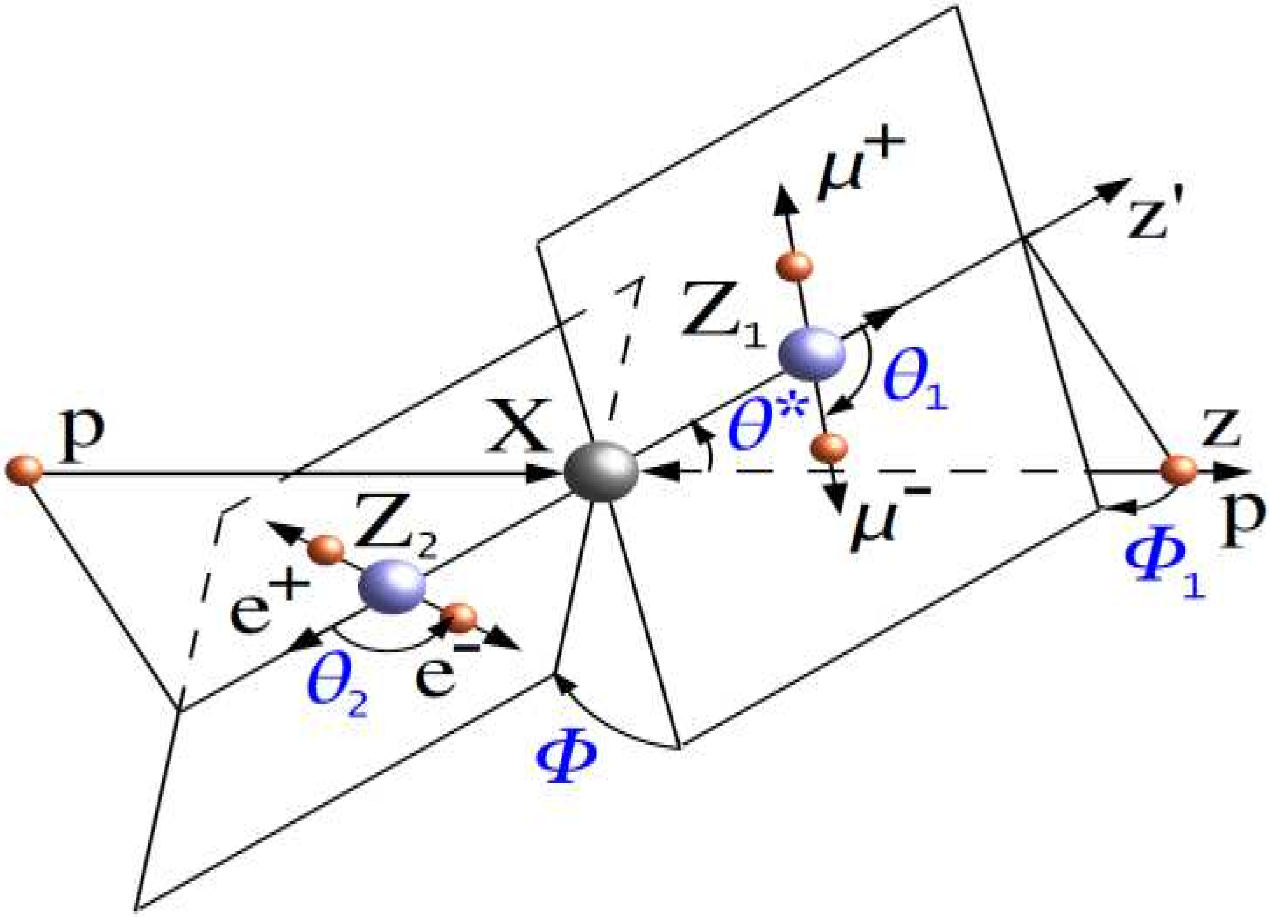

$H \to ZZ^{(*)} \to 4l$ ($l=e,\mu$) : Spin-Parity

Table 9: For an assumed 0^+ hypothesis H_0, the values for the expected and observed p_0-values of the different tested spin and parity hypotheses H_1 for the BDT and J^P-MELA analyses. The results are given combining the $\sqrt{s} = 8$ TeV and $\sqrt{s} = 7$ TeVdata sets. Also given is the observed p_0-value where 0^+ is the test hypothesis and the other spins states are the assumed hypothesis (observed*). These two observed p_0-values are combined to provide the CL_S confidence level for each test hypothesis (i.e. observed p_0-value/(1 - observed* p_0-value)). The production mode is assumed to be 100% ggF.

		BDT analysis				J^P-MELA analysis			
		tested J^P for an assumed 0^+		tested 0^+ for an assumed J^P	CL_S	tested J^P for an assumed 0^+		tested 0^+ for an assumed J^P	CL_S
		expected	observed	observed*		expected	observed	observed*	
0^-	p_0	0.0037	0.015	0.31	0.022	0.0011	0.0022	0.40	0.004
1^+	p_0	0.0016	0.001	0.55	0.002	0.0031	0.0028	0.51	0.006
1^-	p_0	0.0038	0.051	0.15	0.060	0.0010	0.027	0.11	0.031
2^+_m	p_0	0.092	0.079	0.53	0.168	0.064	0.11	0.38	0.182
2^-	p_0	0.0053	0.25	0.034	0.258	0.0032	0.11	0.08	0.116

H→ZZ$^{(*)}$→4l (l=e,μ) : Spin-Parity

Little variation in 0^+ / 2^+ discrimination as a function of qqbar fraction

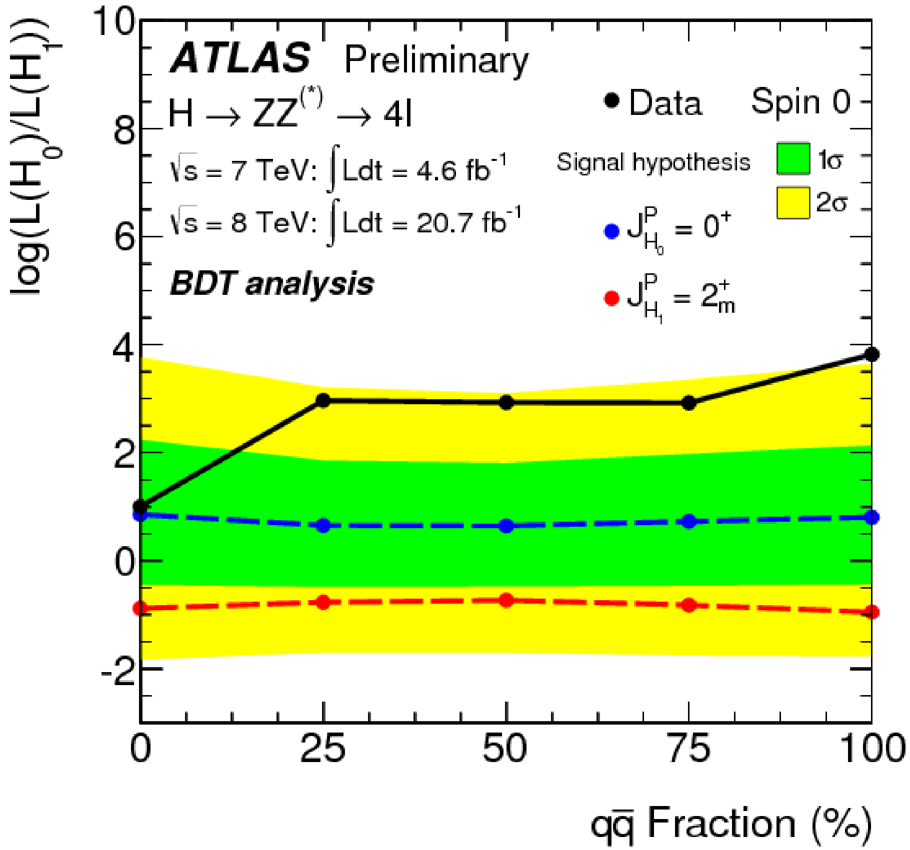

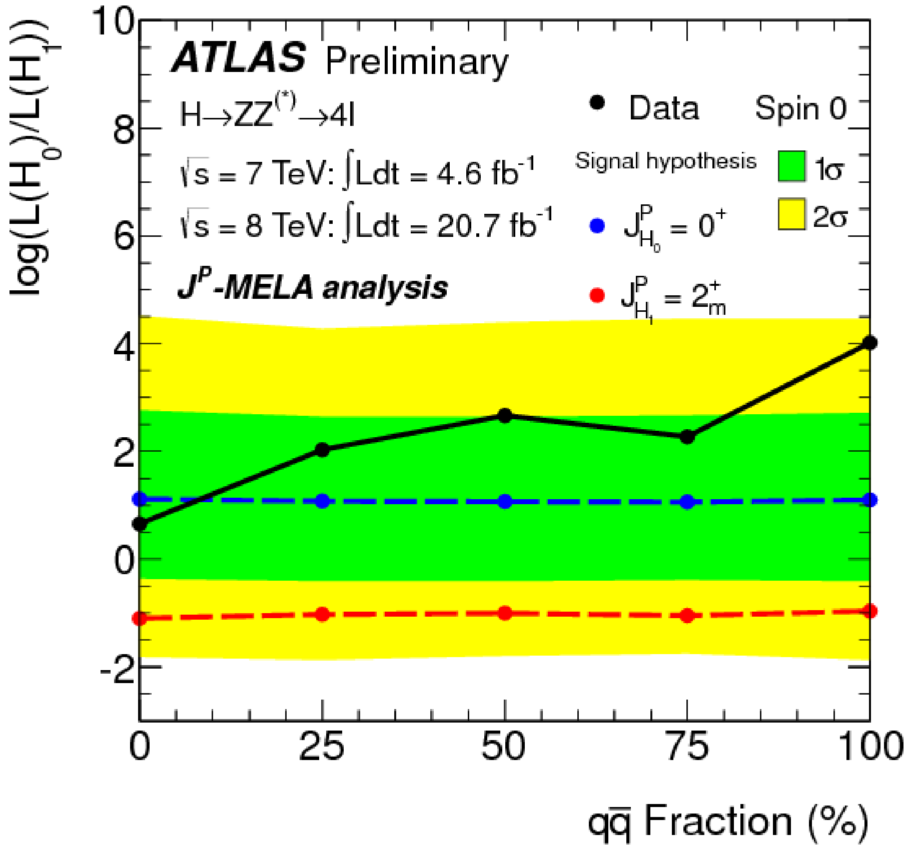

$H \rightarrow WW^{(*)} \rightarrow l\nu l'\nu$ ($l=e,\mu$)

$\sigma \times BR \sim 200$ fb for $m_H \sim 125$ GeV

H→WW$^{(*)}$→lνl'ν (l=e,μ) : Overview

ATLAS-CONF-2012-158

Signal reconstruction

- Broad signal due to undetected neutrinos
- Challenge for missing E_T resolution in harsh pile-up conditions → substantial Drell-Yan background in same-flavor final states

→ analysis focused on different flavor final states for now

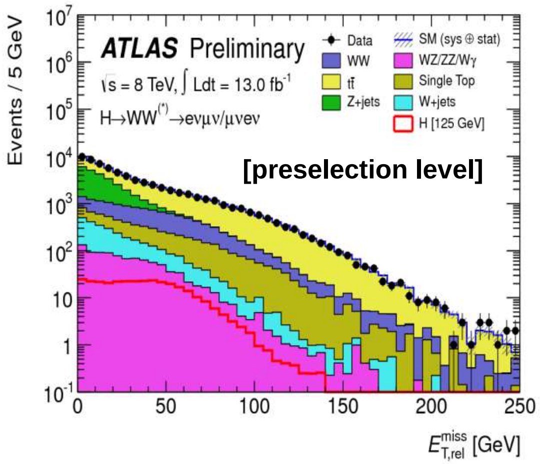

Signal region (0-jet with leading electron)

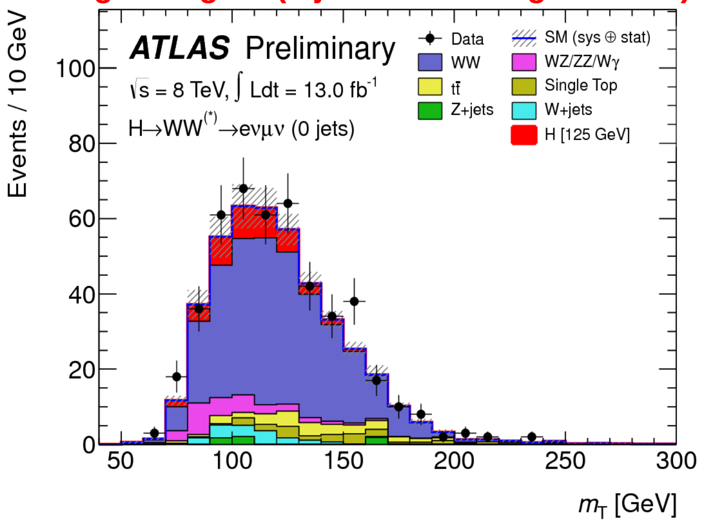

- Two isolated opposite-sign leptons [p_T>25/15 GeV] and large missing E_T
- Exploit signal topology, e.g. from spin-0: low m_{ll}, low $\Delta\Phi_{ll}$
- Use transverse mass as discriminant in final fit

$$m_T = \sqrt{(E_T^{\ell\ell} + E_T^{miss})^2 - |\mathbf{p}_T^{\ell\ell} + \mathbf{E}_T^{miss}|^2}$$

Background control

- Rate/composition largely depends on jet multiplicity
  - ►H+(0-jet): WW, Z/W+jets
  - ►H+(1-jet): WW, top
  - ►H+(≥2-jets): top

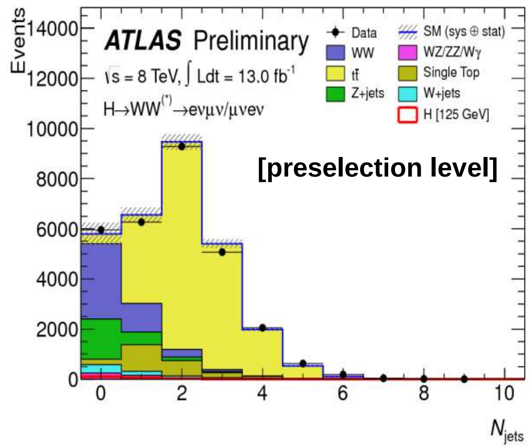

→ Main backnds estimated from signal-free control regions in data

- Analysis in 4 categories: 0/1 jet and leading μ/e

H→WW(*)→lνl'ν (l=e,μ) : background estimates

ATLAS-CONF-2012-158

- Complex mixture of large backgrounds → sensitivity dominated by uncertainties on bknds
- Main backgrounds estimated from signal-free control regions in data
  - WW, top: MC normalised to data in control regions → extrapolation to signal regions
  - W+jets fully estimated from data (including extrapolation factor to signal region)
  - Dibosons (except WW) from MC (validation with W+jets in same-charge region)

Top control region - 1 jet (before rescaling)

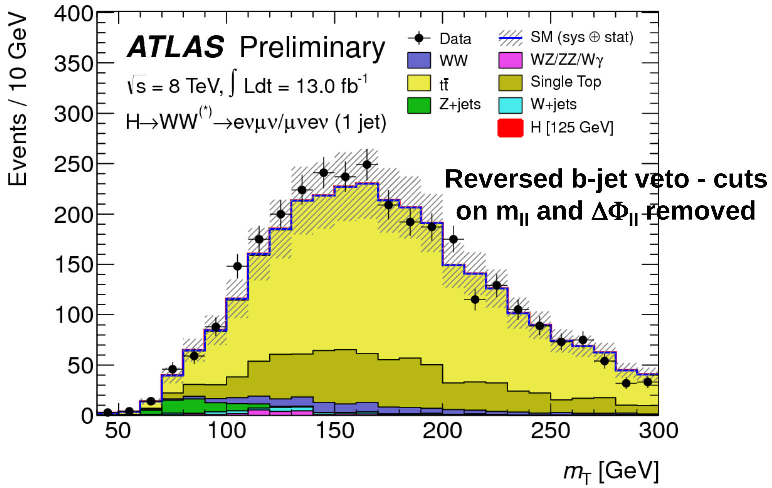

WW control region - 0 jet (before rescaling)

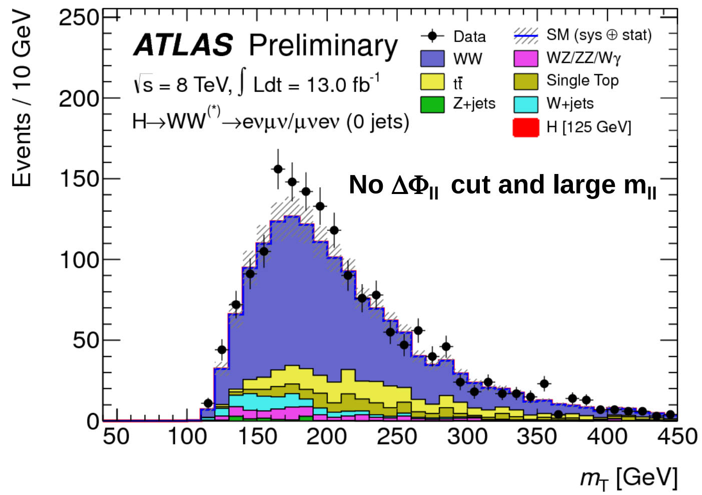

→ MC/data normalisation factor extracted. Good shape agreement.

→Total uncertainty on top in SR: 14%/37% 0/1 jet

→Total uncertainty on WW in SR: 13%/54% 0/1 jet

$H \to WW^{(*)} \to l\nu l'\nu$ ($l=e,\mu$) : Results

ATLAS-CONF-2012-158

Background-subtracted data and signal MC (125 GeV)

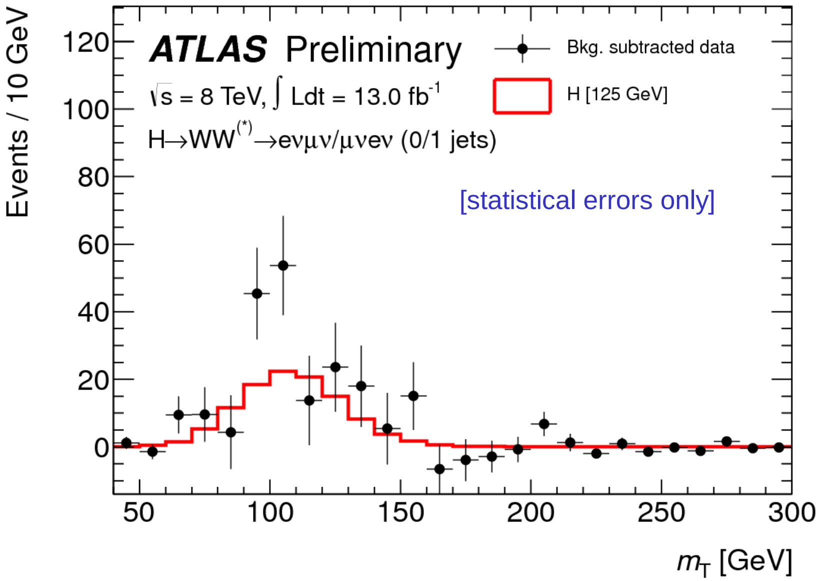

For illustration:

In window $0.75m_H<m_T<m_H$: 564 events observed [448±45 expected from bknd & 63±15 from SM higgs@125 GeV – S/B~0.15]

[excess consistent across all categories]

Broad excess due to poor mass resolution

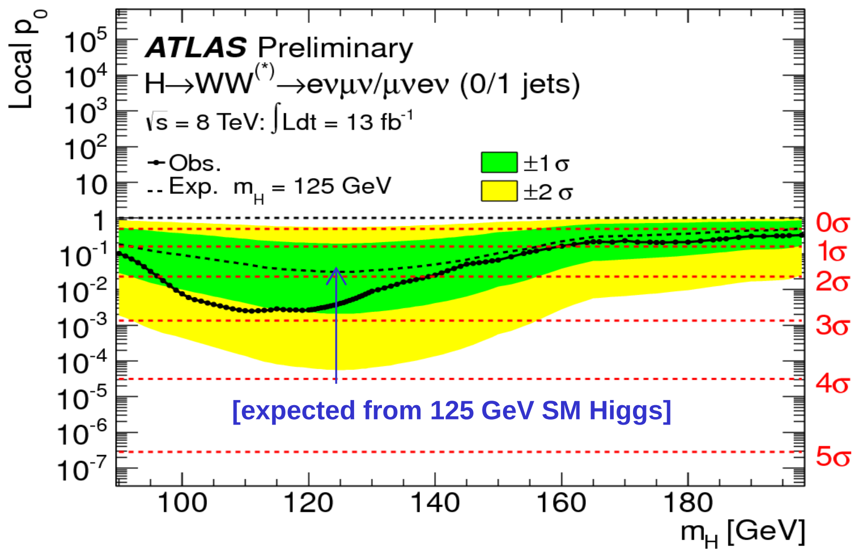

- Observed local significance of the broad excess @ 125 GeV: **2.6σ** (1.9σ expected for SM Higgs).
- Signal strength @ 125GeV **μ=1.5±0.6**

[dominated by systematic uncertainties]

$$\mu = 1.48^{+0.35}_{-0.33}\,(\mathrm{stat})^{+0.41}_{-0.36}\,(\mathrm{syst\ theor})\,^{+0.28}_{-0.27}\,(\mathrm{syst\ exp}) \pm 0.05\,(\mathrm{lumi})$$

$$\sigma(pp \to H)\cdot\mathcal{B}(H \to WW)_{m_H=125\ \mathrm{GeV}} = 7.0\,^{+1.7}_{-1.6}\,(\mathrm{stat})\,^{+1.7}_{-1.6}\,(\mathrm{syst\ theor})\,^{+1.3}_{-1.3}\,(\mathrm{syst\ exp})\ \pm 0.3\,(\mathrm{lumi})\ \mathrm{pb}$$

H→WW(*)→lνl'ν (l=e,μ) : backgrounds

ATLAS-CONF-2012-158

❑ W+jets estimation and same-charge validation region

- Control sample: one lepton fails identification or isolation criteria → fraction of W+jets ~90% (80%) in electron (muon) channel
- Extrapolation in signal region through "fake factor", measured in data (dijet sample)
- Uncertainty on W+jets background, dominated by systematics on fake factor: ~50%
- Shape and normalisation of W+jets & non-WW diboson backgrounds checked in same-charge di-lepton validation region → very good data/MC agreement
- Uncertainty on non-WW diboson backgrounds: 16% (23%) for H+0-jet (H+1-jet)

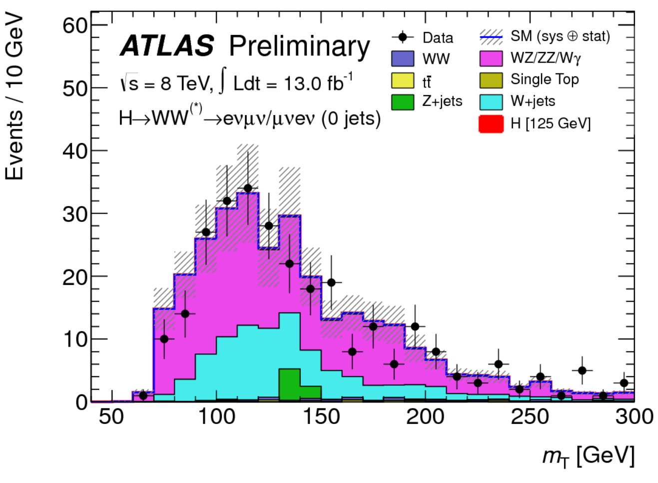

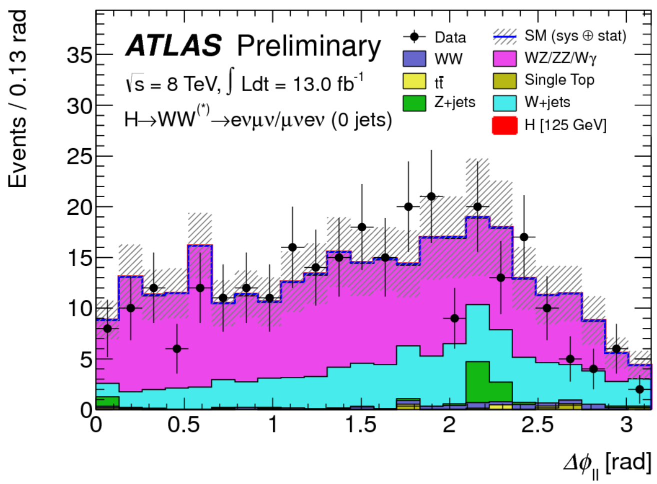

H→WW$^{(*)}$→lνl'ν (l=e,μ) : backgrounds

ATLAS-CONF-2012-158

❑ Top control sample and normalisation

- A major background for channels with >0 jet multiplicicy
- In H+1-jet: control sample = b-jet veto reverted and m_{ll}, $\Delta\Phi_{ll}$ cuts removed
- Small contribution from other backgrounds subtracted (e.g. data-driven for W+jets)
- Normalisation factor applied on MC to match data yield = 1.03±0.02 (stat)
- Uncertainty on top backgrounds in signal region: 14% (37%) for H+0-jet (H+1-jet)

Top control region (1 jet) , before rescaling

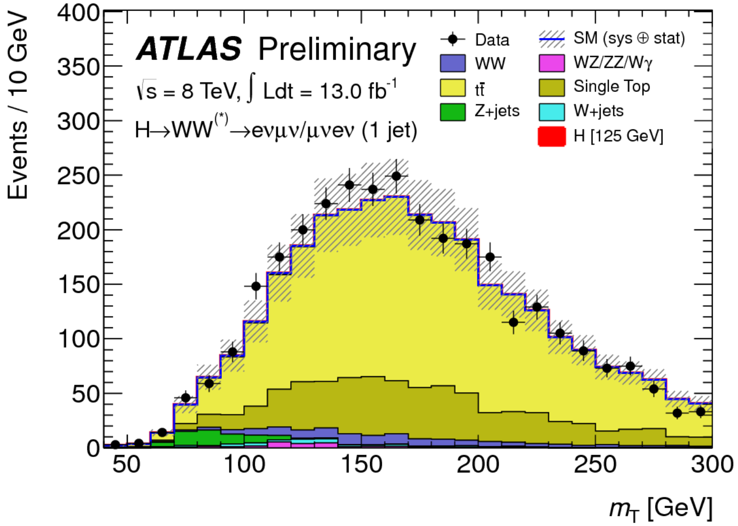

Top control region (1 jet) , after rescaling

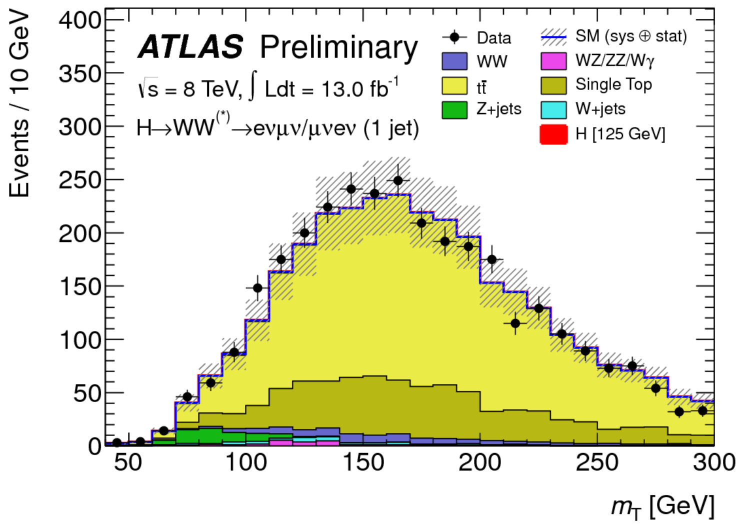

H→WW(*)→lνl'ν (l=e,μ) : backgrounds

ATLAS-CONF-2012-158

❑ WW control sample and normalisation

- control sample = $\Delta\Phi_{ll}$ cut removed and large m_{ll} → 70% (40%) WW events in 0-jet (1-jet)
- Contribution from other backgrounds derived as for signal region
- Large normalisation factor = 1.13±0.04 (stat) for H+0-jet and 0.84±0.08 (stat) for H+1-jet
- But good agreement in kinematic variable shapes m_T, m_{ll}, $\Delta\Phi_{ll}$
- Uncertainty on WW backgrounds in signal region: 13% (54%) for H+0-jet (H+1-jet)

WW control region (0 jet), before rescaling

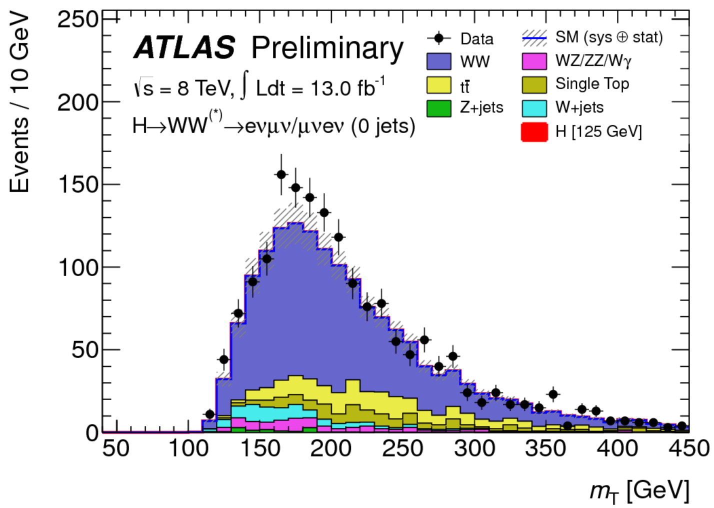

WW control region (1 jet), before rescaling

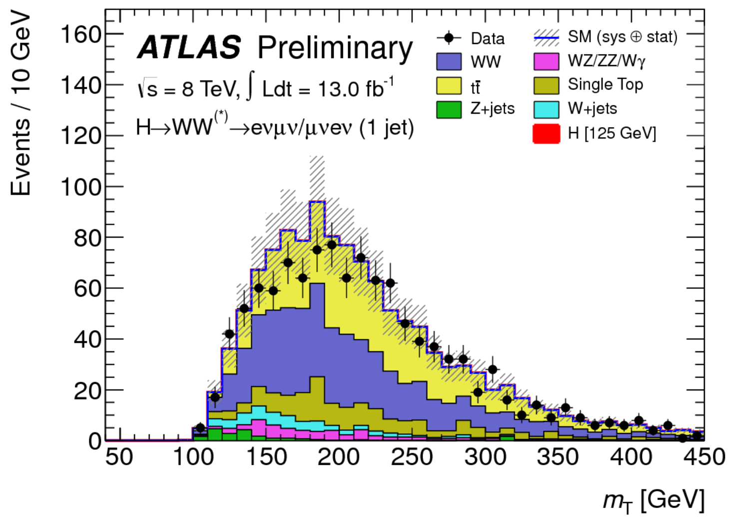

H→WW(*)→lνl'ν (l=e,μ) : signal regions

ATLAS-CONF-2012-158

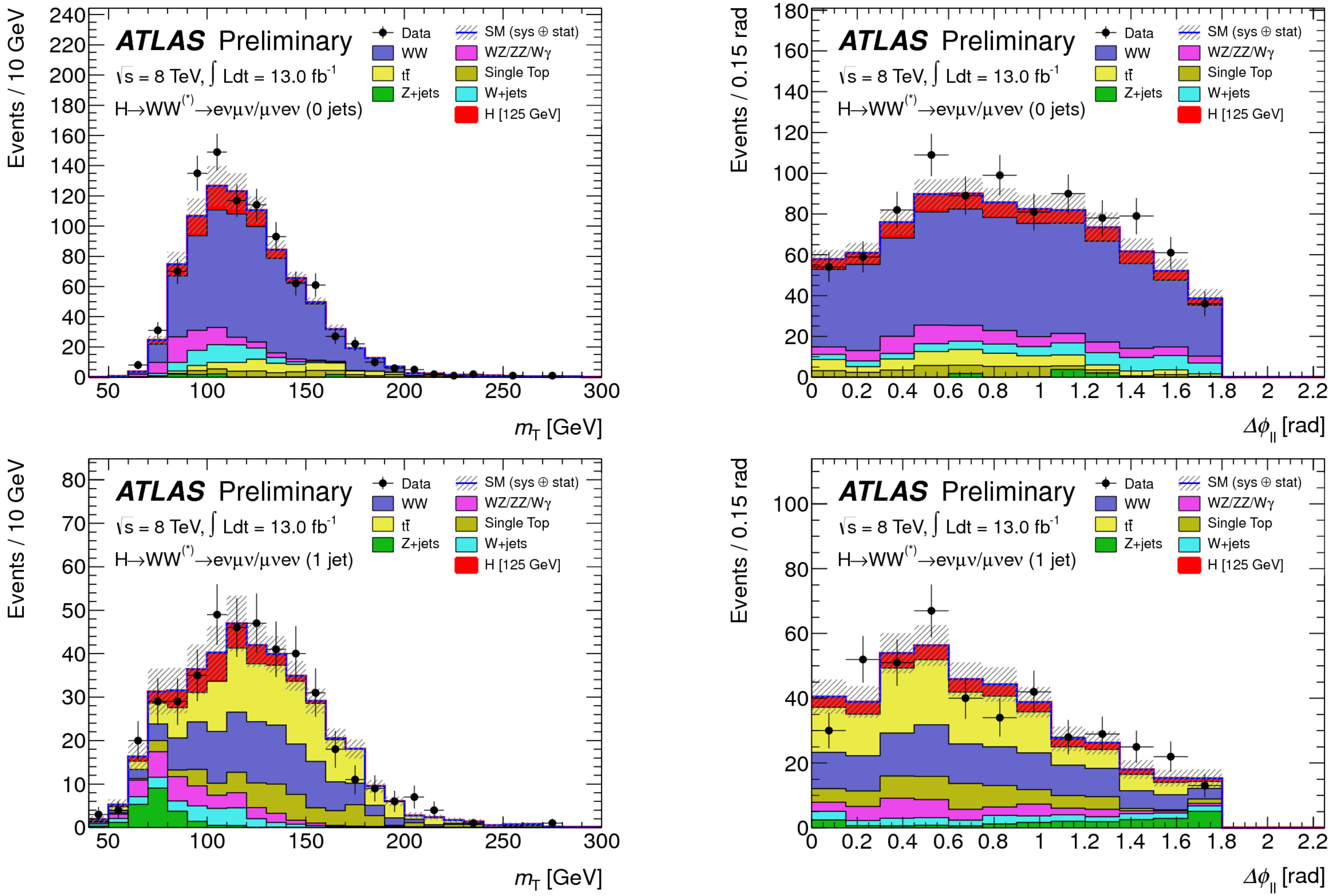

$H \rightarrow WW^{(*)} \rightarrow l\nu l'\nu$ (l=e,μ) : signal regions

ATLAS-CONF-2012-158

Number of events in individual channels after full selection

→ excess consistent across channels

Signal region yield for $e\mu$ and μe channels separately				
	0-jet $e\mu$	0-jet μe	1-jet $e\mu$	1-jet μe
Total bkg.	392 ± 7	382 ± 6	202 ± 6	184 ± 5
Signal	41.8 ± 0.6	33.8 ± 0.5	18.9 ± 0.4	16.0 ± 0.4
Observed	469	448	226	207

In window $0.75m_H < m_T < m_H$

	Signal	WW	$WZ/ZZ/W\gamma$	$t\bar{t}$	$tW/tb/tqb$	Z/γ^* + jets	W + jets	Total Bkg.	Obs.
H+ 0-jet	45 ± 9	242 ± 32	26 ± 4	16 ± 2	11 ± 2	4 ± 3	34 ± 17	334 ± 28	423
H+ 1-jet	18 ± 6	40 ± 22	10 ± 2	37 ± 13	13 ± 7	2 ± 1	11 ± 6	114 ± 18	141

$H \rightarrow WW^{(*)} \rightarrow l\nu l'\nu$ ($l=e,\mu$) : systematics

ATLAS-CONF-2012-158

Leading systematics on event yield

Source (0-jet)	Signal (%)	Bkg. (%)
Inclusive ggF signal ren./fact. scale	13	-
1-jet incl. ggF signal ren./fact. scale	10	-
PDF model (signal only)	8	-
QCD scale (acceptance)	4	-
Jet energy scale and resolution	4	2
W+jets fake factor	-	5
WW theoretical model	-	5
Source (1-jet)	**Signal (%)**	**Bkg. (%)**
1-jet incl. ggF signal ren./fact. scale	26	-
2-jet incl. ggF signal ren./fact. scale	15	-
Parton shower/ U.E. model (signal only)	10	-
b-tagging efficiency	-	11
PDF model (signal only)	7	-
QCD scale (acceptance)	4	2
Jet energy scale and resolution	1	3
W+jets fake factor	-	5
WW theoretical model	-	3

H→WW(*)→lνl'ν (l=e,μ) : signal strength

ATLAS-CONF-2012-158

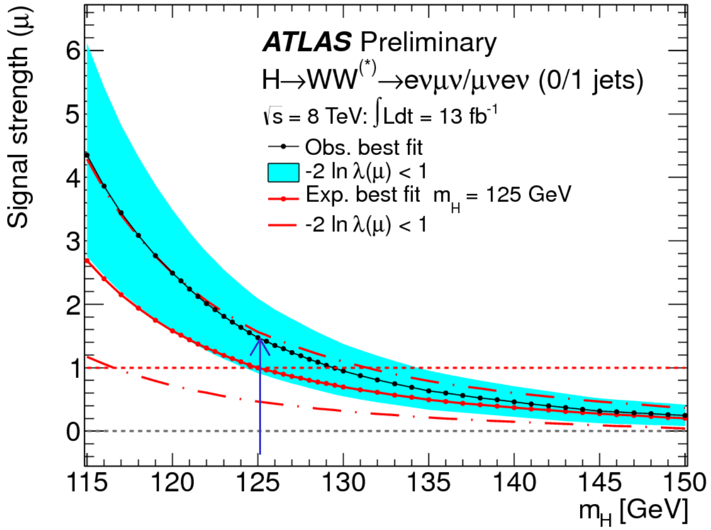

$$\mu = 1.48^{+0.35}_{-0.33}\,(\text{stat})^{+0.41}_{-0.36}\,(\text{syst theor})\,^{+0.28}_{-0.27}\,(\text{syst exp}) \pm 0.05\,(\text{lumi})$$

Increase of fitted signal strength at low m_H due to decrease of expected σ·Br for signal

Table 7: Dominant contributions to the relative uncertainty on the measured signal strength for m_H = 125 GeV. The total relative uncertainty is also given. The large uncertainty on the signal strength from WW normalisation is due to the significant size of this background in comparison with the signal.

Systematics on signal strength

Source	Upward uncertainty (%)	Downward uncertainty (%)
Statistical uncertainty	+23	-22
Signal yield ($\sigma \cdot \mathcal{B}$)	+14	-9
Signal acceptance	+9	-6
WW normalisation, theory	+20	-20
Other backgrounds, theory	+9	-9
W+jets fake rate	+11	-12
Experimental + bkg subtraction	+14	-11
MC statistics	+8	-8
Total uncertainty	+41	-38

Missing ET reconstruction vs pile-up

- Pileup dependence from soft activity in calorimeter
- Including tracking information helps to mitigate effects from pileup interactions
- Missing E_T resolution in Z→μμ events w/wo soft-term vertex fraction (STVF) correction:

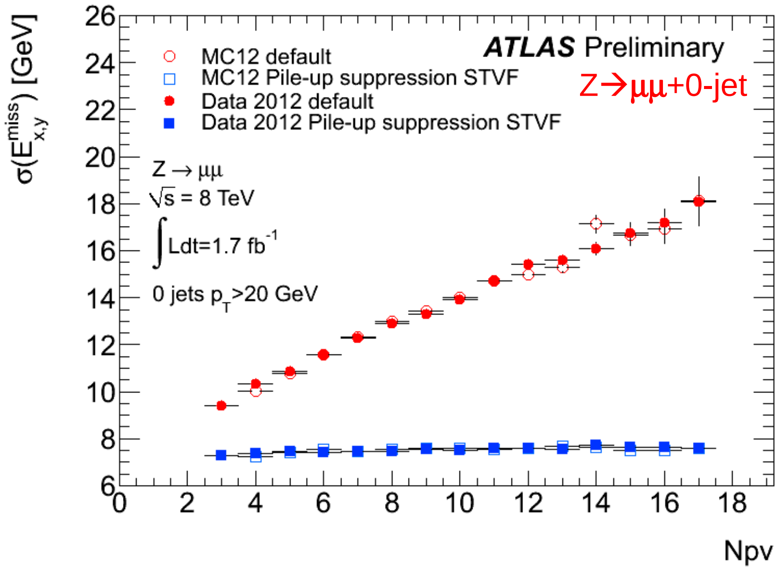

- Missing E_T soft term scaled (event by event) by STVF: ratio of the sum of p_T of tracks associated to the primary vertex and all tracks not associated to reconstructed objects

$$STVF = \left(\sum p_T^{track,PV} \Big/ \sum p_T^{track}\right)_{\substack{unmatched\\objects}}$$

WH→WWW$^{(*)}$→lνlνlν (l=e,μ)

ATLAS-CONF-2012-078

- Dedicated analysis with full 2011 dataset → high sensitivity to H to WW coupling (both production and decay)
- ==3 isolated leptons and large Etmiss. Other cuts: at most 1 jet (without b-tag), small ΔR(<2) between oppositely charged leptons. Events from dilepton H→WW analysis vetoed. 2 categories: “Z enriched” (with SFOS leptons) and “Z depleted” (without)
- Main backgrounds: WZ, Z+jets, top – normalisation and shapes OK in control regions
- Limit at m_H=125 GeV: ~7*SM cross-section – best limit at m_H=165 GeV: 2.7*SM

	$W(H\to WW)$	$Z(H\to WW)$	$V(H\to\tau\tau)$	$H\to ZZ$	Observed	Total Bkg.
Pre-selection	1.78±0.15	3.56±0.30	0.66±0.06	0.97±0.08	2077	2240±260
Z enriched	1.36±0.11	3.50±0.28	0.54±0.05	0.97±0.08	2056	2220±260
At most 1 jet, not b-tagged	1.24±0.12	2.22±0.21	0.48±0.05	0.80±0.07	1801	1960±240
$E_{T,rel}^{miss} > 40$ GeV	0.61±0.05	0.54±0.05	0.10±0.01	0.01±0.01	114	115±10
Z mass veto	0.47±0.05	0.04±0.01	0.04±0.01	−−	13	9.9±2.2
All cuts	0.34±0.06	0.03±0.01	0.02±0.01	−−	3	3.7±0.9
Z depleted	0.43±0.06	0.06±0.01	0.12±0.02	−−	21	12.49±1.07
At most 1 jet, not b-tagged	0.40±0.06	0.04±0.01	0.11±0.02	−−	7	4.9±0.9
$E_{T,rel}^{miss} > 25$ GeV	0.26±0.03	0.02±0.01	0.04±0.01	−−	1	1.22±0.24
All cuts	0.18±0.04	0.01±0.01	0.03±0.01	−−	0	0.25±0.15

Background fully dominated by WZ

Production cross-section limits

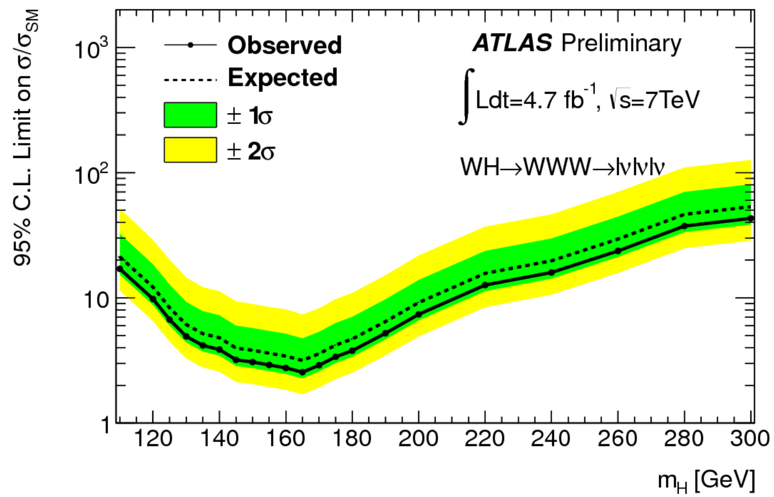

H→Zγ

H→Zγ

ATLAS-CONF-2013-009

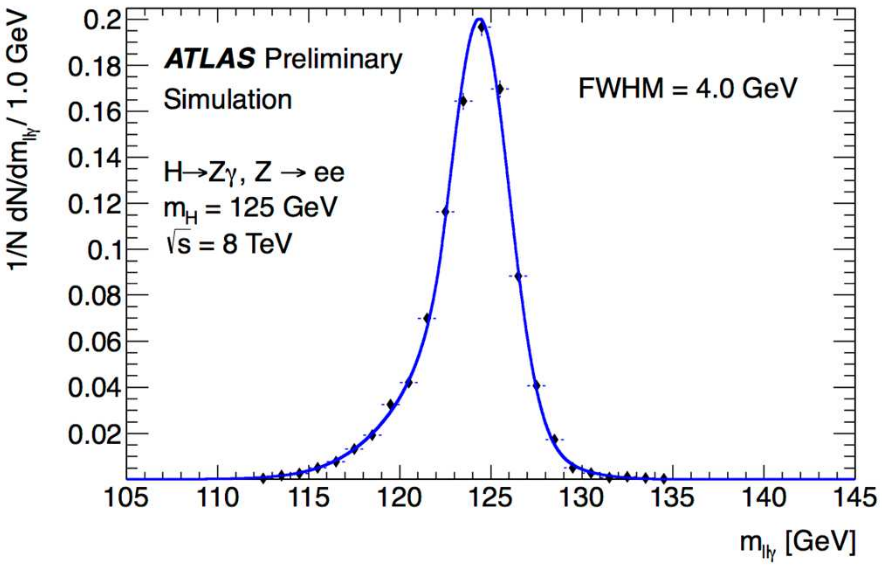

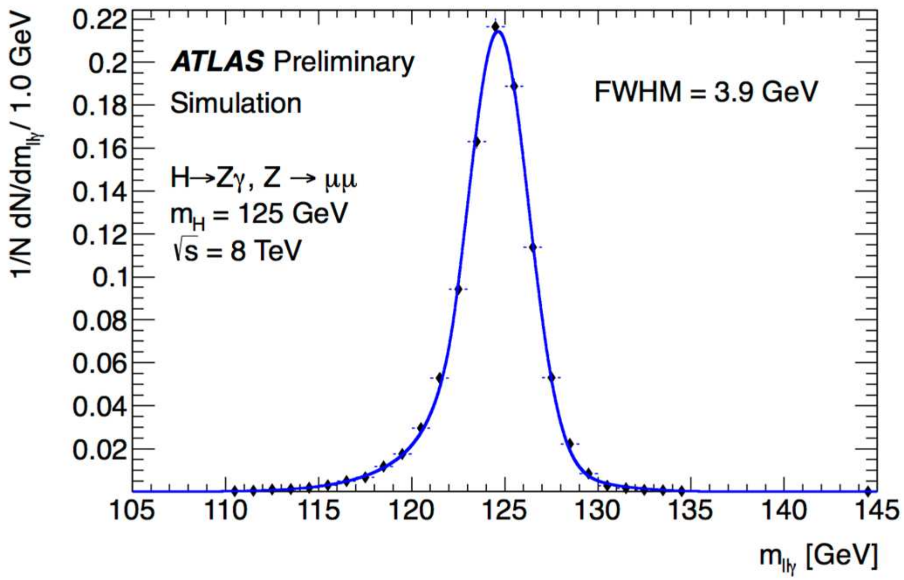

m_H	$Z \to ee$, 7 TeV		$Z \to \mu\mu$, 7 TeV		$Z \to ee$, 8 TeV		$Z \to \mu\mu$, 8 TeV	
[GeV]	ε [%]	S	ε [%]	S	ε [%]	S	ε [%]	S
120	17.1	0.6	22.5	0.7	21.3	4.0	25.8	4.9
125	20.4	0.9	26.5	1.1	24.6	5.9	29.7	7.2
130	23.0	1.1	29.9	1.5	27.3	7.7	32.8	9.3
135	25.1	1.3	32.4	1.7	29.4	9.0	35.1	10.7
140	26.6	1.4	34.1	1.8	30.9	9.5	36.6	11.3
145	27.5	1.4	35.0	1.8	31.7	9.2	37.3	10.8
150	27.9	1.2	35.1	1.5	32.0	8.1	37.2	9.4

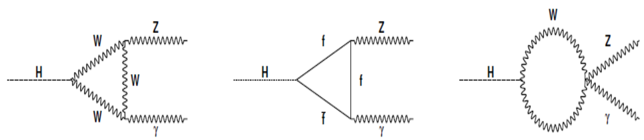

H→Zγ

ATLAS-CONF-2013-009

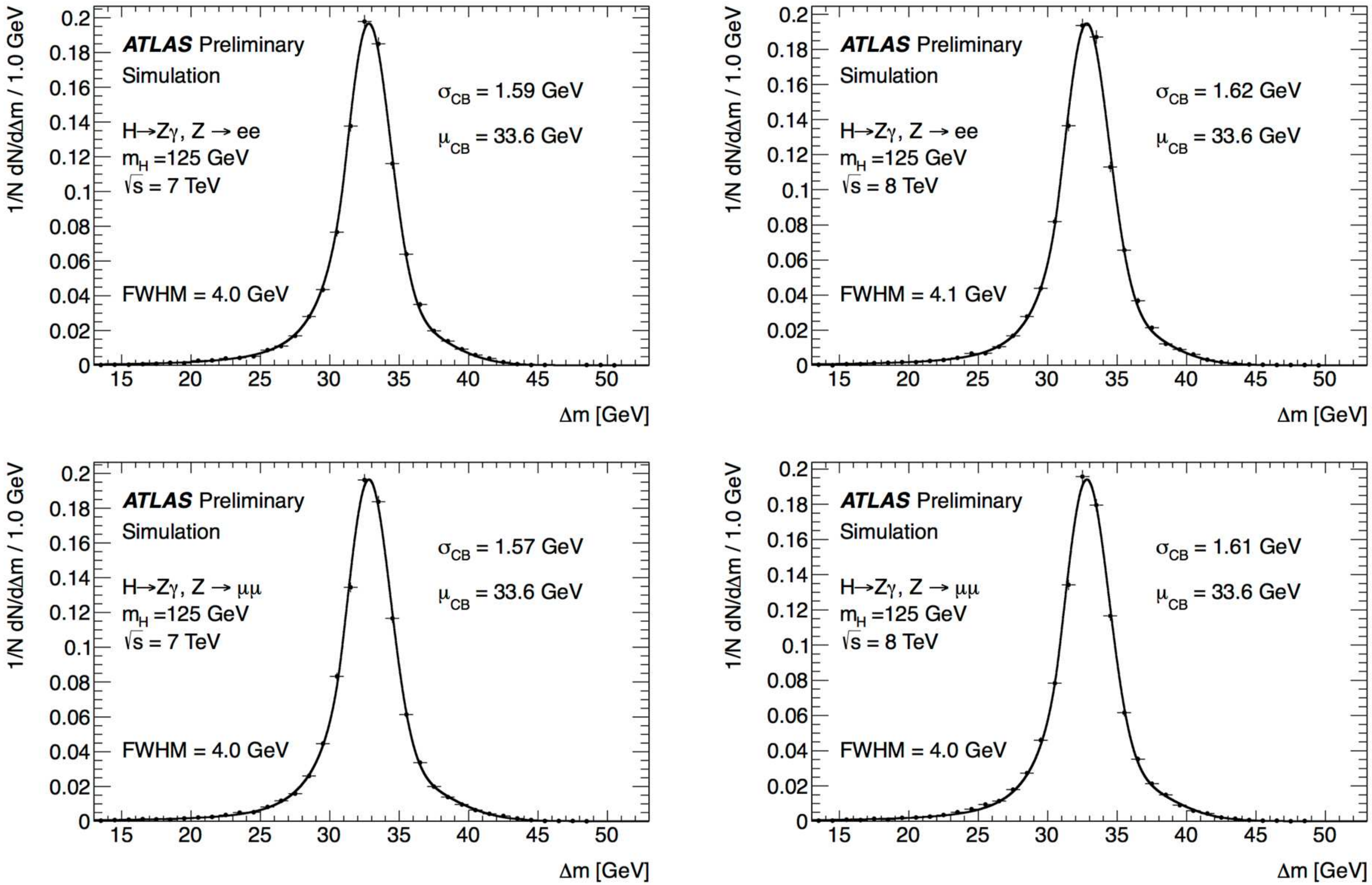

H→Zγ

ATLAS-CONF-2013-009

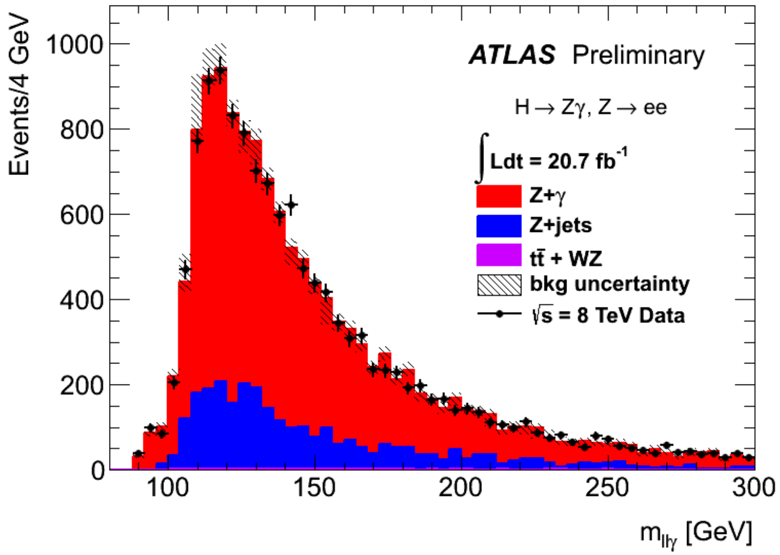

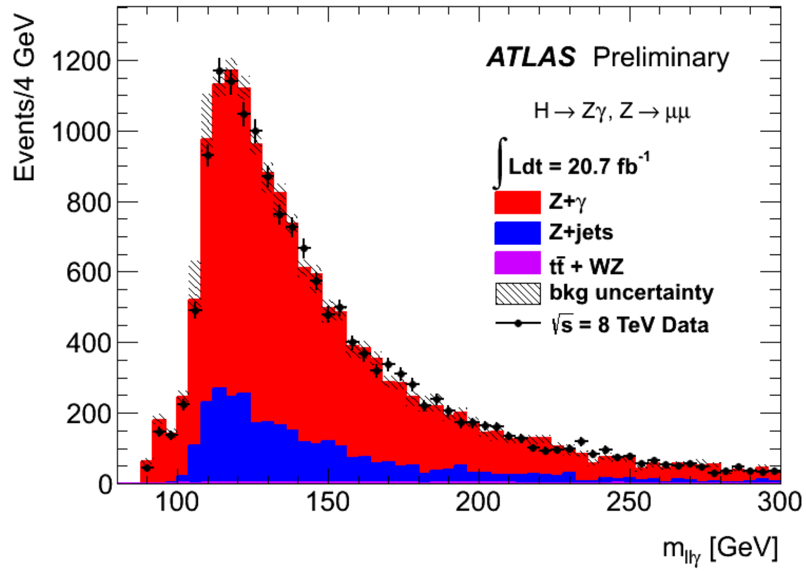

❑ Data-driven background decomposition

- Small backgrounds from ttbar and WZ evaluated from Monte Carlo
- Z+γ / Z+jets contributions estimated in situ from 2D sideband technique [photon ID vs isolation]
- Fractions of backgrounds estimated: 82%/17%/1% for Z+γ/Z+jets/others
- Good agreement data/MC → good understanding of backgrounds
- Decomposition not directly used in Higgs search → bknd extrapolated from data sidebands

H→Zγ

ATLAS-CONF-2013-009

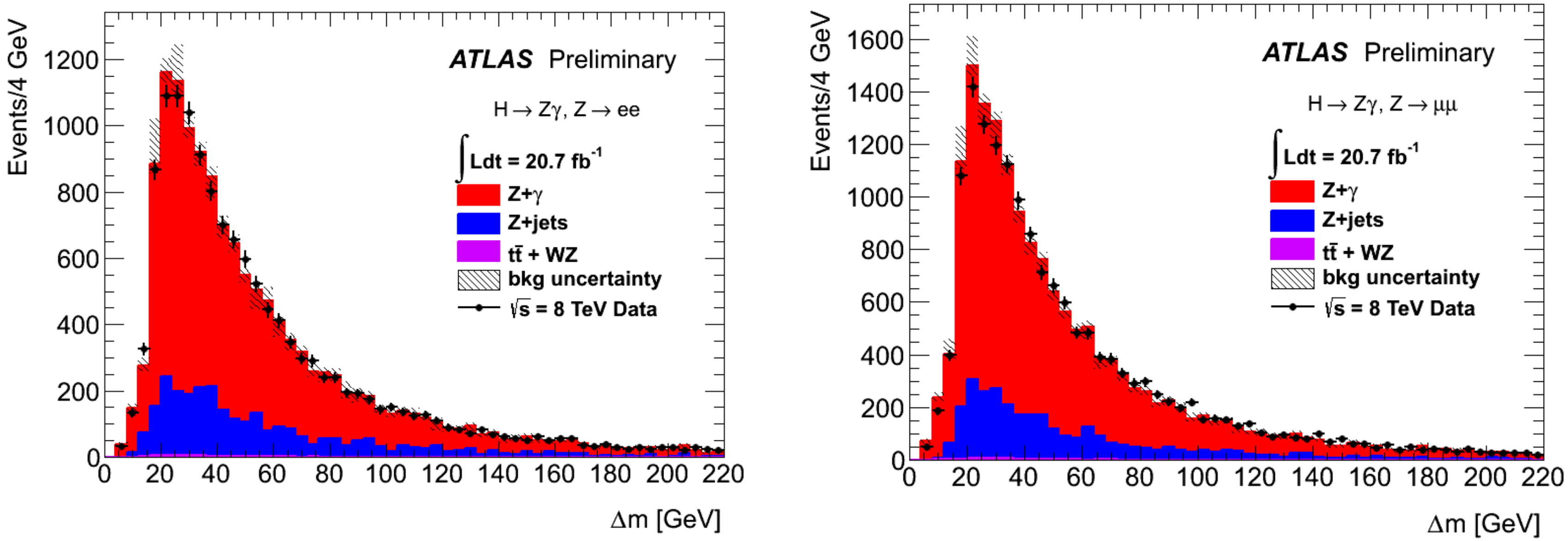

❑ Data-driven background decomposition

- Small backgrounds from ttbar and WZ evaluated from Monte Carlo
- Z+γ / Z+jets contributions estimated in situ from 2D sideband technique [photon ID vs isolation]
- Fractions of backgrounds estimated: 82%/17%/1% for Z+γ/Z+jets/others
- Good agreement data/MC → good understanding of backgrounds
- Decomposition not directly used in Higgs search → bknd extrapolated from data sidebands

H→Zγ

ATLAS-CONF-2013-009

Table 3: Summary of the systematic uncertainties on the signal yield and invariant mass distribution for $m_H = 125$ GeV, at $\sqrt{s} = 8(7)$ TeV.

Systematic Uncertainty	$H \to Z(ee)\gamma(\%)$	$H \to Z(\mu\mu)\gamma(\%)$
Signal Yield		
Luminosity	3.6 (1.8)	3.6 (1.8)
Trigger efficiency	0.4 (0.2)	0.8 (0.7)
Acceptance of kinematic selection	4.0 (4.0)	4.0 (4.0)
γ identification efficiency	2.9 (2.9)	2.9 (2.9)
electron reconstruction and identification efficiency	2.7 (3.0)	
μ reconstruction and identification efficiency		0.6 (0.7)
e/γ energy scale	1.4 (0.3)	0.3 (0.2)
e/γ isolation	0.4 (0.3)	0.4 (0.2)
e/γ energy resolution	0.2 (0.2)	0.0 (0.0)
μ momentum scale		0.1 (0.1)
μ momentum resolution		0.0 (0.1)
Signal Δm resolution		
e/γ energy resolution	5.0 (5.0)	2.4 (2.4)
μ momentum resolution		0.0 (1.5)
Signal Δm peak position		
e/γ energy scale	0.2 (0.2) GeV	0.2 (0.2) GeV
μ momentum scale		negligible

H→Zγ

ATLAS-CONF-2013-009

Δm=$m_{ll\gamma}$-m_{ll} distributions and background-only fit [fit with 3rd order polynomials]

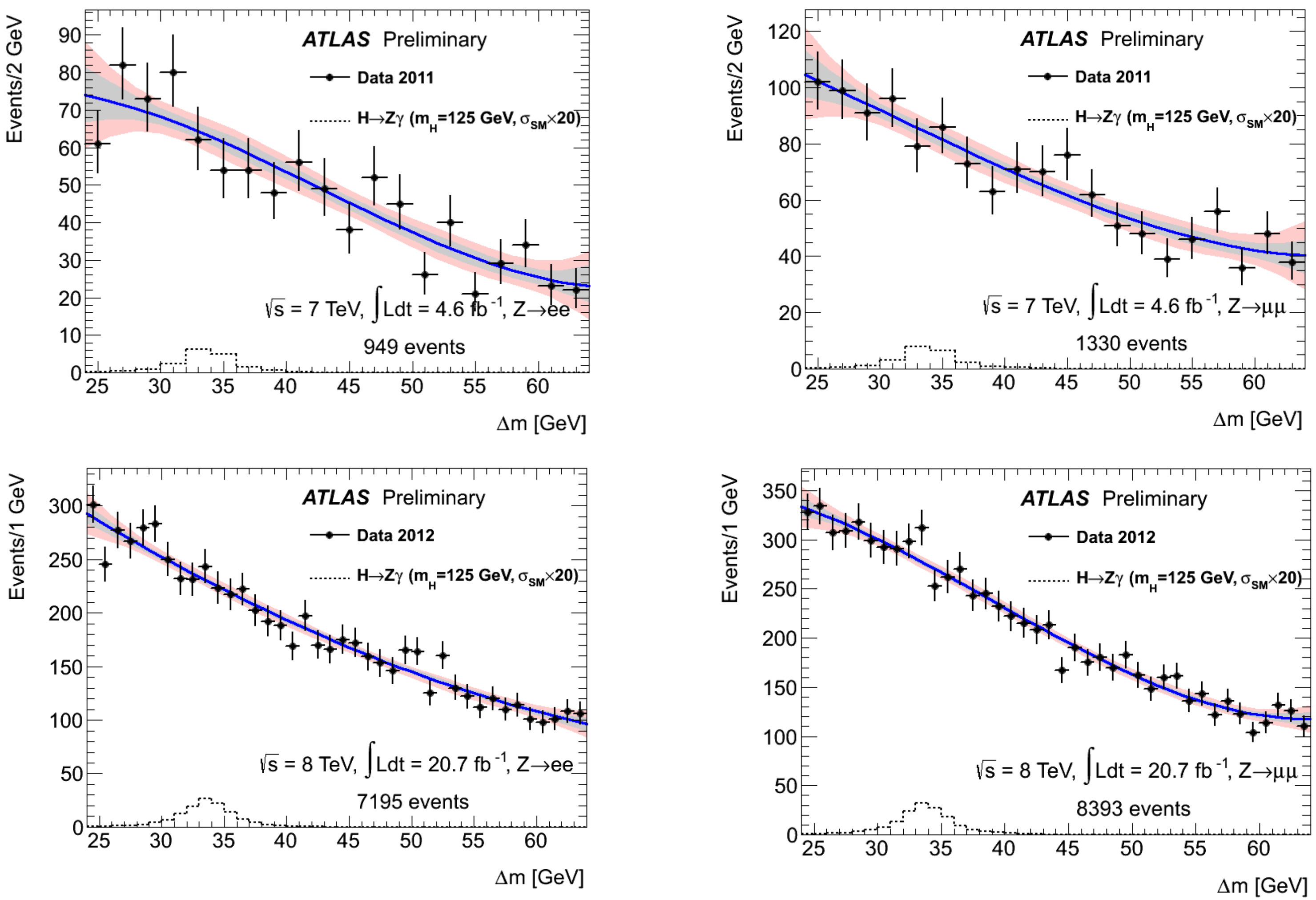

H→Zγ

ATLAS-CONF-2013-009

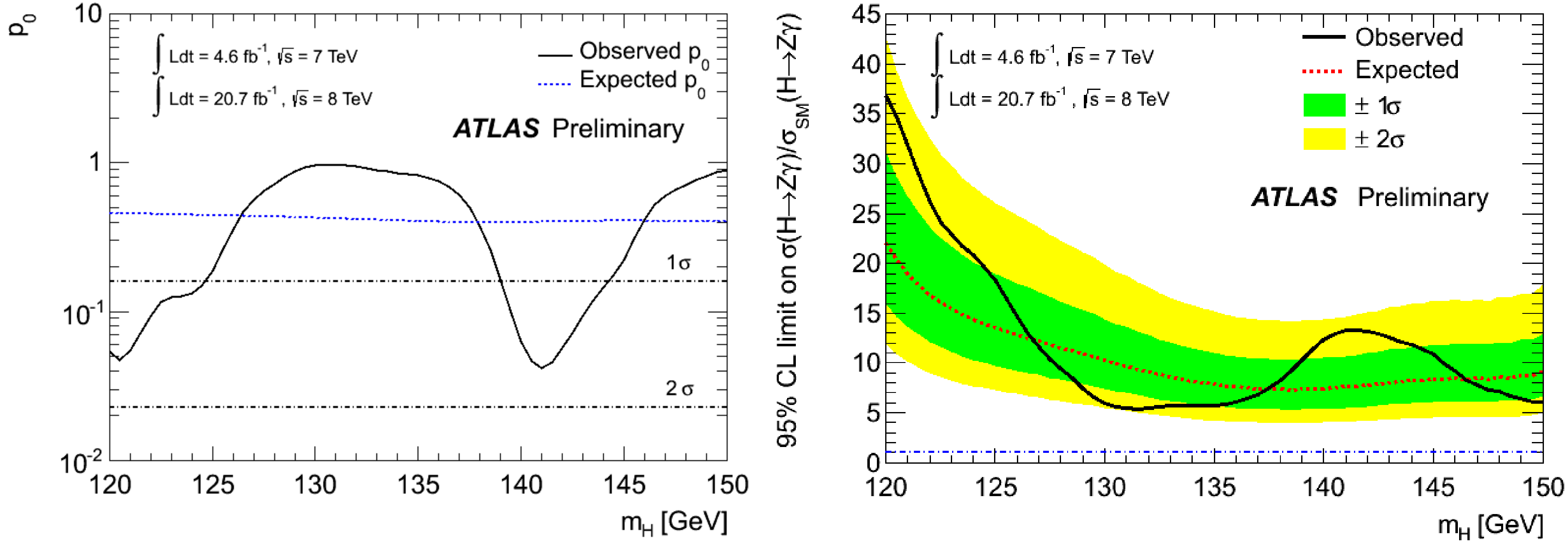

- p_0 at m_H=125 GeV: 0.188 (0.9σ) (expected p_0: 0.043)
- limit at m_H=125 GeV: 18.2×SM cross-section (expected 13.5×SM)

H→Zγ

In addition to H→Zγ followed by Z→ll, H→llγ may receive contributions from internal conversions in H→γγ and from FSR in H→ll

arXiv:1211.6058

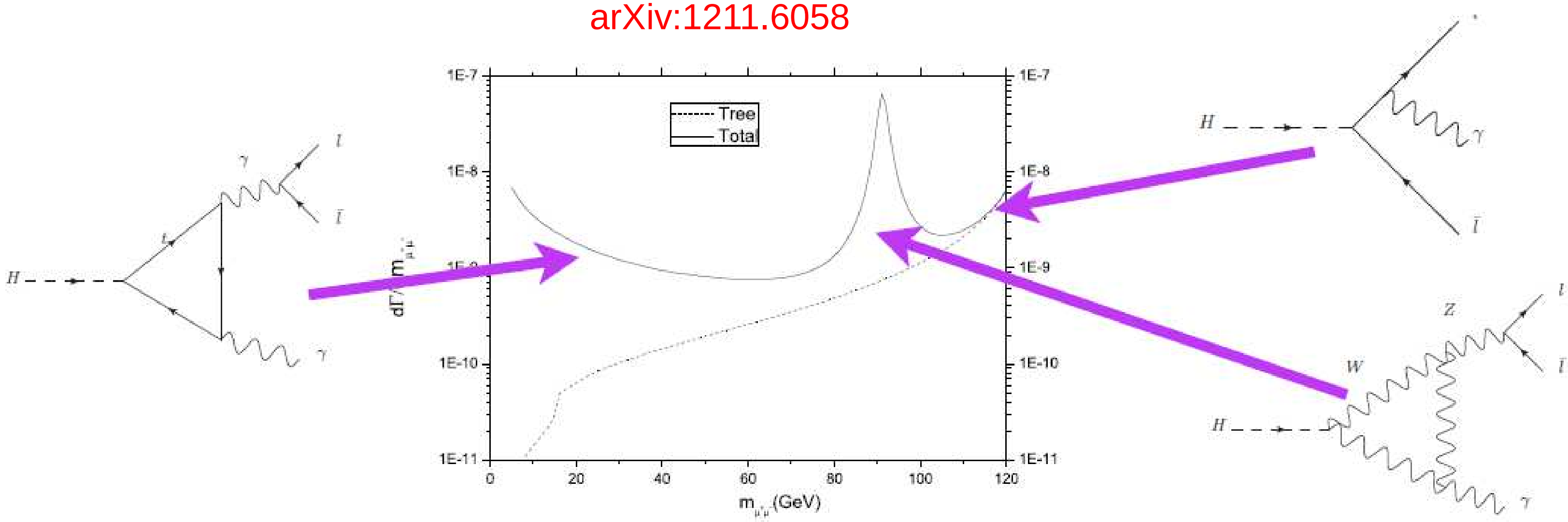

- H→γγ*: <1% of the H→Zγ signal after cuts (e.g. mll cut)
- H→ll*: l and soft γ tend to be collinear → suppressed by p_T^γ and ΔR(l,γ) cuts
- H→ll* peaks in $m_{ll\gamma}$ at m_H but not in Δm → Δm chosen as final discriminant

High-mass searches

High-mass searches in dibosons

❑ High-mass SM Higgs searches

PLB 717 (2012) 29 | PLB 717 (2012) 70 | PLB 718 (2012) 391

- Analyses published with full 2011 dataset (4.7 fb^{-1} @ $\sqrt{s}$=7 TeV) → no excess above SM
- Complement the analyses made with ZZ→4l and WW→lνlν final states at high-mass

H→ZZ→llνν (l=e,μ)

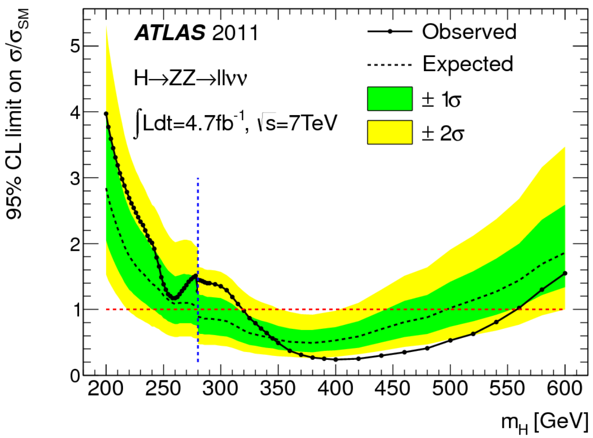

H→ZZ→llqq (l=e,μ)

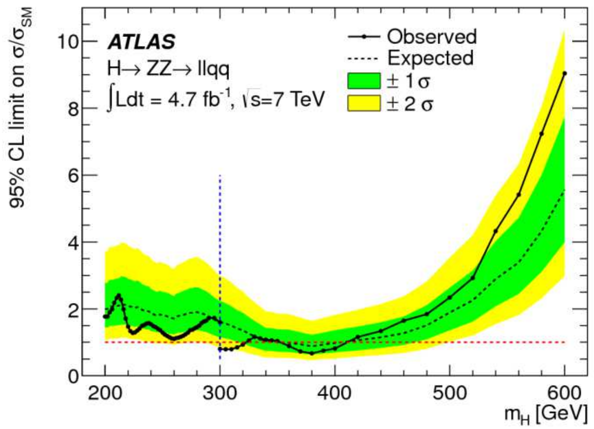

H→WW→lνqq (l=e,μ)

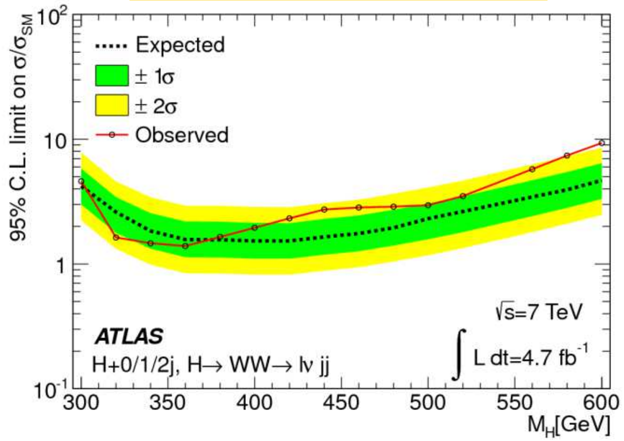

→ Need to be re-interpreted in light of X(125) discovery

- Remark: Z$^{(*)}$Z→llqq final state also used for a low mass Higgs search analysis

ATLAS-CONF-2012-163

$H \rightarrow ZZ \rightarrow ll\nu\nu$ ($l=e,\mu$)

PLB 717 (2012) 29

- Analysis published with full 2011 dataset
- 2 isolated OS leptons (third lepton veto), $|m_{ll}-m_Z|<15$ GeV, b-tag veto – Etmiss and $\Delta\phi_{ll}$ cuts in 2 mass regions (mass-dependent kinematics – boost of Zs increases with m_H)
- Main backgrounds: inclusive Z production, dibosons, top
- SM Higgs exclusion limits at 95% CL: 319-558 GeV (expected: 280-497 GeV)
- Need to be re-interpreted in light of X(125) discovery

m_T distributions in low (left) and high (right) mass signal region

$$m_T^2 \equiv \left[\sqrt{m_Z^2 + |\vec{p}_T^{\,\ell\ell}|^2} + \sqrt{m_Z^2 + |\vec{p}_T^{\,\rm miss}|^2}\right]^2 - |\vec{p}_T^{\,\ell\ell} + \vec{p}_T^{\,\rm miss}|^2$$

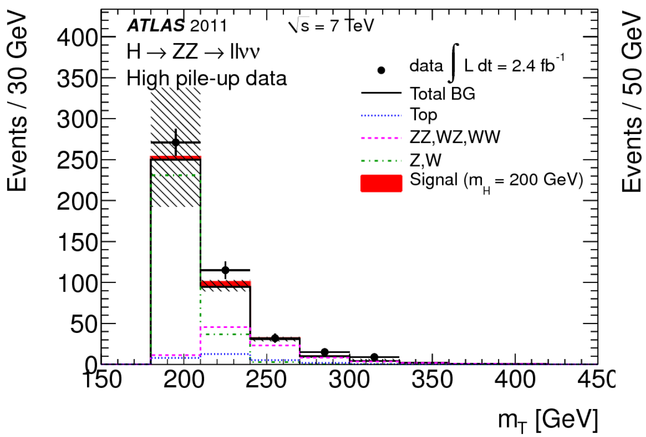

Production cross-section limits

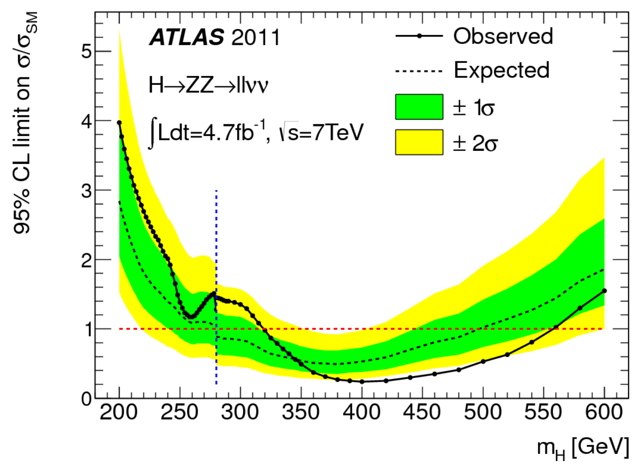

H→ZZ→llqq (l=e,μ)

PLB 717 (2012) 70

- Analysis published with full 2011 dataset for high mass region [200-600] GeV (CONF note ATLAS-CONF-2012-163 for search in low mass range [120-180] GeV)
- 2 isolated OS leptons (third lepton veto), $83<m_{ll}<99$ GeV, Etmiss<50 GeV. 2 jets with $70<m_{jj}<105$ GeV. 2 categories (<2 or =2 b-tags). 2 mass regions (mass-dependent kinematics – boost of Zs increases with m_H)
- Main backgrounds: Z+jets, top – normalisations from control regions (m_{jj} & m_{ll} sidebands)
- SM Higgs exclusion limits at 95% CL: 300-322 & 353-410 GeV (expected: 251-404 GeV)
- Need to be re-interpreted in light of X(125) discovery

m_{lljj} distributions in untagged (left) and tagged (right) high mass signal region

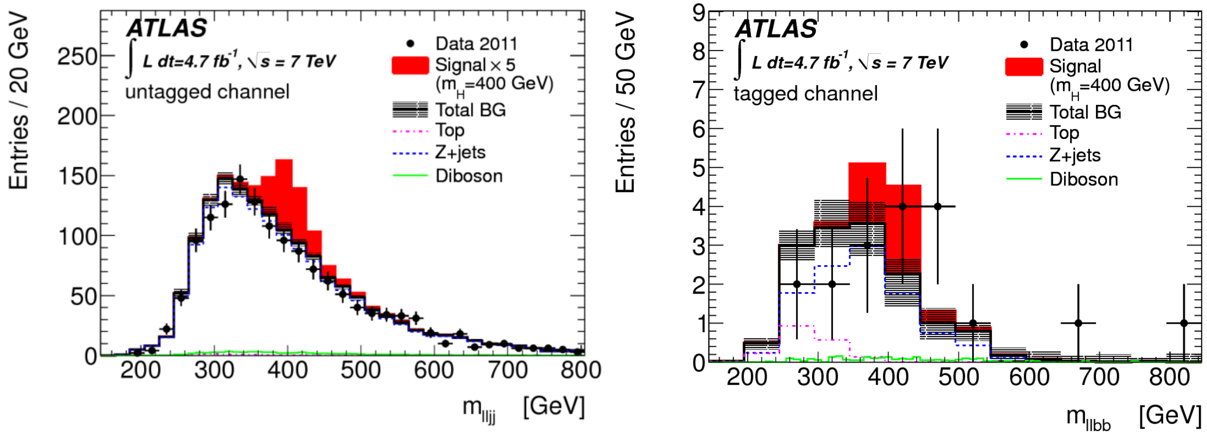

Production cross-section limits

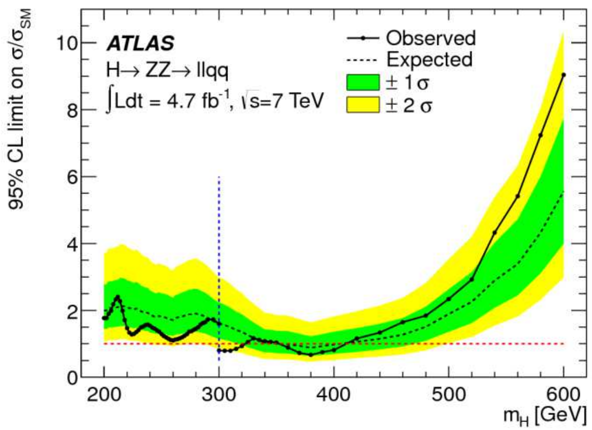

H→WW→lνqq (l=e,μ)

PLB 718 (2012) 391

- Analysis published with full 2011 dataset
- At high m_H, W is highly boosted and produces jets with higher p_T than background W+jets
- Categories H+0/1/2-jets. 1 high-p_T lepton (second lepton veto), large Etmiss, 2 jets (b-tag veto) with $71<m_{jj}<91$ GeV – Invariant mass reconstruction using $m_{l\nu}=m_W$ mass contraint
- Main backgrounds: W+jets (+top & Z+jets)
- Best sensitivity for m_H=400 GeV: 1.9*SM cross-section (expected 1.6)
- Need to be re-interpreted in light of X(125) discovery

Examples of $m_{l\nu jj}$ distributions in 0-jet (left) and 1-jet (right) signal region

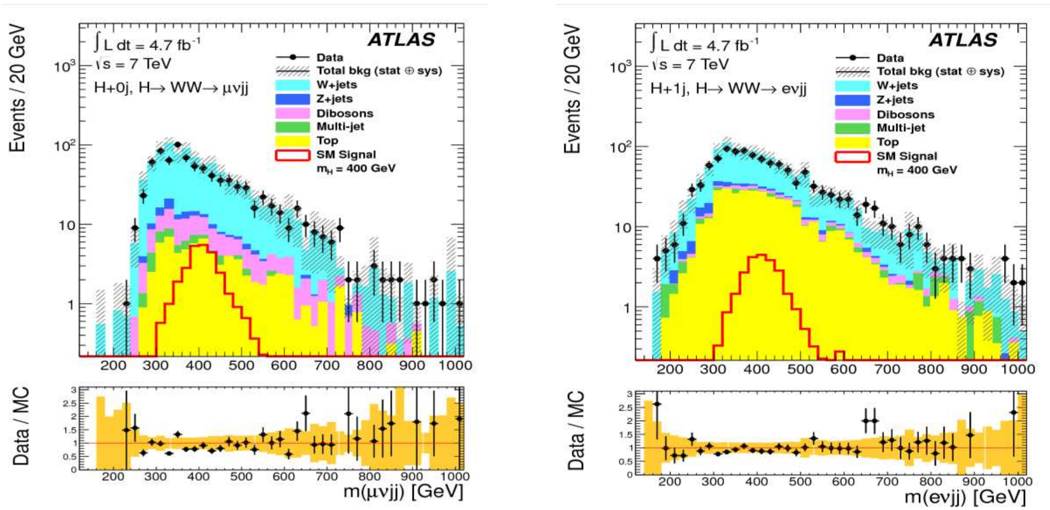

Production cross-section limits

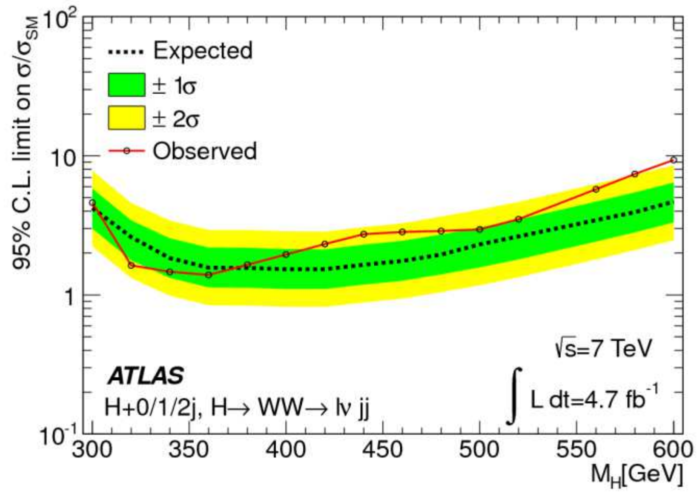

Grand picture (July paper)

PLB 716 (2012) 1-29